


國立交通大學

環境工程研究所

博士論文

利用光 Fenton 法降解與去除水中

加保扶毒性之研究



Application of photo-Fenton process in the
degradation and detoxification of carbofuran
contaminated water

研究生：呂理安

指導教授：林志高 教授

中華民國一百年九月

利用光 Fenton 法降解與去除水中加保扶毒性之研究

**Application of photo-Fenton process in the degradation and
detoxification of carbofuran contaminated water**

研 究 生：呂理安

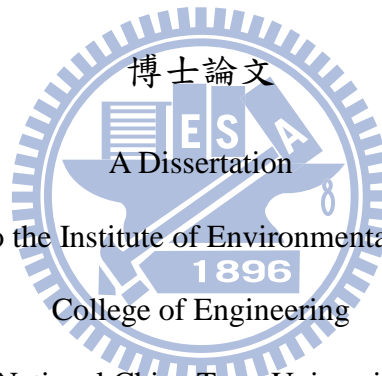
Student: Li-An Lu

指 導 教 授：林志高

Advisor: Jih-Gaw Lin

國立交通大學

環境工程研究所



Submitted to the Institute of Environmental Engineering

College of Engineering

National Chiao Tung University

in partial Fulfillment of the Requirements

for the Degree of

Doctor of Philosophy

in

Environmental Engineering

Sep, 2011

Hsinchu, Taiwan, Republic of China

中華民國一百年九月


利用光 Fenton 法降解與去除水中加保扶毒性之研究

研究生:呂理安

指導教授:林志高 教授

國立交通大學環境工程研究所 博士班

中文摘要



加保扶為氨基甲酸鹽類之殺蟲劑，易從施作場址滲出進而污染地表水與地下水。由於加保扶之毒性不利於生物處理，僅高級氧化法可以在短時間內降解加保扶。因此，高級氧化法中之光化學氧化法（例如光 Fenton 法），被視為處理加保扶最具有潛力技術之一。本研究中將探討 UV 照射時間、初始加保扶濃度、pH 值以及過氧化氫合三價鐵之加藥量等操作因子，對於光 Fenton 法處理受農藥加保扶污染水體之影響，並由加保扶以及溶解性有機碳 (dissolved organic carbon, DOC) 去除率評估光 Fenton 法之處理效率。實驗結果顯示除了初始加保扶濃度外，其餘操作因子對於加保扶以及 DOC 去除效率皆有正面影響。加保扶濃度 50 mg L^{-1} 條件下，當過氧化氫和三價鐵加藥量分別大於 $4 \text{ mg L}^{-1} \text{ min}^{-1}$ 以及 35 mg L^{-1} 時，加保扶與 DOC 去除率並沒有顯著的提升。此外，光 Fenton 法降解與礦化加保扶之最佳 pH 值為 3。在 pH 值 3 以及過氧化氫和三價鐵加藥量分別控制在 $4 \text{ mg L}^{-1} \text{ min}^{-1}$ 與 35 mg L^{-1} 之條件下，濃度 50 mg L^{-1} 之加保扶可以在 30 分鐘之內完全降解，同時反應 120 分鐘後礦化率可達 93%。

本研究主要目的為藉由二因子中央合成設計與反應曲面法，找出三價鐵 ($1-100 \text{ mg L}^{-1}$) 與過氧化氫 ($1-10 \text{ mg L}^{-1} \text{ min}^{-1}$) 最適之加藥量，同時建立不同反應時間下，加保扶和 DOC 去除率以及 BOD_5/DOC 比例等反應變數之二階多項式。實驗結果顯示，DOC 之去除率與系統中過氧化氫加藥量高度相關，如欲在短時間內達到較高之礦化率，則須添加較多之過氧化氫。由加保扶去除率與 BOD_5/DOC 比例實驗結果分析發現，降解 100 mg L^{-1} 加保扶最適之三價鐵與過氧化氫加藥量分別為 59 mg L^{-1} 以及 $5.4 \text{ mg L}^{-1} \text{ min}^{-1}$ 。在此操作條件下，加保扶可在 30 分鐘完全去除，同時反應 60 分鐘後 DOC 去除率約 41%，過氧化氫與三價鐵之比例介於 0.75 到 9.04 之間。另外，Microtox[®] 毒性試驗與 BOD_5/COD 比例實驗結果顯示，在最適加藥條件下，45 分鐘為結合光 Fenton 法與生物處理之最適反應時間，暴露 15 分鐘之 Microtox[®] 毒性單位可下降至 10，且 BOD_5/DOC 比例由初始 0 上升至 0.38。毒性單位之下降與生物降解性之提升，表示此時出流水水質為生物較易分解之水質特性。此外，平均氧化狀態(average oxidation state, AOS) 以及碳氧化狀態 (carbon oxidation state, COS) 兩指標分別由 -0.03 增加至 0.42 與 1.82，顯示在光 Fenton 法處理加保扶過程中，經氧化產生有機之中間產物。而中間產物分析結果顯示，有五種中間產物在光 Fenton 降解加保扶程序中產生，推論在氨基甲酸鹽之 C-O 鍵與咪喃環之 3-C 位置皆被氧化。綜合以上結果，對於受加保扶污染水體之處理，光 Fenton 法為結合生物處理程序極具潛力之前處理單元。

關鍵字：生物降解性、加保扶、中央合成設計、光 Fenton 法、反應曲面

Abstract

Carbofuran, a pesticide belong to the category of carbamate derivative, will contaminate surface and groundwater through leaching from applied site. Since carbofuran exhibits a special biorefractory character and require longer biodegradation time, its complete degradation in a shorter time could only be achieved by advanced oxidation processes. Therefore, photochemical oxidation i.e. photo-Fenton process has been considered as a promising technology for the degradation of carbofuran. The effects of irradiation time, carbofuran concentration, pH, H₂O₂ dosage rate and Fe³⁺ dosage on photo-Fenton treatment of carbofuran were evaluated in this study. The treatment efficiency was estimated based on the reductions of carbofuran concentration and dissolved organic carbon (DOC). The outcomes demonstrate that all the parameters had positive effect on carbofuran degradation except carbofuran concentration. With carbofuran concentration of 50 mg L⁻¹, no significant improvement in the carbofuran and DOC removals was observed when the H₂O₂ dosage rate and Fe³⁺ dosage were increased beyond 4 mg L⁻¹ min⁻¹ and 35 mg L⁻¹, respectively. Furthermore, the value of pH 3 was found to be the best suitable for carbofuran degradation and mineralization under the photo-Fenton process. At pH value of 3, carbofuran (50 mg L⁻¹) was completely degraded within 30 min and 93% DOC removal was achieved after 120 min reaction under H₂O₂ dosage rate 4 mg L⁻¹ min⁻¹ and Fe³⁺ dosage 35 mg L⁻¹.

A two factor central composite design along with response surface methodology was employed to estimate the favorable H₂O₂ dosage rate (1-10 mg L⁻¹ min⁻¹) and Fe³⁺ dosage (1-100 mg L⁻¹) in the photo-Fenton treatment of carbofuran and to develop the second-order polynomial equations in terms of carbofuran and DOC removals and BOD₅/DOC ratio as responses with different reaction times. DOC removal is found to

be highly related with H_2O_2 concentration in the system. Therefore, high loading of H_2O_2 dosage rate must be employed to achieve high carbofuran mineralization within a short reaction time. Based on the results of carbofuran removal and BOD_5/DOC ratio, H_2O_2 dosage rate of $5.4 \text{ mg L}^{-1} \text{ min}^{-1}$ and Fe^{3+} dosage of 59 mg L^{-1} were found to be the favorable reagent dosages for carbofuran degradation. Carbofuran (100 mg L^{-1}) was completely removed within 30 min reaction and 41% DOC removal was reached at these conditions. Moreover, the $\text{H}_2\text{O}_2/\text{Fe}^{3+}$ ratio was found to be varied from 0.75 to 9.04 within 60 min reaction. Based on the results of Microtox[®] test and BOD_5/COD ratio at the favorable reagent dosages, a reaction of 45 min was chosen as the appropriate time for coupling the photo-Fenton process with biological treatment. Under these conditions, 96% carbofuran removal was achieved, the toxicity unit (TU) measured with 15 min exposure was decreased to 10 and the biodegradability evaluated by BOD_5/COD ratio was increased from 0 to 0.38. The reduction of TU and increase of biodegradability represented an easily biodegradable effluent. Moreover, average oxidation state and carbon oxidation state were increased from -0.03 to 0.42 and 1.82, respectively, which revealed the strong mineralization and generation of oxidized organic intermediates during the photo-Fenton treatment of carbofuran. Furthermore, five major carbofuran intermediates were identified, which indicate that C-O bond of the carbamate group and 3-C position of the furan ring were oxidized as a result of the photo-Fenton reaction. The results obtained in this study demonstrate that the photo-Fenton process is a promising pretreatment method before the application of biological treatment for carbofuran removal from contaminated water/wastewater.

Keyword: Biodegradability; Carbofuran; Central composite design; Photo-Fenton; Response surface methodology

誌謝

回想起過去六年博士生涯實在感觸良多，要感謝的人實在太多了。首先感謝指導教授林志高老師從碩士以來細心指導，除了專業知識學習以外，同時也提供很多獨立思考判斷與領導能力學習機會。另外，口試期間也承蒙高正忠老師、邱求三老師、李俊福老師以及馬英石老師於百忙之中抽空閱讀論文以及在颱風天前來參與博士論文口試，並提供許多寶貴意見與指導，使得論文整體架構與內容更加完善，提升論文品質。其中特要感謝馬英石學長於實驗內容討論與論文投稿給予莫大協助，細心解答研究中遭遇各項難題。同時也要感謝邱求三老師提供實驗相關器材與設備，使得研究得以順利完成。此外，還要感謝 Dr. Kumar 以及 Dr. Daverey 在英文編修方面提供協助，並給予練習說英文之機會。

研究過程中，最要感謝家人全力支持，得以全心投入研究無後顧之憂完成學業。以及女朋友心渝兩年半來之陪伴，豐富了枯燥之研究生活。也要感謝研究室學長姐秀鳳、曉芬、宏邦、人傑與至誠，以及學弟妹 Remya、義雄、珮琦、怡湘、彥良、琪婷、彥汝、偉志、裕盛、欣倩、青洲、信杰、瑞興、紹謙、維芬、紘瑩、依璇、彥均、怡君、維倫、茜如、珮芸、信翰與南維，在實驗以及生活上諸多協助。最後，僅將此論文與榮耀獻給你們。

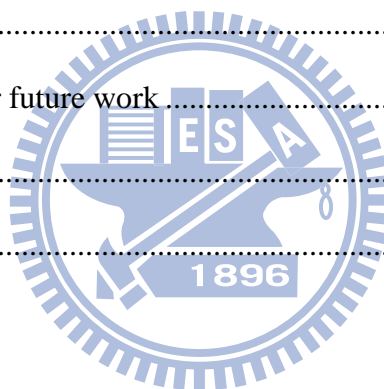
呂理安 謹誌於交通大學環工所

Table of contents

中文摘要	i
Abstract.....	III
誌謝	V
Table of contents.....	VI
List of tables	IX
List of figures	XI
Chapter 1 Introduction.....	1
1.1 Research background.....	1
1.2 Research motivation	3
1.3 Research objective	4
Chapter 2 Literature review.....	5
2.1 Pesticides	5
2.2 Carbofurn.....	6
2.2.1 Characteristics of carbofuran.....	6
2.2.2 Environmental fate	9
2.2.3 Effects on animals	11
2.2.4 Effects on Humans.....	11
2.2.5 Treatment techniques for aqueous carbofuran.....	11
2.2.6 Degradation intermediates and pathways of carbofuran by AOPs.....	13
2.3 Advanced oxidation processes	16
2.4 Fenton process	19
2.4.1 Electro-Fenton treatment.....	21

2.4.2 Anodic Fenton treatment	23
2.4.3 Heterogeneous Fenton treatment	24
2.4.4 Photo-Fenton treatment	25
2.5 Factors affecting photo-Fenton process	26
2.6 Integrating AOPs and biological process in water and wastewater treatment	30
2.7 Experimental design methodology	31
Chapter 3 Materials and methods	36
3.1 Chemical reagents	36
3.2 Experimental apparatus	36
3.4 Experimental procedure	40
3.5 Experimental design and data analysis	40
3.6 Analytical measurements	42
3.6.1 Analysis of carbofuran concentration	42
3.6.2 Analysis of H ₂ O ₂ concentration	44
3.6.3 Analysis of DOC concentration	44
3.6.4 Microtox [®] test	45
3.6.5 Identification of intermediates	45
3.6.6 Other analytical techniques	46
3.7 Carbofuran removal kinetics	46
Chapter 4 Results and discussions	47
4.1 Effect of irradiation time on carbofuran degradation	48
4.2 Effect of carbofuran concentration on carbofuran degradation	48
4.3 Effect of initial pH on carbofuran degradation	50
4.4 Effect of H ₂ O ₂ dosage rate on carbofuran degradation	55
4.5 Effect of Fe ³⁺ dosage on carbofuran degradation	60

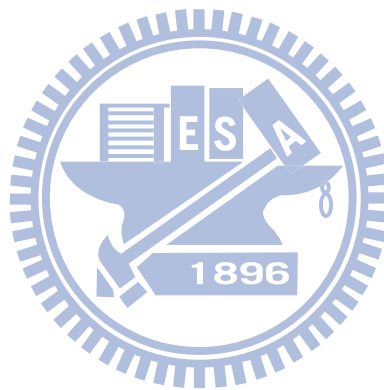
4.6 Chemical degradability of carbofuran	64
4.7 CCD of experiments for the photo-Fenton process	66
4.7.1 The regression model coefficients	67
4.7.2 Influence of H ₂ O ₂ dosage rate and Fe ³⁺ dosage on response	72
4.7.3 Favorable reagent dosages for carbofuran degradation under the photo-Fenton as a pretreatment process	77
4.8 Degradation pathway	79
4.9 Toxicity and oxidation state assessment	83
4.10 Biodegradability assessment.....	85
Chapter 5 Conclusions and recommendations.....	87
5.1 Summary of findings	87
5.2 Recommendations for future work	89
Chapter 6 References.....	90
Curriculum vitae	102



List of tables

Table 2-1. Annual usage of carbofuran in Taiwan.....	7
Table 2-2. Identity and physical/chemical properties of carbofuran.	8
Table 2-3. Toxicity of carbofuran on different spicies.....	12
Table 2-4. Comparison of carbofuran degradation under different treatment techniques.	14
Table 2-4. Comparison of carbofuran degradation under different treatment techniques (continued).....	15
Table 2-5. The advantage and disadvantage of each Fenton process.	22
Table 2-6. The independent and dependent variables of experimental design selected in Fenton processes.....	33
Table 2-6. The independent and dependent variables of experimental design selected in Fenton processes (contined)	34
Table 3-1. Experimental conditions for carbofuran degradation.....	41
Table 3-2. Experimental design along with coded and natural levels for two independent variables.....	43
Table 4-1. Effect of various pH on carbofuran and DOC removals (Fe^{3+} dosage at 35 mg L^{-1} , H_2O_2 dosage rate at 4 mg $\text{L}^{-1} \text{min}^{-1}$ and carbofuran 50 mg L^{-1}).....	53
Table 4-2. Effect of various H_2O_2 dosage rates on carbofuran and DOC removals (Fe^{3+} dosage at 35 mg L^{-1} , pH 3 and carbofuran 50 mg L^{-1}).	58
Table 4-3. Summarization of carbofuran degradation, DOC removal and the ratio of DOC removal/carbofuran degradation by the photo-Fenton reaction at various H_2O_2 dosage rates (Fe^{3+} 35 mg L^{-1} , pH 3 and carbofuran 50 mg L^{-1}).	59

Table 4-4. Effect of various Fe^{3+} dosages on carbofuran and DOC removals under H_2O_2 dosage rates 0.8 and 4 $\text{mg L}^{-1} \text{min}^{-1}$ at pH 3 and carbofuran 50 mg L^{-1}	62
Table 4-5. Carbofuran and DOC removals under various experimental conditions.	65
Table 4-6. Experimental results of CCD for the photo-Fenton degradation of carbofuran (pH 3 and carbofuran 100 mg L^{-1}).....	68
Table 4-7. Estimated regression coefficient and corresponding P-value for response...	69
Table 4-8. Optimum levels of H_2O_2 dosage rate and Fe^{3+} dosage for maximum carbofuran and DOC removals and BOD_5/DOC ratio.....	77
Table 4-9. Comparison of the simulated data of carbofuran removal and DOC removal with experimental data.....	79

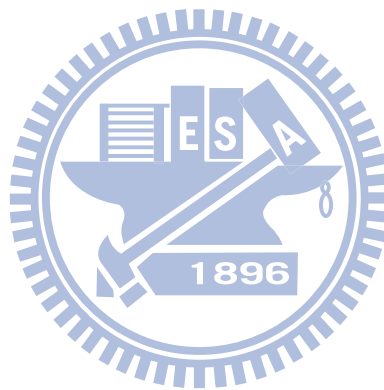


List of figures

Fig. 2-1. Proposed degradation mechanism of carbofuran by Fe (III) aquacomplexes [5].	17
Fig. 2-2. Proposed oxidative degradation pathway of carbofuran by AFT [63]......	18
Fig. 2-3. Speciation of Fe(III) species in water at 1×10^{-3} M total iron, ionic strength 0.1 M, and 25°C. Dashed line regions are supersaturated with respect to amorphous ferricoxyhydroxides [89]......	30
Fig. 3-1. Schematic diagram of the experimental setup.	37
Fig. 3-2. Flowchart of the research.....	39
Fig. 4-1. The profiles of (a) carbofuran (b) DOC removals with time (Fe^{3+} dosage at 5 mg L^{-1} , H_2O_2 dosage rate at $0.1 \text{ mg L}^{-1} \text{ min}^{-1}$ and pH 3).	49
Fig. 4-2. The profiles of (a) carbofuran (b) DOC removals with time at pH 3, using H_2O_2 : $1.3 \text{ mg L}^{-1} \text{ min}^{-1}$, Fe^{3+} : 10 mg L^{-1} (A and B) and H_2O_2 : $1.3 \text{ mg L}^{-1} \text{ min}^{-1}$, Fe^{3+} : 40 mg L^{-1} (C and D) (Solid points represent carbofuran 21 mg L^{-1} and hollow points represent carbofuran 81 mg L^{-1}).	51
Fig. 4-3. The profiles of (a) carbofuran (b) DOC removals with time at various pH (Fe^{3+} dosage at 35 mg L^{-1} , H_2O_2 dosage rate at $4 \text{ mg L}^{-1} \text{ min}^{-1}$ and carbofuran 50 mg L^{-1}).	52
Fig. 4-4. The profiles of (a) carbofuran (b) DOC removals with time at various H_2O_2 dosage rates (Fe^{3+} dosage at 35 mg L^{-1} , pH 3 and carbofuran 50 mg L^{-1}).	56
Fig. 4-5. Profiles of residual H_2O_2 with time at various H_2O_2 dosage rates (Fe^{3+} 35 mg L^{-1} , pH 3 and carbofuran 50 mg L^{-1}).	58

Fig. 4-6. Profiles of pH at various H ₂ O ₂ dosage rates (Fe ³⁺ dosage at 35 mg L ⁻¹ , pH 3 and carbofuran 50 mg L ⁻¹).	59
Fig. 4-7. The profiles of (a) carbofuran (b) DOC removals with time under various Fe ³⁺ dosages at pH 3 and carbofuran 50 mg L ⁻¹ (Solid points represent H ₂ O ₂ dosage rate 0.8 mg L ⁻¹ min ⁻¹ and hollow points represent H ₂ O ₂ dosage rate 4 mg L ⁻¹ min ⁻¹).	61
Fig. 4-8. Profiles of residual H ₂ O ₂ with time under various Fe ³⁺ dosages at pH 3 and carbofuran 50 mg L ⁻¹ (Solid points represent H ₂ O ₂ dosage rate 0.8 mg L ⁻¹ min ⁻¹ and hollow points represent H ₂ O ₂ dosage rate 4 mg L ⁻¹ min ⁻¹).	63
Fig. 4-9. Profiles of pH with time under different Fe ³⁺ dosages at pH 3 and carbofuran 50 mg L ⁻¹ (Solid points represent H ₂ O ₂ dosage rate 0.8 mg L ⁻¹ min ⁻¹ and hollow points represent H ₂ O ₂ dosage rate 4 mg L ⁻¹ min ⁻¹).	63
Fig. 4-10. Experimental and calculated values for carbofuran and DOC removals and BOD ₅ /DOC ratio in the photo-Fenton degradation of carbofuran.	71
Fig. 4-11. Normal probability plots of responses (a) carbofuran removal at 45 min (b) carbofuran removal at 60 min (c) DOC removal at 45 min (d) DOC removal at 60 min (e) BOD ₅ /DOC ratio at 60 min.	73
Fig. 4-12. Plots of residuals versus predicted values for responses (a) carbofuran removal at 45 min (b) carbofuran removal at 60 min (c) DOC removal at 45 min (d) DOC removal at 60 min (e) BOD ₅ /DOC ratio at 60 min.	74
Fig. 4-13. The response surface and contour plot as a function of H ₂ O ₂ dosage rate and Fe ³⁺ dosage of (a) carbofuran removal at 60 min (b) DOC removal at 45 min (c) BOD ₅ /DOC ratio at 60 min.	75
Fig. 4-14. GC-MS spectra of carbofuran and its degradation intermediates (RT means retention time).	81
Fig. 4-15. Proposed degradation pathways of carbofuran by photo-Fenton process	

(dotted lines reflect the hypothesized carbofuran degradation pathway).....	82
Fig. 4-16. Variations in the Microtox [®] test, AOS and COS as a function of reaction time (H ₂ O ₂ dosage rate at 5.4 mg L ⁻¹ min ⁻¹ , Fe ³⁺ dosage at 59 mg L ⁻¹ , pH 3 and carbofuran 100 mg L ⁻¹).....	84
Fig. 4-17. Variations in the BOD ₅ and BOD ₅ /COD ratio as a function of reaction time (H ₂ O ₂ dosage rate at 5.4 mg L ⁻¹ min ⁻¹ , Fe ³⁺ dosage at 59 mg L ⁻¹ , pH 3 and carbofuran 100 mg L ⁻¹).....	85



Chapter 1

Introduction

1.1 Research background

Carbofuran is a broad spectrum carbamate pesticide and nematicide, which has been used against various foliar pests observed in fruits, vegetables and forest crops. It accounts about 9-18% of the total insecticides produced every year in Taiwan [1]. This carbamate pesticide is highly soluble in fresh water (350 mg L^{-1} , 25°C) [2]; therefore, it is susceptible to leaching and percolation through agricultural fields. Recent findings reported the presence of carbofuran in surface water and groundwater which illustrate the fact that carbofuran can enter ground water through leaching and surface water through runoff from applied fields [3-6] and the half-life of carbofuran in water ranges between 690 days at pH 5 and 7 days at pH 8 [5]. Carbofuran usage has received intensive concern not only due to its high solubility but also due to its high oral toxicity. The LD_{50} for carbofuran is $5\text{-}13 \text{ mg kg}^{-1}$ body weight in rats whereas the LD_{50} for atrazine (a triazine herbicide of low to moderate toxicity) is 1300 mg kg^{-1} [5,7,8].

Hydrolysis and microbial degradation are the two most important mechanisms determining the stability of carbofuran in the environment. It is resistant to biological treatment methods; therefore, microbial degradation of this pesticide, i.e. biodegradation, requires longer time and specific microorganisms. Several treatment techniques including both physicochemical and biological methods could be applied for treating

pesticide contaminated water. However, few techniques are sufficiently broad-based and convenient for real-time applications [9]. Since carbofuran exhibits a special biorefractory character and requires longer biodegradation time, its complete degradation in a shorter time could only be achieved by using strong oxidizing agents.

Advanced oxidation processes (AOPs) have been extensively investigated for water and wastewater treatments. These processes could be applied as the sole treatment process or as a pretreatment for improving the biodegradability of pesticide containing wastewater prior to the biological treatments [10-12]. Several studies have proven that AOPs are promising and attractive alternatives in the treatment of organic pollutants that are either toxic or refractory to the biological treatments [13-16]. AOPs mainly rely on the generation of highly oxidative free radicals, in most cases the hydroxyl radical ($\cdot\text{OH}$) with an E^0 of 2.8 V/SHE [17]. A variety of effective AOPs such as ultrasonic irradiation, direct photolysis, ultra-violet (UV) irradiation in the presence of ozone or Fenton reagent, electro-Fenton, anodic Fenton treatment (AFT), TiO_2 as a photocatalyst and ultrasound penetration have been successfully applied for carbofuran degradation in contaminated water [3,5,18-23]. Among these processes, the Fenton treatment has revealed very high efficiency in the mineralization of biorefractory pesticides and other organic pollutants [13,24-28]. In addition, it is simple, non-expensive and can be operated under the conditions of low temperature and atmospheric pressure [27].

The major drawbacks of Fenton treatment are (1) the continuous addition of Fe^{2+} and H_2O_2 for further oxidation of organic compound owing to the very slow regeneration of Fe^{2+} and (2) the production of large volume of ferric hydroxide sludge [29-31]. The photo-Fenton reaction, a combination of H_2O_2 and UV irradiation less than 400 nm with Fe^{3+} or Fe^{2+} , is a promising treatment, which can produce relatively more $\cdot\text{OH}$ compared to the Fenton treatment. Subsequently, the regenerated Fe^{2+} could

undergo further reaction with more H_2O_2 molecules, produce new $\cdot OH$ and form a reaction cycle [32,33]. In the past, the photo-Fenton treatment has shown very high efficiency in the mineralization of biorefractory pesticides and other organic pollutants [13,24-28].

1.2 Research motivation

Comparing to biological treatment, the major limitation of AOPs is their relatively high operational costs for complete oxidation of organic compounds [34,35]. In order to reduce the operational cost and achieve high performance of AOPs, the operation conditions must be optimized. For such a goal, the statistical based optimization methodology such as the central composite design (CCD) is appropriate to be applied in a multifactor system with minimum number of well-chosen experiments [31,36]. The CCD is a modern experimental design approach, which has been widely used in several applications [13,37-39] to fit the experimental data and develop a statistically significant second-order polynomial equation. Along with response surface methodology (RSM), it is possible to assess the conditions that could yield the most desirable response. Besides, the response surface plots can be constructed to locate the optimum points of the multifactor system [16].

A step forward in the cost reduction of pesticide bearing wastewater treatment could be achieved by combining the AOPs with a conventional biological treatment [11,12,15,40-42]. The combination of the photo-Fenton process (as a pretreatment) followed by biological treatment has great potential for enhancing the biodegradability of pesticide contaminated wastewater [12,34,43,44]. Nevertheless, incomplete oxidation may result the formation of more toxic intermediates than the parents, which can

decrease the biodegradability [35,44]. Therefore, the biodegradability and toxicity assessment of degradation intermediates are essential for evaluating the success of the photo-Fenton process as a pretreatment for pesticide contaminated wastewater treatment.

1.3 Research objective

As carbofuran exhibits a special refractory character to biodegradation methods, this study was focused on its oxidation and detoxification. Goals of this study were listed below:

- (1) Investigate the degradation/mineralization extend of carbofuran and estimate the effects of irradiation time, carbofuran concentration, pH, H₂O₂ dosage rate and Fe³⁺ dosage on photo-Fenton treatment of carbofuran.
- (2) Develop the second-order equations in terms of carbofuran and DOC removals and BOD₅/DOC ratio at different time using CCD along with RSM to find out the favorable dosage conditions.
- (3) Investigate the variations of toxicity and biodegradability with reaction time under favorable reagent dosages to find out the appropriate time to coupling photo-Fenton process with biological treatment.
- (4) Identify the intermediates produced under favorable reagent dosages to propose the possible degradation pathway.

Chapter 2

Literature review

2.1 Pesticides

Pesticides include a variety of compounds such as insecticides, nematocides and herbicides. They are carcinogenic and mutagenic substances, and commonly used to protect the plant from pest attack. The widespread use of pesticide throughout the agricultural industry has resulted in mixed impacts. On one hand, utilization of pesticides produces an enormous increase in agricultural productivity. On the other hand, improper applications of pesticides, the disposal of rinse water from pesticide containers and spray equipment, and the disposal of unused, unwanted, or obsolete pesticide stocks create soil and groundwater pollution problems, resulting not only the impact on the ecosystem but a risk to human health. Moreover, recent findings that cite the presence of pesticides in drinking water supplies illustrate the fact that some fraction of pesticides applied to agricultural lands can be transported off site and into surface waters [45]. The pesticides concentration in air, surface waters, soil, flora and fauna is increasing day by day, and at present, it constitutes a major problem owing to their repeated and indiscriminate use in agriculture [9,18,46-48]. In addition to their toxicity character by themselves, the hazardous potential is increased by the possibility of generating organohalogen compounds through their reactions with chloro derivatives [18]. Hence,

to meet the world wide problem of environmental protection and pollution control, it is necessary to detect, separate, identify and determine pesticide residues in the ecosystem. Later, the pollutant can be removed from the medium [46]. The use of wide range of pesticides makes research extremely difficult for developing a single method for the removal of pesticides. Many approaches either independent or in conjunction have been considered for pesticide removal, including chemical oxidation, photo degradation, biological degradation, coagulation, incineration and adsorption, but only few are sufficiently broad-based and convenient to the user [49].

2.2 Carbofurn

2.2.1 Characteristics of carbofuran

Carbofuran ($C_{12}H_{15}NO_3$, 2,3-dihydro-2,2-dimethylbenzofuran-7-yl methylcarbamate) is a broad spectrum carbamate pesticide and nematicide that kills insects, mites, and nematodes on contact or after ingestion. It is used against foliar pests including wireworms, white grubs, weevils, stem borers, aphids and several other insects observed in the fruits, vegetables, and forest crops [50]. Formulations of carbofuran are used worldwide in agricultural applications. In 1995, more than 2200 tons of carbofuran was applied in United States [3]. Carbofuran annual usage in Italy is about 1200 tons [51]. In Taiwan, carbofuran accounts for about 9-18% of insecticides production per year as shown in Table 2-1 [52]. As a result of its widespread use; air, food, surface water and underground water are contaminated with carbofuran and its metabolites, which may affect human health. Carbofuran is highly toxic to animals and humans both by oral and inhalation routes and therefore, may pose a serious threat to

Table 2-1. Annual usage of carbofuran in Taiwan.

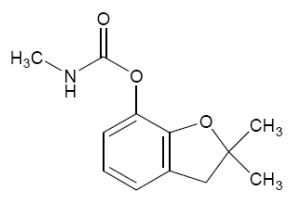
Year	2005	2006	2007	2008	2009	2010
Usage of total						
insecticide	14	12	9	12	18	15
(%)						
carbofuran/	2,302/	1809/	1,407/	1,803/	2,564/	2,310/
total insecticide	16,288	15,478	15,016	14,493	14,075	15,645
(ton)						

those in contact with it in manufacturing and formulation plants or in crop fields [50].

The detailed physical and chemical characteristics of carbofuran are listed in Table 2-2.

The use of carbofuran has received intensive concern not only due to its heavy use but also due to its high oral toxicity. The oral LD₅₀ of carbofuran is 11 mg kg⁻¹ body weight in rats [5]. In comparison to this, the LD₅₀ of parathion (an extremely toxic organophosphorus pesticide) is 8 mg kg⁻¹ whereas the LD₅₀ of atrazine (a triazine herbicide of low to moderate toxicity) is 1300 mg kg⁻¹ [53]. Carbofuran is highly soluble in fresh water (350 mg L⁻¹) [2]. Furthermore, the organic carbon partition coefficient ranges from 14 to 160 indicating carbofuran will leach significantly into the aqueous phase [3]. It is well known that carbofuran is more persistent than other carbamate or organophosphorus insecticides [50]. Normally, carbofuran is moderately persistent in water due to its chemical stability and retains its biological activity in a single application [5,54]. Therefore, the development of new methodology for the removal of carbofuran in fresh water has received much attention in recent years.

Table 2-2. Identity and physical/chemical properties of carbofuran.

Property	Information
Pesticide type	Insecticide
IUPAC name	2,3-dihydro-2,2-dimethyl-benzofuran-7-yl methylcarbamate
Chemical structure	
Molecular formula	$C_{12}H_{15}NO_3$
Molecular weight	221.3 g mol^{-1}
Color/Form/Odor	White crystalline solid with slight phenolic odor
Melting point	$153-154^{\circ}\text{C}$
Boiling point	150°C
Vapor pressure	$3.4 \times 10^{-6} \text{ mm Hg (} 25^{\circ}\text{C)}$
Henry's Law Constant	$3.9 \times 10^{-9} \text{ atm m}^3 \text{ mol}^{-1}$
Octanol/Water partition (Kow) Log Kow	2.32
Solubility	In water 350 mg L^{-1} and in acetone 150, acetonitrile 140, benzene 40, cyclohexone 90, dimethylformade 270 and dimethyl sulfoxide 250 (all in g kg^{-1} at 25°C).
Specific gravity	1.18 at 20°C

Source: US Environmental Protection Agency [7]

2.2.2 Environmental fate

(1) In plant:

Carbofuran is rapidly taken up by plants through the roots from soil and water and is translocated mainly into the leaves. The main metabolite in plants has been identified as 3-hydroxycarbofuran [8]. However, levels of 3-hydroxycarbofuran and other degradation products in plants are influenced by factors, i.e. plant age, soil type, pesticide formulation, application method and rate, and weather conditions. Oxidation of unconjugated 3-hydroxycarbofuran yields 3-ketocarbofuran which rapidly hydrolyzes to less toxic 3-ketocarbofuran phenol. Accordingly, 3-ketocarbofuran is not detected as a terminal residue in plants above trace levels. Residue analyses indicated that carbofuran and 3-hydroxycarbofuran are the compounds that occur most often in plant tissues after treatment [55].

(2) In soil:

Carbofuran is degraded in soil mainly by hydrolysis, microbial action and photodecomposition. Carbofuran is also decomposed by sunlight irradiation, resulting in generation of 2-hydroxyfuradan and furadan phenol [56]. Its persistence depends on pH, soil type, temperature, moisture content and the microbial population. The adsorption and desorption characteristics which determine the movement of carbofuran through the soil profile, their bioavailability, microbial degradability and persistence depend upon soil properties such as organic matter content, clay content and the physicochemical properties of the pesticide, i.e., size, shape, solubility in water, pK values and polarity [50]. Degradation products in soil include carbofuran phenol,

3-hydroxycarbofuran and 3-ketocarbofuran; field studies have indicated a half-life of around 150 d in soil [51]. It has been found that carbofuran is susceptible to leaching and reported that carbofuran is the most mobile among the eight major pesticides applied to the soils in Taiwan [57]. Moreover, carbofuran has also been classified under the category of highly mobile compounds. If carbofuran is applied into the soil, around 1 to 5 cm depth, more than 11% of the applied carbofuran can be transported to surface waters and entered groundwater in runoff [58].

(3) In water:

Carbofuran is degraded in water by hydrolysis, microbial decomposition and photolysis. In aqueous medium, carbofuran hydrolyses to produce alcohols, amines, and carbon dioxide [3]. Hydrolysis half-lives in water at 25°C of 690, 57 and 7 d have been reported at pH levels of 6.0, 7.0 and 8.0, respectively [59]. The laboratory study shows that half-lives of carbofuran in deionized water are approximately 3.1 h and 41.6 h when exposed to 300 nm light and to direct sunlight, respectively [60]. Carbofuran is increasingly detected in surface water and ground water of at least seven states in USA [3,18]. The available data show that carbofuran has been frequently detected as a ground water contaminant in America as well as in Europe and Asia over the last two decades. It has been found in surface water that serves as a drinking water source for Sacramento and groundwater in different states of USA with the concentration between 1 and 500×10^{-6} mM [61,62]. It also found in soil leachate, groundwater and surface water in Carchi, Ecuador [4] and contaminated with seawater at area of Laysan Island in 1998 [60].

2.2.3 Effects on animals

Carbofuran is highly toxic after acute oral administration. The oral LD₅₀ values ranged from 0.2 to 39 mg kg⁻¹ of body weight as listed in Table 2-3. Toxic signs observed were typical for cholinesterase inhibition; salivation, cramps, trembling and sedation were observed within minutes after administration and lasted for up to 3 d. WHO has classified carbofuran as highly hazardous insecticide [8].

2.2.4 Effects on Humans

Acute toxic clinical effects resulting from carbofuran exposure in humans appear to be completely reversible and have been successfully treated with atropine sulfate. However, treatment should occur as soon as possible after exposure because acute carbofuran toxicosis can be fatal; younger age groups are more susceptible than adults [55]. In addition, carbofuran is poisonous to human if swallowed, inhaled, or absorbed through the skin; patients are cautioned not to breathe carbofuran dust, fumes, or spray mist; and treated areas should be avoided for at least 2 days [8].

2.2.5 Treatment techniques for aqueous carbofuran

Due to stringent drinking water standards, the U.S. EPA prescribes maximum contaminant level (MCL) for carbofuran in drinking water at 40 µg L⁻¹ (Canada 90 µg L⁻¹, Taiwan 20 µg L⁻¹). The European Union has set a maximum admissible concentration of 0.5 µg L⁻¹ for the sum of all pesticides and 0.1 µg L⁻¹ for an individual compound in drinking water [6]. The treatment of carbofuran has become a worldwide

Table 2-3. Toxicity of carbofuran on different species.

Species	LD ₅₀ (mg kg ⁻¹)
Rats	5-13
Dogs	19
Fulvous ducks	0.238
Bobwhite quail	12
Pheasant	4.15
Chickens	25-39
Bluegill sunfish	0.24
Rainbow trout	0.38
House sparrow	1.3

Source: World Health Organization [8]; California Public Health Goal [56]

issue and forced the development of processes to solve this problem. It is well known that photolysis, microbial degradation and hydrolysis are main degradation pathways of carbofuran in the environment [5,60]. Carbofuran is resistant to biological treatment methods; therefore, microbial degradation of this pesticide, i.e. biodegradation, requires longer time and specific microorganisms. Direct photolysis and photo oxidation may contribute to carbofuran transformation in natural waters [3]. Several treatment techniques including both physicochemical and biological methods could be applied for treating pesticide contaminated water. However, few techniques are sufficiently broad-based and convenient for real-time applications [9]. Since carbofuran exhibits a special biorefractory character and requires longer biodegradation time, its complete degradation in a shorter time could only be achieved by utilizing strong oxidizing agents. A variety of effective treatment techniques such as ultrasonic irradiation, direct

photolysis, ultra-violet (UV) irradiation in the presence of ozone or Fenton reagent, electro-Fenton, anodic Fenton treatment (AFT), TiO₂ as a photocatalyst and ultrasound penetration have been successfully applied for carbofuran degradation in contaminated water [3,5,18-23]. These treatments (Table 2-4) have shown that AOPs are useful in treating carbofuran and giving a more effective performance than using single oxidants and concluded that •OH is effective in degrading carbofuran. Among the AOPs, the photo-Fenton process has greater potential in decomposition of carbofuran comparing with other AOPs due to the formation of more •OH than the other processes.

2.2.6 Degradation intermediates and pathways of carbofuran by AOPs

Some researchers have carried out the investigations on the degradation intermediates of carbofuran by different AOPs treatments. It has been reported that 2,2-dimethyl-2,3-dihydro-benzofuran-7-ol, an intermediate produced due to the cleavage of the carbamate group of carbofuran, was identified by GC/MS in the hydrolysis, photolysis, photocatalysis and AFT treatment of carbofuran [5,19,48,61,63]. With further oxidizing on the furan ring, 2,2-dimethyl-2,3-dihydro-benzofuran-7-ol, 7-hydroxy-2,2-dimethyl-benzofuran-3-one and 2,2-dimethyl-2,3-dihydro-benzofuran-3,7-diol were generated. These two byproducts were also found as intermediates of carbofuran degradation by AFT treatment. In addition, more byproducts with lower toxicity than their parent compound were identified in the treated carbofuran solution, particularly the heterocyclic ring opened byproducts, such as 3-phenoxy 1-propanol, 2-ethyl 1-hexanol, 2-butoxyl ethanol. Based on the decrease of TOC or COD during the degradation process, it could be anticipated that the benzene ring was opened and the mineralization reaction to carbon dioxide occurred. According to the intermediates

Table 2-4. Comparison of carbofuran degradation under different treatment techniques.

Treatment method	Carbofuran concentration (mg L^{-1}) / working volume (mL)	Experimental conditions	Reaction time (min)	Carbofuran removal (%)	TOC removal (%)	Reference
UV + Fe^{3+}	10/20	pH 2.8, $\text{Fe}^{3+} 8 \times 10^{-4} \text{ mol L}^{-1}$, 990-W UV lamp ($\lambda < 300 \text{ nm}$)	50	90	70 (25 h)	[5]
Ultrasonic irradiation	29/700	1800 W, 20 kHz Argon: Oxygen (4:1)	60	86	-	[3]
UV	100/350	Temp., pH 3	60	67	-	[18]
Ozone	100/350	Temp., pH 2, pressure 0.265 kPa	30	90	-	[18]
Fenton	100/350	pH 3, $\text{H}_2\text{O}_2 170 \text{ mg L}^{-1}$, $\text{Fe}^{2+} 28 \text{ mg L}^{-1}$	50	40	-	[18]
UV + TiO_2	200/100	pH 7, 64-W UV lamps ($\lambda 365 \text{ nm}$), 100 mg TiO_2	300	100	100	[19]

Table 2-4. Comparison of carbofuran degradation under different treatment techniques (continued).

Treatment method	Carbofuran concentration (mg L^{-1}) / working volume (mL)	Experimental conditions	Reaction time (min)	Carbofuran removal (%)	TOC removal (%)	References
Fenton	50/1000	pH 3, H_2O_2 200 mg L^{-1} , Fe^{2+} 5 mg L^{-1} 300 W, 20 kHz	30	57	10	[20]
Sono-Fenton	50/1000	pH 3, H_2O_2 100 mg L^{-1} , Fe^{2+} 10 mg L^{-1}	30	100	14	[23]
Photo-Fenton	50/300	pH 2.8, H_2O_2 340 mg L^{-1} , Fe^{3+} 2.8 mg L^{-1} , 16 14-W UV lamps (λ 300-400 nm)	30	100	91 (2 h)	[9]

detected, the possible photocatalytic degradation of carbofuran was proposed by Katsumata *et al.* (2005) and shown in Fig. 2-1 [5]. According to this pathway, the carbamate group is appeared to be the primary attack site by the hydroxyl radical. At the same time, unstable carbamic acid was formed and rapidly degraded to methylamine and carbon dioxide. After the removal of carbamate group, the hydroxyl radicals continuously attack at C-3 position of the furan ring and form a carbonyl group. The hydroxyl radicals attack at C-2 position of the furan ring and further lead to the cleavage of the ring and demethylation. The aromatic intermediate is presumably further oxidized through ring-rupturing reaction into aliphatic compounds.

In another case, a suggested oxidation pathway of carbofuran by anodic Fenton treatment (AFT) was proposed by Wang and Lemley (2003) and shown in Fig. 2-2 [63]. The result is similar to the photocatalytic degradation of carbofuran. The carbamate group appears to be the first group removed by the hydroxyl radical and during AFT treatment. And then the hydroxyl radical continues attack by substituting a hydroxyl group for one of H atoms at 3-C of the furan ring. Further oxidation eliminates another H atom at 3-C and a carbonyl group is formed.

2.3 Advanced oxidation processes

AOPs are characterized by the presence of free radicals, i.e. hydroxyl radicals, as the oxidants under atmospheric temperature and pressure and extensively investigated for water and wastewater treatments. A technology in water and wastewater treatment using AOPs is considered to be fast and effective in this respect; it has shown great potential in the treatment of pollutants and a wide range of applications in groundwater treatment and municipal wastewater sludge destruction. These processes could be

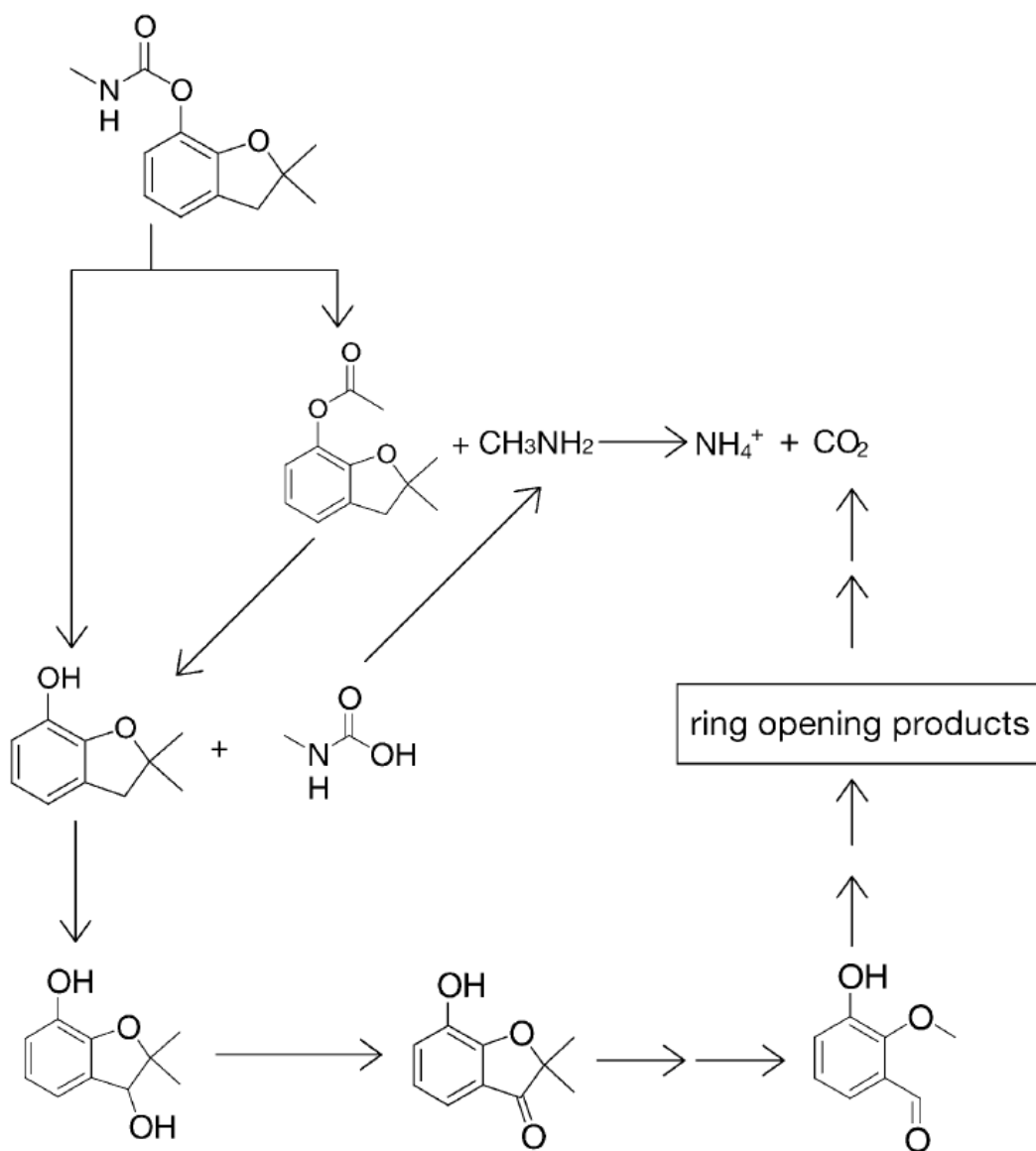


Fig. 2-1. Proposed degradation mechanism of carbofuran by Fe (III) aquacomplexes [5].

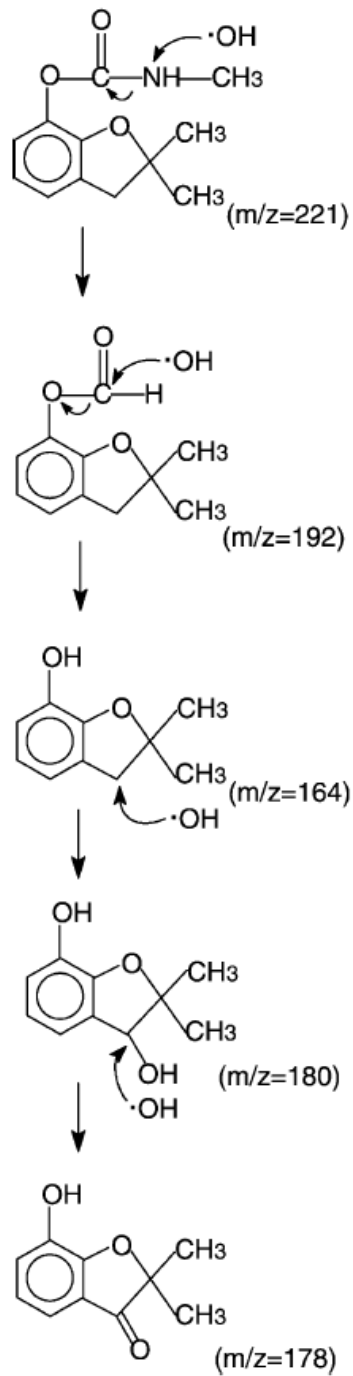


Fig. 2-2. Proposed oxidative degradation pathway of carbofuran by AFT [63].

applied as the sole treatment process or as a pretreatment for improving the biodegradability of pesticide containing wastewater prior to the biological treatments [11,12].

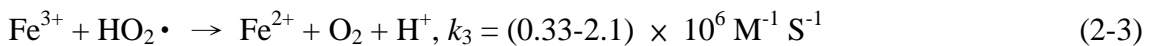
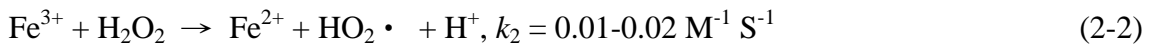
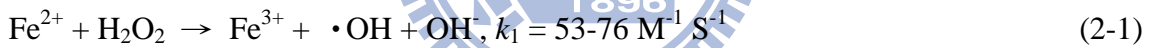
AOPs mainly rely on the generation of highly oxidative free radicals. In most cases the $\cdot\text{OH}$ with an E^0 of 2.8 V/SHE, are considered to be promising and attractive alternatives in the treatment of organic pollutants that are either toxic or refractory towards biological treatments and, therefore, these processes have wide range of applications in wastewater treatment [13-16]. The $\cdot\text{OH}$ produced can achieve three goals: (1) the reduction of COD; (2) convert the constituents of organic pollutants into simple, relatively harmless, and inorganic molecules (i.e., CO_2 , H_2O) (3) the detoxification and enhancement of the biodegradability in order to make next biological treatment possible [62]. A variety of effective degradation procedures have been developed in the field of chemical treatment of water for the elimination of pesticides: ultrasonic irradiation, direct photolysis, heterogeneous photocatalytic [64], UV irradiation in the presence of ozone or Fenton reagent, membrane anodic Fenton treatment, Fenton-coagulation [65] and TiO_2 as a photocatalyst [5,31,43,66]. Though, AOPs have many advantages including fast reaction rate, non-selective to pollutants and degrading refractory materials, one common disadvantage is high consumption of electrical energy for devices such as ozonizers, UV lamps, ultrasounds and heater, which results in rather high treatment cost.

2.4 Fenton process

It was developed in the 1890s by Henry John Horstman Fenton. He reported that H_2O_2 could be activated by Fe^{2+} salts to oxidize tartaric acid. In 1934, Haber and Weiss

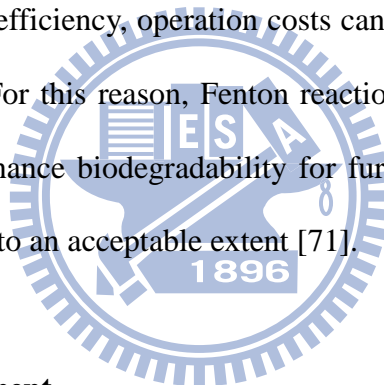
proposed that the active oxidant produced by Fenton reaction is $\cdot\text{OH}$, one of the most powerful oxidants known. Fenton treatment has received even more extensive attention because of its broad-spectrum of target compounds, strong oxidation ability, fast reaction rate, and the simplicity of the treatment equipment. Besides, the process is simple and non-expensive, operating at low temperature and at atmospheric pressure [27].

The Fenton method requires H_2O_2 , Fe^{2+} salts and acidic pH. Comparing with other bulk oxidants, H_2O_2 is inexpensive, safe and easy to handle and no lasting environmental threat since it readily decomposes to water and oxygen. The mechanism of the Fenton reaction with H_2O_2 and Fe^{2+} is shown in Eq. 2-1 to 2-3. Furthermore, Fe^{3+} produced can react with H_2O_2 to form Fenton-like reaction (Eq. 2-2) and generate less powerful hydroperoxyl radical ($\text{HO}_2\cdot$, E^0 1.42 V/SHE) [33,67-69]. Therefore, the ferric ion can be used instead of ferrous ion in Fenton process.



The reaction rate of the Fenton reaction (k_1) is much faster than the Fe^{2+} regeneration rate (k_2 and k_3), therefore the addition of Fe^{2+} and H_2O_2 is required to keep the reaction proceed. The major advantages of the Fenton's reagent are: (1) both iron and H_2O_2 are cheap and non-toxic; (2) there is no mass transfer limitation due to its homogeneous catalytic nature; (3) there is no additional energy involved in using catalyst; (4) the process is technologically simple. The main disadvantages of Fenton

reaction are (1) the continuous addition of Fe^{2+} and H_2O_2 for further oxidation of organic compound owing to the very slow regeneration rate of Fe^{2+} ; (2) the production of large volume of ferric hydroxide sludge [29-31]; (3) requirement of an acidic reaction condition (usually pH at 2.5-3.5) which could consume a lot of acid and require neutralization of low pH effluent prior to drainage [70]. In order to overcome these drawbacks and to improve treatment efficiency, several modified Fenton process like electro-Fenton, anodic Fenton, heterogeneous Fenton and photo-Fenton treatment are developed. The advantages and disadvantages of each Fenton process are listed in Table 2-5. Using Fenton process for the treatment of organic compounds in water and wastewaters reveals high removal efficiency under optimal experimental conditions. Even with optimal removal efficiency, operation costs can be an important limitation in the selection of treatment. For this reason, Fenton reaction may be recommended as a pre-treatment process to enhance biodegradability for further biological treatment and reduce the operational costs to an acceptable extent [71].



2.4.1 Electro-Fenton treatment

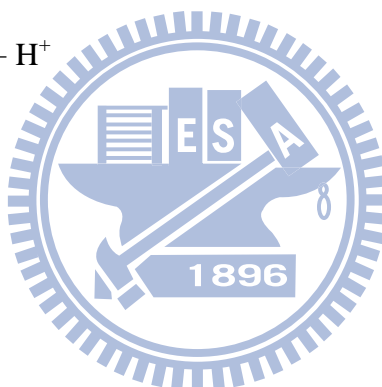
Recently, indirect electro-chemical oxidation methods such as electro-Fenton are being developed for wastewater remediation. In these environmentally clean electrochemical techniques, H_2O_2 is continuously generated in an acidic contaminated solution (Eq. 2-4) from the two-electron reduction of O_2 at reticulated vitreous carbon, mercury pool, carbon-felt and O_2 -diffusion cathodes [72].



Table 2-5. The advantage and disadvantage of each Fenton process.

Process	Advantage	Disadvantage	Reference
Fenton	<ol style="list-style-type: none"> 1. Cost-effective 2. Simple handling 3. No additional energy involved 	<ol style="list-style-type: none"> 1. Continuous addition of reagents 2. Production of ferric hydroxide sludge 3. Requirement of acidification and neutralization 	[73-75]
Electro-Fenton	<ol style="list-style-type: none"> 1. Allowing better control of the process 2. Avoiding the addition of H₂O₂ 	<ol style="list-style-type: none"> 1. Additional energy consumption 2. Requirement of acidification and neutralization 3. Low current density and low reaction rate 	[17,22,72]
Anodic Fenton	<ol style="list-style-type: none"> 1. Avoiding the addition of iron ion 2. Effluent pH is neutral 	<ol style="list-style-type: none"> 1. Additional energy consumption 2. Not simple handling 	[30,63]
Heterogeneous Fenton	<ol style="list-style-type: none"> 1. Recycle of iron source 2. Lower H₂O₂ consumption 	<ol style="list-style-type: none"> 1. Requirement of acidification and neutralization 2. Low reaction rate 3. Iron source leaching at acid pH 	[42,76,77]
Photo-Fenton	<ol style="list-style-type: none"> 1. Reduction of ferric hydroxide sludge formation 2. Without continuous addition of iron ion 3. More •OH generated 4. Simple handling 	<ol style="list-style-type: none"> 1. Additional energy consumption 2. Requirement of acidification and neutralization 	[22,78,79]

The two main sources of $\cdot\text{OH}$ are anodic water oxidation (Eq. 2-5) and classical Fenton's reaction between Fe^{2+} and H_2O_2 by adding small amounts of Fe^{2+} as catalyst into the acidic solution. Fe^{3+} species generated from Fenton's reaction revert to Fe^{2+} by different reduction processes, involving H_2O_2 and/or organic intermediate radicals, as well as the direct reduction of Fe^{3+} on the cathode, allowing the propagation of the Fenton's reaction by a catalytic cycle [80]. The reduction of Fe^{3+} by H_2O_2 takes place in two steps (Eq. 2-6 and Eq. 2-7), and also produces $\text{HO}_2\cdot$ as the anodic oxidation of H_2O_2 (Eq. 2-8).



2.4.2 Anodic Fenton treatment

AFT was proposed as an improvement of the classic Fenton treatment and the electrochemical Fenton treatment. The reaction treatment is separated into two half-cells. Ferrous ion is generated from iron in anodic half-cell by electrolysis (Eq. 2-9), whereas water is reduced in the cathodic half-cell. H_2O_2 is pumped into the anodic half-cell. In the cathodic half-cell, water is reduced on a graphite cathode (Eq. 2-10).



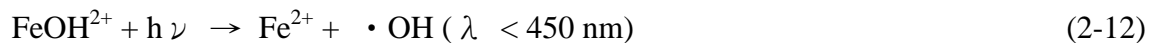
The AFT has several significant advantages over Fenton treatment and electrochemical Fenton treatment. First, the ferrous ion is delivered into the treatment system by electrolysis, overcoming the difficulty of handling hygroscopic ferrous salt. Secondly, the pH of the treatment effluent can be partially neutralized by combining effluents from the anodic and cathodic half-cells of the AFT. Thirdly, the Fenton reaction can occur in an optimal pH environment in the anodic half-cell, keeping the treatment efficiency high [63].

2.4.3 Heterogeneous Fenton treatment

Homogeneous Fenton processes (such as AFT, electro-Fenton) have a significant disadvantage: homogeneously catalyzed reactions need 50-80 mg L⁻¹ of iron ions in solution, which is quite above 2 mg L⁻¹ in treated water regulated by the European Union directives [67]. In addition, the removal/treatment of the sludge-containing iron ions (the precipitate of ferric hydroxide) at the end of the treatment require large amount of chemicals and increase treatment cost. To overcome the disadvantages, the use of heterogeneous catalysts usually called heterogeneous Fenton is developed. Iron oxides such as goethite [81], zeolite [77] and magnetites are effective catalysts for catalytic H₂O₂ oxidation. However, it has been demonstrated that iron oxide catalysts lose their activity because of leaching effects of metallic catalysts under acidic condition. The leaching and deactivation of the catalyst are still challenges for developing advantageous catalyst for oxidation of wastewaters. Even catalysts used in heterogeneous Fenton treatment can be easily removed from the effluent, Mantzavinos (2003) reported that homogeneous Fenton process is more effective than heterogeneous ones [73].

2.4.4 Photo-Fenton treatment

The degradation rate of target compound is enhanced with an irradiation applied and the process is called photo-Fenton reaction. The photo-Fenton reaction, a combination of H₂O₂ and UV irradiation less than 450 nm with Fe³⁺ or Fe²⁺, is a promising treatment process which can produce more •OH in comparison to Fenton reaction. When Fe³⁺ ions are added to the system, the Fe(OH)²⁺ complex is formed at the acidic environment as shown in Eq. 2-11. The positive effect of irradiation on the degradation rate is due to the photoreduction of Fe(OH)²⁺ to Fe²⁺ as shown in Eq. 2-12 [68]. Subsequently, the regenerated Fe²⁺ can further react with more H₂O₂ molecules, produce new •OH as Eq. 2-1 and form a reaction cycle [32,33]. It has three advantages, i.e. (1) facilitate the Fenton treatment without continuous addition of external Fe²⁺; (2) reduce the ferric hydroxide sludge formation [28,33]; (3) one mole of H₂O₂ can produce two moles of •OH according to Eq. 2-13 [28,33]. The more •OH generated than Fenton reaction is considered to be responsible for high efficiency of the photo-Fenton process. With irradiation of a light source, the performance of photo-Fenton was reported to be positively enhanced compared to the Fenton reaction [27,28,66].



In the past, the photo-Fenton treatment has shown very high efficiency in the mineralization of biorefractory pesticides and other organic pollutants [13,24-28].

Recently, it has been proven that the irradiation of Fe^{3+} with H_2O_2 enhances the reaction rate of oxidant production through the involvement of $\cdot\text{OH}$ and high valence iron intermediates responsible for the direct attack to organic matter [26,68]. The advantages of the photodegradation process as an oxidative treatment are economical, rapid degradation and simple handling. Therefore, the photocatalytic reaction would be applied to wastewater treatment as a new developing methodology for reducing levels of pesticides and endocrine disrupting chemicals. However, high electrical energy demand and chemical reagents consumption are major drawbacks of photo-Fenton process [31]. In order to reduce the operational cost and achieve high performance, the experimental conditions, i.e. pH, temperature and dosages of reactants, must be optimized.

2.5 Factors affecting photo-Fenton process

Many studies have shown the effectiveness of photo-Fenton process in the decomposition of various refractory organic compounds [27,28,33,68,82]. In order to achieve high removal efficiency, the optimal operation conditions must be investigated. This would be an extremely difficult and time consuming work due to involvement of several factors such as wavelength and intensity of light source, the dosages of H_2O_2 and Fe^{3+} , $\text{H}_2\text{O}_2/\text{Fe}^{2+}$ ratio, the initial pH, reaction temperature and concentration of target compound. The previous research works remarked in literature generally shows the following facts:

(1) Wavelength of irradiation:

As shown in Eq. 2-12, photo-Fenton reaction can only be activated with

wavelength of irradiation up to 450 nm. The performance of photo-Fenton process is highly related to the wavelength of irradiation as the quantum yield of Eq. 2-12 is wavelength dependent. The quantum yields of $\cdot\text{OH}$ and ferrous ion formation decrease with the increasing in wavelength of irradiation. For example, the quantum yields of $\cdot\text{OH}$ are 0.14 and 0.017 at 313 nm and 360 nm, respectively [83]. On the other hand, the quantum yield of Fe^{2+} formation is about 1.0-1.2 with irradiation wavelength in the range of 250-450 nm (UV/visible) and decreases with wavelength greater than 450 nm [84].

(2) Light intensity:

Light intensity is one of the few parameters that affect the performance of photo-Fenton reaction on target compounds. The organic conversion in the presence of UV irradiation ($\lambda < 400$ nm) in the literature is found to be linear to the incident radiant flux. Glatzmaier *et al.* (1990) and Glatzmaier (1991) reported that the decomposition rates of dioxin and polychlorinated biphenyls increased with increasing intensity of photons [85,86].

(3) H_2O_2 dosage:

Several researchers have reported that higher dosage of H_2O_2 increased the extent of TOC degradation [71]. However, the degradation efficiency decreases with further increase of H_2O_2 dosage. This effect can be explained by the fact that overdosed H_2O_2 competes the $\cdot\text{OH}$ with the organic matter (Eq. 2-14) and the less oxidizing $\text{HO}_2\cdot$ generated reduces the amount of highly oxidative $\cdot\text{OH}$ present in the system (Eq. 2-15) [16,42,74].



(4) Fe^{3+} dosage:

The Fe^{3+} concentration has a positive effect on the oxidation performance and higher Fe^{3+} concentration stimulate H_2O_2 decomposition. Further increase in Fe^{2+} concentrations results in decrease in removal efficiency due to scavenging effects of Fe^{2+} regenerated on $\cdot\text{OH}$ as shown in Eq. 2-16. The optimal initial Fe^{3+} concentration depends on the initial H_2O_2 concentration as well as waste composition [71,74,78,82,87]. Therefore, determination of their optimal ratio is necessary for better treatment performance.



(5) $\text{H}_2\text{O}_2/\text{Fe}^{3+}$ ratio:

The performance of photo-Fenton reaction is significantly affected by reagent dosages, i.e. $\text{H}_2\text{O}_2/\text{Fe}^{3+}$ ratio. Several researchers reported that the optimum Fe^{3+} dosage depends on H_2O_2 dosage as well as pollutant composition [26,28,88]. Xu *et al.* (2007) reported that optimum $\text{H}_2\text{O}_2/\text{Fe}^{3+}$ ratio was found to be 10 for solar photo-Fenton treatment of wastepaper pulp effluent [26]. Torrades *et al.* (2008) also indicated that optimum $\text{H}_2\text{O}_2/\text{Fe}^{3+}$ ratio for Fenton and photo-Fenton treatment of wheat straw black liquor was 12 [28]. As different authors reported different values of $\text{H}_2\text{O}_2/\text{Fe}^{3+}$ ratio, it is important to determine the optimum $\text{H}_2\text{O}_2/\text{Fe}^{3+}$ ratio for better removal efficiency.

(6) pH:

An acidic pH is required for the photo-Fenton process with an optimal value often around 3 [27]. The decrease of oxidation yield of the process at higher pH values (pH > 3) is due to the precipitation of Fe³⁺ as Fe(OH)₃, which could hinder the reaction between Fe³⁺ and H₂O₂. Under excess H⁺ at low pH condition (pH < 3), H⁺ reacts with •OH via Eq. 2-17 and produce water [33]. The consumption of •OH decreases the oxidation performance of target compounds. It has been widely reported in the literature that the optimum pH for the photo-Fenton reaction is around 3 owing to the concentration of Fe(OH)²⁺ (dominant Fe³⁺ species formed in the photo-Fenton reaction at pH 2-3) is highest at pH 3 as shown in Fig. 2-3 [14,25]. For example, Bautista *et al.* (2007) find out the optimal pH at 3 in the treatment of cosmetic wastewaters [74]. Oliveira *et al.* (2006) showed that the optimum pH is close to 3-3.5 in the degradation of 2,4-dichlorophenol, since oxidation rate decreases at high pH values. Below pH 3, the use of more acid seems to be useless [87]. Low pH values of the effluents limit the application of the photo-Fenton process while its combination with biological processes, since acidification of influent and neutralization of effluents increase the process cost.



(7) Temperature:

Higher temperature can increase the extent and rate of TOC degradation under low reagent dosage or inadequate reagent ratios [28,68]. Santos *et al.* (2007) reported that higher temperature (70°C) produces a faster reaction rate in decomposition of phenolic mixtures [69].

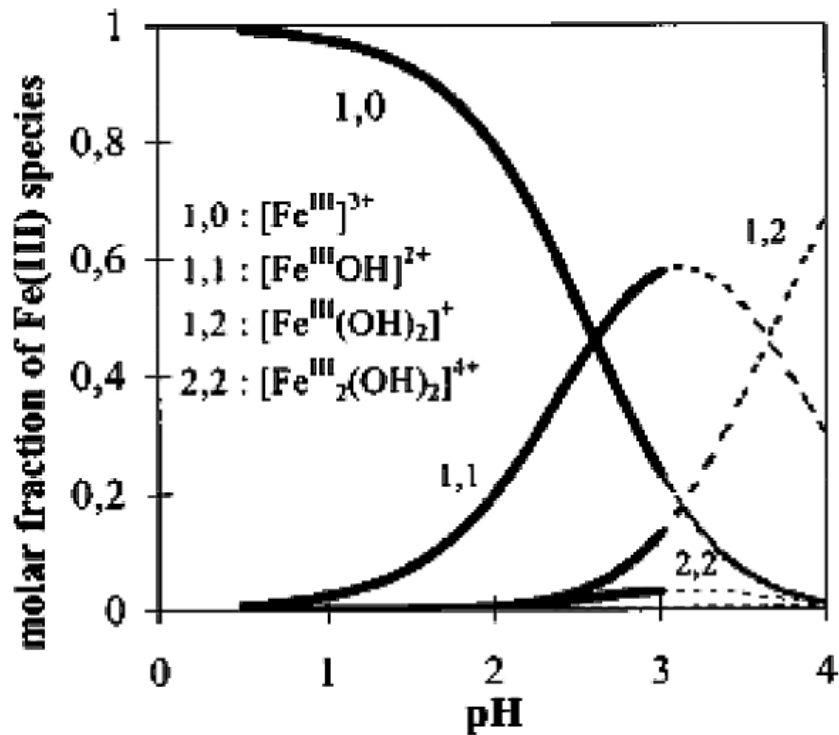


Fig. 2-3. Speciation of Fe(III) species in water at 1×10^{-3} M total iron, ionic strength 0.1 M, and 25°C. Dashed line regions are supersaturated with respect to amorphous ferricoxyhydroxides [89].

(8) Concentration of pollutant

Initial concentration of target compounds is the most important parameter affecting the removal efficiency in the Fenton reaction. Catalkaya and Kargi (2007) indicated that mineralization efficiencies obtained at low pesticide concentrations were higher than those obtained at high pesticide concentrations [16].

2.6 Integrating AOPs and biological process in water and wastewater treatment

Photo-Fenton and other AOPs for wastewater treatment have shown their

worthiness in the field of toxic compounds elimination, but their use remains limited due to high operation costs, high electrical energy demand in generation of UV irradiations, chemical reagents consumption [66]. Specially, the production of photons with artificial light sources requires an important energy input. A step forward in the cost reduction of pesticide bearing wastewater treatment could be achieved by combining the AOPs with a conventional biological treatment [11,12,15,40-42]. The combination of the photo-Fenton process (as a pretreatment) followed by biological treatment has great potential for enhancing the biodegradability of pesticide contaminated wastewater [12,34,43,44]. Nevertheless, incomplete oxidation may result the formation of more toxic intermediates than the parents, which can decrease the biodegradability [35,44]. Therefore, the biodegradability and toxicity assessment of degradation intermediates are essential for evaluating the success of the photo-Fenton process as a pretreatment for pesticide bearing wastewater treatment. In the integrated processes, the variation of biodegradability as a function of the chemical reaction conditions is needed to be determined. Methods for measuring biodegradability, commonly used, are BOD₅ and BOD₅/COD or BOD₅/TOC. Then, a classical biological method can be employed to deal with pretreated effluent. Hence, the combination of photo-Fenton as a preliminary treatment, followed by a biological treatment can be considered as an appropriate methodology for the complete removal of carbofuran from the aqueous system.

2.7 Experimental design methodology

Comparing with biological treatment, the major limitation of AOPs is their relatively high operational costs for complete oxidation of organic compounds [34,35].

In order to reduce the operational cost and achieve high performance of AOPs, the experimental conditions, i.e. pH, temperature and dosages of reactants as shown in Table 2-6, must be optimized. The traditional approach of changing one variable at a time while fixing all other variables constant to investigate the effect of parameter on the response is a time consuming method especially while multifactor and several responses considered. Moreover, this approach has limitation in assuming that various parameters don't have interacted effect between variables. To overcome these drawbacks, the statistical based optimization methodology which consider interaction effect between variables, such as the CCD, is appropriate to be applied in a multifactor system with minimum number of well-chosen experiments [31,36].

The CCD is a modern experimental design approach, which has been widely used in several applications [13,37-39] to fit the experimental data and develop a statistically significant second-order polynomial equation. The CCD is a star design including factorial design, axial or star point and central point (three to five replicates). The total number of experiments (N) required for CCD is determined as per the Eq. 2-18 [39,90,91], where K represents the number of independent variables and n_c is the central point. Due to the varying units of the different factors (actual values), independent variables are normalized in the form of dimensionless coded values ($-\alpha$, -1, 0, 1, α), which is also useful to obtain more accurate estimate of the regression coefficient and reduce the interrelationship between linear and quadratic terms [87,92]. The value of α was calculated by Eq. 2-19. The transformation of natural variable into coded value (-1 and +1) is made according to the Eq. 2-20 [76].

$$N = 2^K + 2K + n_c \quad (2-18)$$

Table 2-6. The independent and dependent variables of experimental design selected in Fenton processes.

Method	Target compound	Experimental condition	Independent variable	Dependent variable	Reference
Fenton	Orange II	pH 3 2 h	Temp (10-64°C) H ₂ O ₂ (102-646 mg L ⁻¹) H ₂ O ₂ :Fe ²⁺ (4-20)	Color TOC	[93]
Fenton	Olive oil processing wastewater	4 h	pH (3-5) H ₂ O ₂ :Fe ²⁺ (1.67-8.33) Wastewater concentration (40-100%)	COD Color Aromatocity Total phenolics	[37]
Fenton	2,4-dichlorophenol	pH 3.5 3 h	Temp (20-40°C) H ₂ O ₂ (200-212 mg L ⁻¹) Fe ²⁺ (3.5-6.5 mg L ⁻¹)	2,4-dichlorophenol (5, 10, 20 min)	[87]

Table 2-6. The independent and dependent variables of experimental design selected in Fenton processes (continued)

Method	Target compound	Experimental condition	Independent variable	Dependent variable	Reference
Fenton	Diuron	pH 4.2 Temp 23-25°C 4 h	Diuron (1-25 mg L ⁻¹) H ₂ O ₂ (1.5-340 mg L ⁻¹) Fe ²⁺ (0.25-56 mg L ⁻¹)	TOC Diuron Adsorbable organic xalogen (AOX)	[16]
Photo-Fenton	Cellulose bleaching effluents	Sun light pH 3 15 min 400 nm	Temp (30-70°C) H ₂ O ₂ (1000-10000 mg L ⁻¹) Fe ²⁺ (50-450 mg L ⁻¹)	TOC	[31]
Photo-Fenton	2-chlorophenol	pH 2.5 30 min	H ₂ O ₂ (200-700 mg L ⁻¹) Fe ²⁺ (3-87 mg L ⁻¹)	TOC	[68]
Photo-Fenton	Imidacloprid	365 nm pH 2.8	H ₂ O ₂ (98-452 mg L ⁻¹) Fe ²⁺ (11-39 mg L ⁻¹)	TOC	[82]

$$\alpha = (2^K)^{1/4} \quad (2-19)$$

$$\frac{U_i}{\alpha} = \frac{X_i - (X_{i,\max} + X_{i,\min})/2}{(X_{i,\max} - X_{i,\min})/2} \quad (2-20)$$

where U_i and X_i are the natural and coded values of independent variables. $X_{i,\max}$ and $X_{i,\min}$ are the maximum and minimum values of independent variables, respectively.

RSM is used along with different type of experiment designs, i.e. factorial design and CCD, for optimization by least squares technique to assess the conditions that could yield the most desirable response [16,31,37]. A full second-order polynomial equation and its corresponding regression coefficients for two factors are as shown in Eq. 2-21.

$$Y = \beta_0 + \beta_1 X_1 + \beta_2 X_2 + \beta_{11} X_1^2 + \beta_{22} X_2^2 + \beta_{12} X_1 X_2 \quad (2-21)$$

where Y represents predicted response; X_1 and X_2 represents independent variables; the set of regression coefficients consist the intercept (β_0), linear (β_1, β_2), interaction (β_{12}) and quadratic coefficients (β_{11}, β_{22}) [37].

For the purpose of applying effectively AOPs in the wastewater treatment, the optimization of operational parameters plays an important role in target compounds degradation. For such a goal, experimental design along with RSM has been used extensively in several applications to generate a quadratic model and yield the most desirable response that considers the synergistic and antagonist effects between the variables [13,31,93]. Besides, the response surface plot can be constructed to locate the optimum point of the multifactor system [16].

Chapter 3

Materials and methods

3.1 Chemical reagents

Carbofuran was obtained from Shida Chemical Industries (Taoyuan, Taiwan) and was used as received (HPLC grade > 98% purity). Titanium sulfate (TiSO_4 , 5% w/w) was purchased from Nacalai Tesque (Japan) and H_2O_2 (33%, w/w) was supplied by Panreac Chemicals (Spain). Stock solution of Fe^{3+} (1000 mg L^{-1}) was prepared by dissolving ferric sulfate (Yakuri Pure Chemicals, Japan) in double distilled water. The HPLC grade methanol was used in carbofuran analysis. All other chemicals were reagent grade and the solutions were prepared using double distilled water.

3.2 Experimental apparatus

Fig. 3-1 shows the schematic diagram of the experimental setup used for carbofuran degradation. A 1.6 L double-walled reactor was used in all experiments. Several ports were provided on the reactor for feeding the reactants and sampling the solution. Moreover, pH and temperature probes were fixed in the reactor. A Teflon-coated stirrer was installed in the reactor to mix the solution at 175 rpm. During the experiment, H_2O_2 was added continuously into reactor at a flow rate of 1 mL min^{-1}

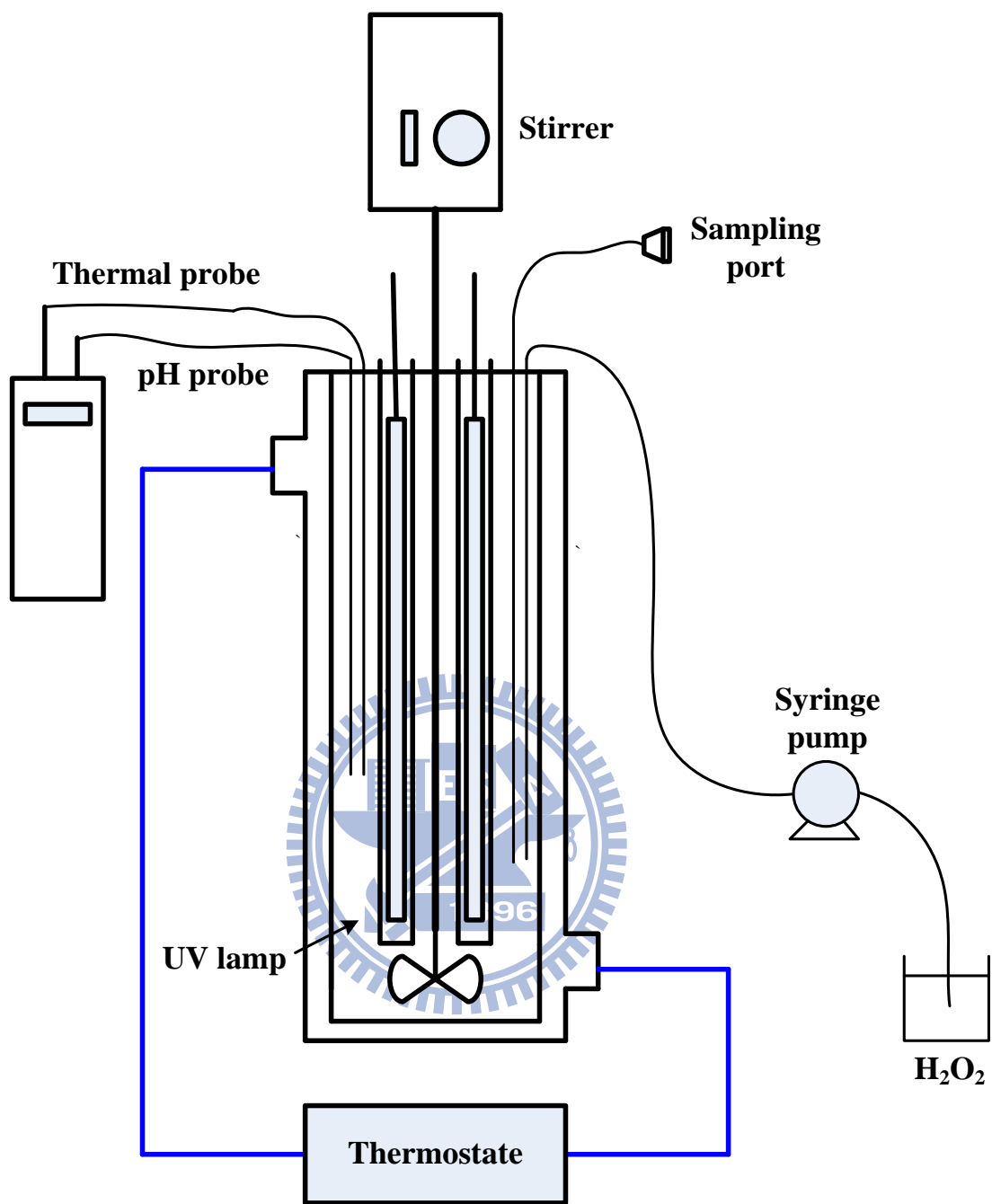


Fig. 3-1. Schematic diagram of the experimental setup.

with a syringe pump. Two 8-W monochromatic UV lamps of 312 nm (with emission range between 280 nm and 360 nm) were placed axially in the reactor and kept in place with a quartz sleeve; the UV intensity of one 8-W UV lamp at 312 nm is $60 \mu\text{W cm}^{-2}$. The reaction temperature was maintained at $25 \pm 1^\circ\text{C}$ during all the experiments by using a water bath.

3.3 Experimental overview

The present study was divided into three stages as shown in Fig. 3-2. In stage 1, the effects of operating parameters including irradiation time, carbofuran concentration, pH, H_2O_2 dosage rate and Fe^{3+} dosage were investigated. The carbofuran removal was fitted using the pseudo-first order reaction model to determine the kinetic parameters. Furthermore, a number of control experiments including H_2O_2 , Fe^{3+} , UV, $\text{Fe}^{3+} + \text{H}_2\text{O}_2$, UV + Fe^{3+} and UV + H_2O_2 were carried out to evaluate the efficiency of each process in carbofuran degradation and mineralization.

The CCD along with RSM was employed to find out the favorable reagent dosages for carbofuran degradation under the photo-Fenton process in the stage 2. The effects of H_2O_2 dosage rate ($1\text{-}10 \text{ mg L}^{-1} \text{ min}^{-1}$) and Fe^{3+} dosage ($1\text{-}100 \text{ mg L}^{-1}$) were evaluated and the second-order polynomial equations in terms of carbofuran and DOC removals and BOD_5/DOC ratio with different reaction times were developed.

Stage 3 was intended to evaluate the potential of the photo-Fenton process as a pretreatment of carbofuran under favorable reagent dosages obtained in stage 2. BOD_5 , BOD_5/COD ratio, average oxidation state (AOS), carbon oxidation state (COS) and Microtox[®] test were used to investigate the variations of toxicity and biodegradability during the degradation and mineralization of carbofuran and to assess the appropriate

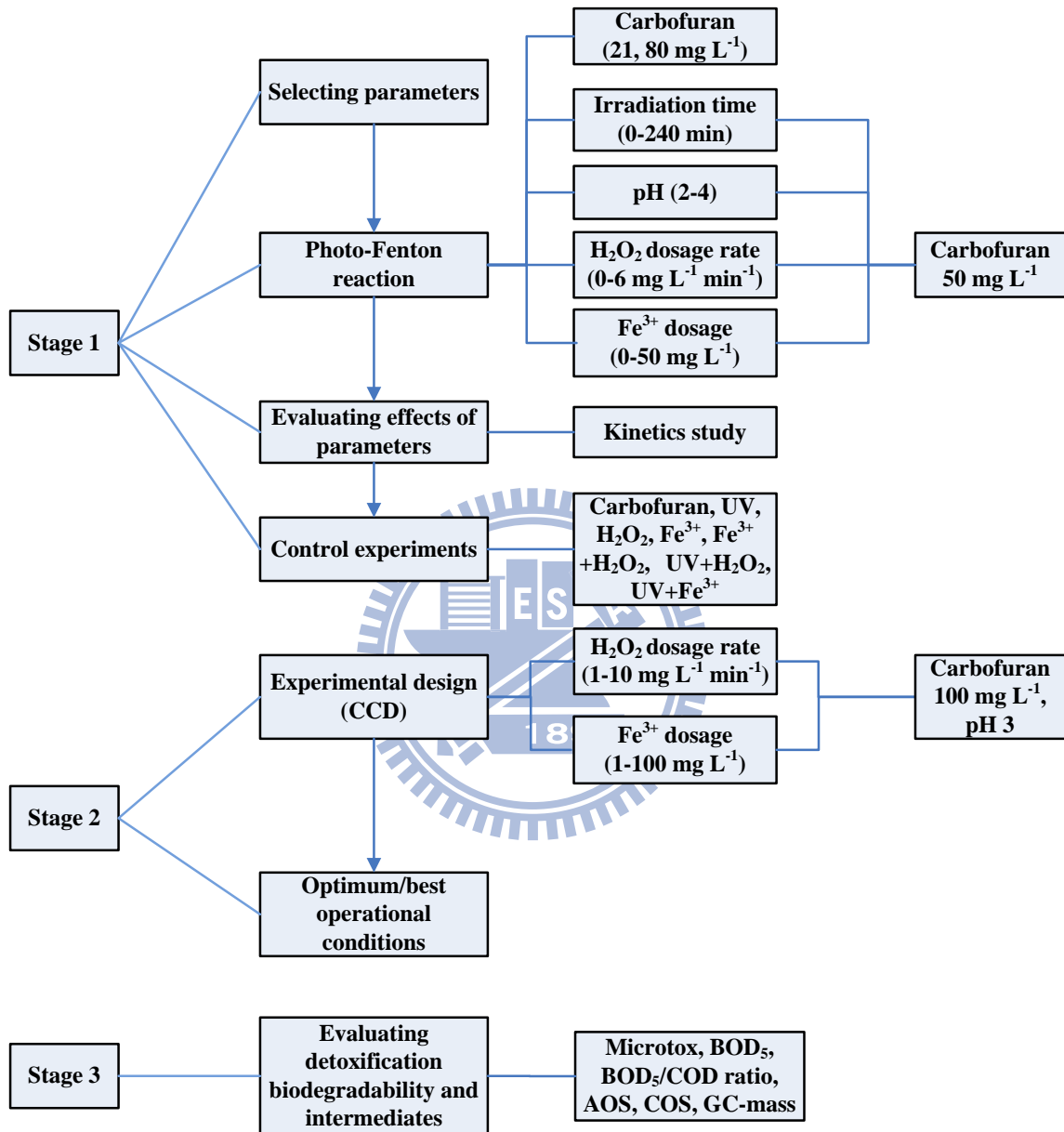


Fig. 3-2. Flowchart of the research.

time for coupling the photo-Fenton process with biological treatment. Moreover, the intermediates of carbofuran produced during the photo-Fenton treatment were identified by GC/MS.

3.4 Experimental procedure

Stock solution of carbofuran was prepared by dissolving 200 mg of carbofuran in 1 L double distilled water. Exactly 1 L of diluted carbofuran solution corresponding to a required initial concentration was added into the reactor. The initial pH was adjusted to a pre-determined level using 0.1 N H₂SO₄. Subsequently, a designed quantity of Fe³⁺ was pumped into the reactor and the contents were mixed thoroughly. The UV lamps were turned on for 15 min before experiment then mark the starting point of the experiment. The H₂O₂ was simultaneously added into the reactor at a constant flow rate. At regular time intervals, 8 mL of sample was withdrawn from the reactor and filtered through a 0.45 μm membrane filter paper. Finally, the samples were analyzed for residual carbofuran, BOD₅, COD, DOC, H₂O₂ and carbofuran intermediates. The experimental conditions for the carbofuran degradation are shown in Table 3-1.

3.5 Experimental design and data analysis

In order to correlate the independent variables, i.e. H₂O₂ dosage rate and Fe³⁺ dosage, and dependent variables, i.e. carbofuran and DOC removals and BOD₅/DOC. Predetermined ranges of independent variables, i.e. H₂O₂ dosage rate (1, 2.3, 5.5, 8.7 and 10 mg L⁻¹ min⁻¹) and Fe³⁺ dosage (1, 15, 51, 86 and 100 mg L⁻¹), were selected for CCD. Three replications of central points (runs 4, 5, 6) were selected for CCD to check the reproducibility of data and evaluate the experimental error of the results and total 11

Table 3-1. Experimental conditions for carbofuran degradation

Experiments	carbofuran concentration (mg L ⁻¹)	pH	Reaction time (min)	H ₂ O ₂ dosage rate (mg L ⁻¹ min ⁻¹)	Fe ³⁺ dosage (mg L ⁻¹)	Sampling time (min)
Effect of irradiation time	50	3	240	0.1	5	0, 5, 10, 15, 20, 30, 40, 60, 80, 100, 120, 160, 200 and 240
Effect of pH		2, 2.5, 3, 3.5 and 4		4	35	
Effect of H ₂ O ₂ dosage rate	50	3	120	0, 0.5, 1.25, 4, 5 and 6	35	0, 5, 10, 15, 20, 30, 40, 60, 80, 100 and 120
Effect of Fe ³⁺ dosage		3		0.8 and 4	5, 20, 35 and 50	
Chemical degradability	50	3	120			0, 5, 10, 15, 20, 30, 40, 60, 80, 100 and 120
control				0	0	
UV				0	0	
H ₂ O ₂				4	0	
Fe ³⁺				0	35	
Fe ³⁺ + H ₂ O ₂				4	35	
UV + H ₂ O ₂				4	0	
UV + Fe ³⁺				0	35	
Experimental design				1, 2.3, 5.5, 8.7 and 10	1, 15, 51, 86 and 100	
Investigation of toxicity, biodegradability and intermediates	100	3	60	5.4	59	0, 5, 10, 15, 20, 30 45 and 60

photo-Fenton experiments shown in Table 3-2 were randomized by the statistical software to minimize systematic errors. The coded and natural levels of independent variables for the experimental design are shown in Table 3-1. Due to the varying units of the different factors (actual values), H_2O_2 dosage rate and Fe^{3+} dosage were normalized in the form of dimensionless coded values from $-\alpha$ to α , which is also useful to obtain more accurate estimate of the regression coefficients and to reduce the interrelationship between linear and quadratic terms [92]. In this study, the α coded value of a two factor CCD was 1.414. A second-order polynomial equation and its corresponding regression coefficients were obtained from the experimental data using the MINITAB[®] 14 statistical software.

3.6 Analytical measurements

The analysis included measurements of pH, carbofuran concentration, H_2O_2 concentration, DOC, BOD_5 , COD, Microtox[®] test and intermediates. The description of each measurement was summarized as follows:

3.6.1 Analysis of carbofuran concentration

Carbofuran concentration in the samples was analyzed by the high performance liquid chromatography (HPLC) (Hitachi Co., Japan) equipped with a Hitachi L-2420 UV detector and a RP-18 GP 250 separation column (250 mm \times 4.6 mm i.d., Kanto Chemicals, Japan). Exactly 20 μL of sample was injected manually and analyzed at 280nm. The mobile phase, composed of methanol and water (50:50, v/v), was pumped at a flow rate of 1 mL min^{-1} . Under these separation conditions, the retention time of

Table 3-2. Experimental design along with coded and natural levels for two independent variables.

Experimental run	x_1^1		x_2^2	
	Coded value	Natural value (mg L ⁻¹ min ⁻¹)	Coded value	Natural value (mg L ⁻¹)
1	-1	2.3	-1	15
2	-1	2.3	1	86
3	0	5.5	1.414	100
4	0	5.5	0	51
5	0	5.5	0	51
6	0	5.5	0	51
7	0	5.5	-1.414	1
8	1	8.7	1	86
9	1.414	10.0	0	51
10	-1.414	1.0	0	51
11	1	8.7	-1	15

¹ x_1 , H₂O₂ dosage rate (mg L⁻¹ min⁻¹)

² x_2 , Fe³⁺ dosage (mg L⁻¹)

carbofuran was observed around 12 min. The method detection limit (MDL) for analysis of carbofuran is 0.16 mg L^{-1} . The percentage carbofuran removed was expressed as Eq. 3-1, where C_0 is the initial concentration of carbofuran (mg L^{-1}) and C_t is the residual concentration of carbofuran at reaction time t (mg L^{-1}).

$$\text{Carbofuran removal (\%)} = (1 - C_t/C_0) \times 100\% \quad (3-1)$$

3.6.2 Analysis of H_2O_2 concentration

For determining the residual H_2O_2 concentration, the samples were mixed with 5% titanium sulfate solution (the volume ratio of H_2O_2 sample to titanium sulfate solution was 10:1 v/v) and analyzed using a spectrophotometer (Hitachi U-3010, Japan) at 412 nm [94]. The residual H_2O_2 was measured for two purposes: (1) to make sure that the H_2O_2 supplied in the system is sufficient and (2) to compare the residual H_2O_2 with the variation of carbofuran concentration and DOC removal. The MDL for analysis of H_2O_2 is 0.04 mg L^{-1} .

3.6.3 Analysis of DOC concentration

Carbofuran mineralization was estimated in term of DOC concentrations. A TOC analyzer (O.I. Analytical Model 1030) was used for measuring the DOC of the samples. For the DOC measurements, potassium phthalate solutions ($5\text{-}80 \text{ mg L}^{-1}$) were used as the calibration standard. The MDL for analysis of DOC is 0.06 mg L^{-1} . The DOC removal (%) of carbofuran was calculated by using Eq. 3-2, where DOC_0 is the initial DOC value of carbofuran (mg L^{-1}) and DOC_t is the residual DOC value of carbofuran at reaction time t (mg L^{-1}).

$$\text{DOC removal (\%)} = (1 - \text{DOC}_t/\text{DOC}_0) \times 100\% \quad (3-2)$$

3.6.4 Microtox[®] test

Acute toxicity of initial carbofuran solution and the samples collected at different time periods of the photo-Fenton reaction were measured by the Microtox[®] test using *Vibrio fischeri* strain. Microtox[®] test was performed using a model M500 analyzer and standard procedures recommended by the Microbics Corporation, USA. Toxicity is generally expressed as EC₅₀ value, i.e. the concentration of sample that causes a 50% reduction of the bioluminescence (*Vibrio fischeri*). In this paper, toxicity was evaluated at 5 and 15 min from the time of mixing at various dilutions with the *Vibrio fischeri*. Before conducting the Microtox[®] test, the pH value of the samples was adjusted to 7. Moreover, the EC₅₀ value used in this study was converted to toxicity unit (TU) using Eq. 3-3. Thus, TU is inversely proportional to EC₅₀ value, lower EC₅₀ value relates to a higher TU.

$$\text{TU} = 100/\text{EC}_{50} \quad (3-3)$$

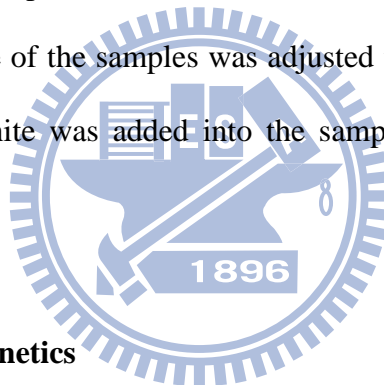
3.6.5 Identification of intermediates

The major carbofuran degradation intermediates formed during the photo-Fenton reaction were identified using the GC/MS technique. A mixture of sample and dichloromethane (5:1 v/v) was shaken vigorously in a rotary shaker at 150 rpm for 30 min, and subsequently, analyzed in a Shimadzu GC/MS-QP2010 equipped with a HP-5 capillary column (30 m × 0.25 mm i.d., thickness of 0.25 μm). Helium was used as the carrier gas at a flow rate of 1.5 mL min⁻¹. The GC oven temperature was programmed as

follows: initially held at 80°C for 2 min, increased to 210°C at a rate of 10°C min⁻¹ and held for 3 min, then raised from 210 to 310°C at a rate of 30°C min⁻¹ and finally held at 310°C for 2 min. The injector and detector temperatures were maintained at 220 and 250°C, respectively. The mass spectrometer was operated in the full-scan electron-impact (EI) mode at 70 eV.

3.6.6 Other analytical techniques

The pH and temperature were monitored continuously by a pH and temperature meter (Suntex TS-2), respectively. In the biodegradability test, variations in BOD₅ and COD at different stages of the photo-Fenton reaction were measured as per the Standard Methods [95]. The pH value of the samples was adjusted to 7 for the analysis of BOD₅ and sodium hydrogen sulphite was added into the samples to remove residual H₂O₂ before analysis of COD.



3.7 Carbofuran removal kinetics

The pseudo-first order reaction model as shown in Eq. 3-4 was used to study the carbofuran removal kinetics, where, C_0 and C_t are the concentrations of carbofuran (mg L⁻¹) at reaction times zero and t , respectively. k_{app} is the apparent rate constant (min⁻¹) and t is the reaction time (min). The rate constants were estimated based on the linear plot of $\ln(C_0/C_t)$ versus t .

$$\ln(C_0/C_t) = k_{app}t \quad (3-4)$$

Chapter 4

Results and discussions

There were numbers of well chosen experiments carried out in this study. Based on the results obtained, this chapter is divided into ten major sections listed as follows:

- 4.1 Effect of irradiation time on carbofuran degradation
- 4.2 Effect of carbofuran concentration on carbofuran degradation
- 4.3 Effect of initial pH on carbofuran degradation
- 4.4 Effect of H₂O₂ dosage rate on carbofuran degradation
- 4.5 Effect of Fe³⁺ dosage on carbofuran degradation
- 4.6 Chemical degradability of carbofuran
- 4.7 CCD of experiments for the photo-Fenton process
- 4.8 Degradation pathway
- 4.9 Toxicity and oxidation state assessment
- 4.10 Biodegradability assessment

Many studies have shown that the performance of the photo-Fenton process is highly related to the operating parameters. In order to achieve high removal efficiency, the optimum operation conditions must be investigated. Therefore, experiments were carried out to study the effects of operating parameters including irradiation time, carbofuran concentration, pH, H₂O₂ dosage rate and Fe³⁺ dosage on the degradation and mineralization of carbofuran and their results are described in sections 4.1-4.5.

Control experiments such as H_2O_2 , Fe^{3+} , UV, $\text{Fe}^{3+} + \text{H}_2\text{O}_2$, UV + Fe^{3+} and UV + H_2O_2 were also carried out to evaluate the efficiency of each process and their results are summarized in section 4.6. The favorable reagent dosages obtained by CCD along with RSM were discussed and reported in section 4.7. The degradation pathway of carbofuran degradation under favorable reagent dosages is proposed and discussed in section 4.8 based on the intermediates identified. Finally, the appropriate time for coupling the photo-Fenton process with biological treatment has been discussed according to the variations of toxicity and biodegradability at favorable reagent dosages in sections 4.8 and 4.9, respectively.

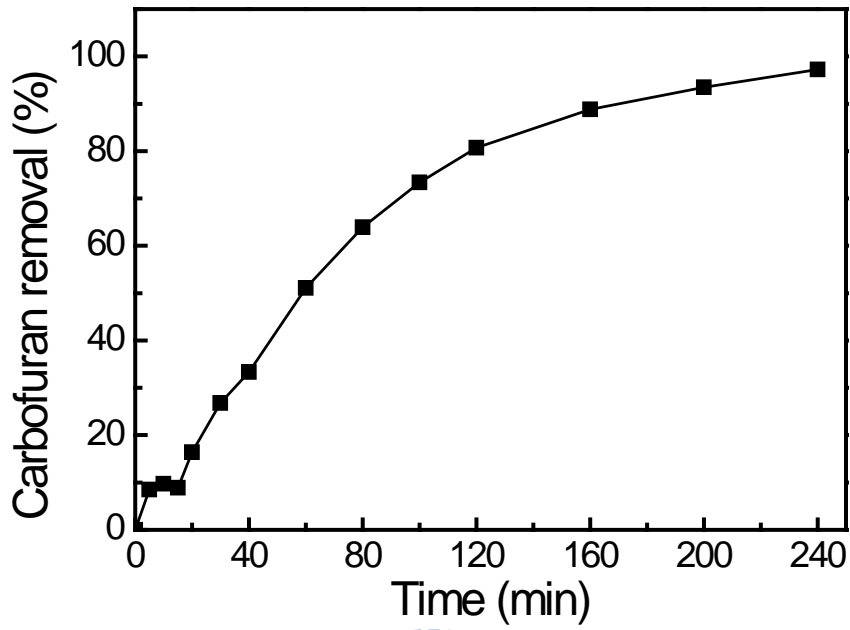
4.1 Effect of irradiation time on carbofuran degradation

The effect of irradiation time was evaluated under an initial carbofuran concentration of 50 mg L^{-1} and pH 3 with the Fe^{3+} dosage at 5 mg L^{-1} and H_2O_2 dosage rate at $0.1 \text{ mg L}^{-1} \text{ min}^{-1}$. The profiles of carbofuran and DOC removals are shown in Fig. 4-1. After 240 min, carbofuran and DOC removals were reached around 97% and 42%, respectively. These results indicate that even with low dosage of Fe^{3+} and dosage rate of H_2O_2 , it is possible to obtain higher carbofuran degradation as well as its mineralization. However, no significant increase in the carbofuran removal was observed between 120-240 min (less than 10%). The DOC removal profile indicates that carbofuran mineralization rate could be enhanced by increasing the UV irradiation time.

4.2 Effect of carbofuran concentration on carbofuran degradation

In order to investigate the effect of carbofuran concentration for the photo-Fenton degradation of carbofuran, the experiments were repeated at 21 and 80 mg L^{-1}

(a)



(b)

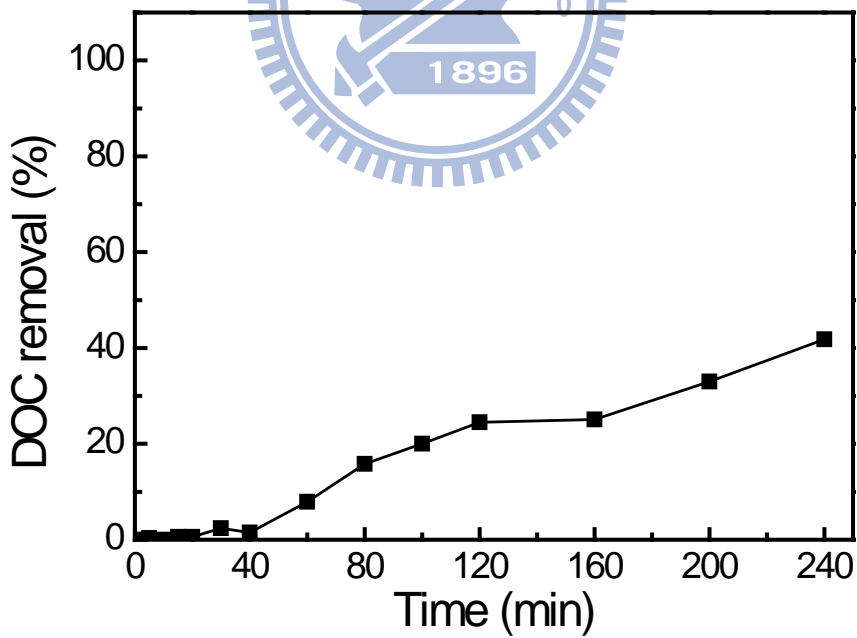
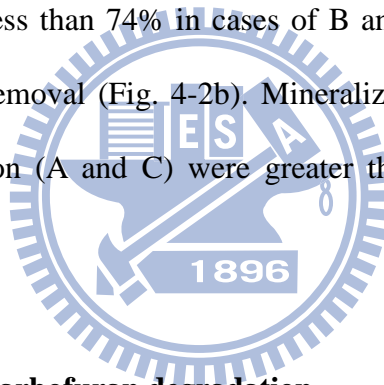


Fig. 4-1. The profiles of (a) carbofuran (b) DOC removals with time (Fe^{3+} dosage at 5 mg L^{-1} , H_2O_2 dosage rate at $0.1 \text{ mg L}^{-1} \text{ min}^{-1}$ and pH 3).

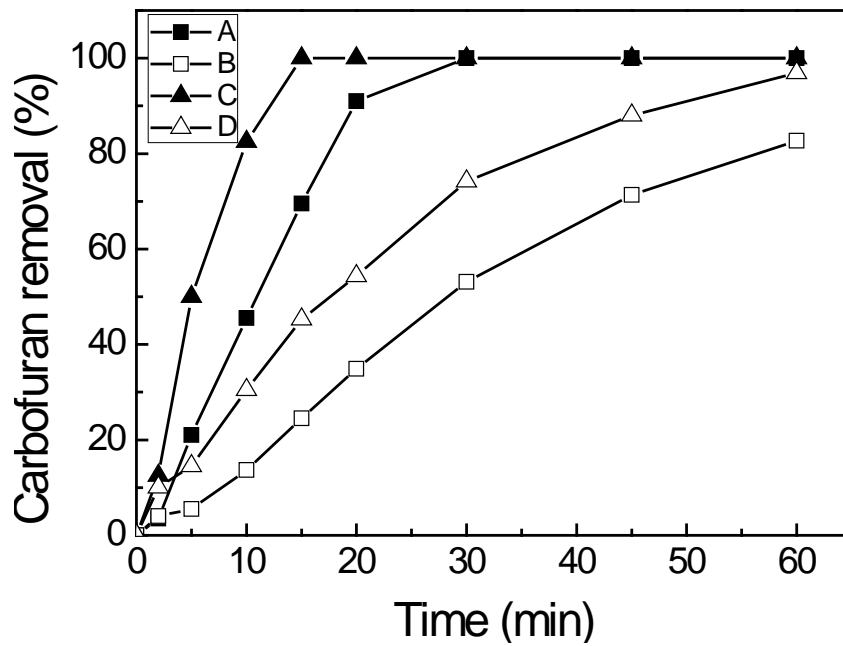
carbofuran concentration with two different reagent dosages at pH 3, i.e. H₂O₂ dosage rate of 1.3 mg L⁻¹ min⁻¹, Fe³⁺ dosage of 10 mg L⁻¹ and H₂O₂ dosage rate of 1.3 mg L⁻¹ min⁻¹, Fe³⁺ dosage of 40 mg L⁻¹. Fig. 4-2 shows the trend of degradation and mineralization of carbofuran with the reaction time. It can be noticed in Figs. 4-2a and b that carbofuran concentration has great negative effect on carbofuran degradation and mineralization, regardless of the amount of H₂O₂ dosage rate and Fe³⁺ dosage employed. The reduction of carbofuran removal accompanies with the increase of carbofuran concentration. In addition, carbofuran removal increased with increasing of limiting factor Fe³⁺ dosage at high carbofuran concentration (Fig. 4-2a). After 30 min of reaction, carbofuran were completely removed in cases of A and C. However, the carbofuran removal has reached only less than 74% in cases of B and D. Similar variations were also determined for DOC removal (Fig. 4-2b). Mineralization efficiencies obtained at low carbofuran concentration (A and C) were greater than those at high carbofuran concentration (B and D).



4.3 Effect of initial pH on carbofuran degradation

The photo-Fenton reaction is strongly pH dependent as solution pH will affect the generation of $\cdot\text{OH}$, the oxidation performance and the species concentration of Fe³⁺ complex in aqueous solution. The experiments were conducted using 50 mg L⁻¹ carbofuran concentration at various pH values (2-4) with Fe³⁺ dosage of 35 mg L⁻¹ and H₂O₂ dosage rate of 4 mg L⁻¹ min⁻¹. The effect of initial pH on the carbofuran degradation in the photo-Fenton process is shown in Fig. 4-3 and Table 4-1. As shown in Fig. 4-3, the profiles demonstrate that the removals of carbofuran and DOC are greatly affected by the initial pH level. Almost 100% degradation of carbofuran was

(a)



(b)

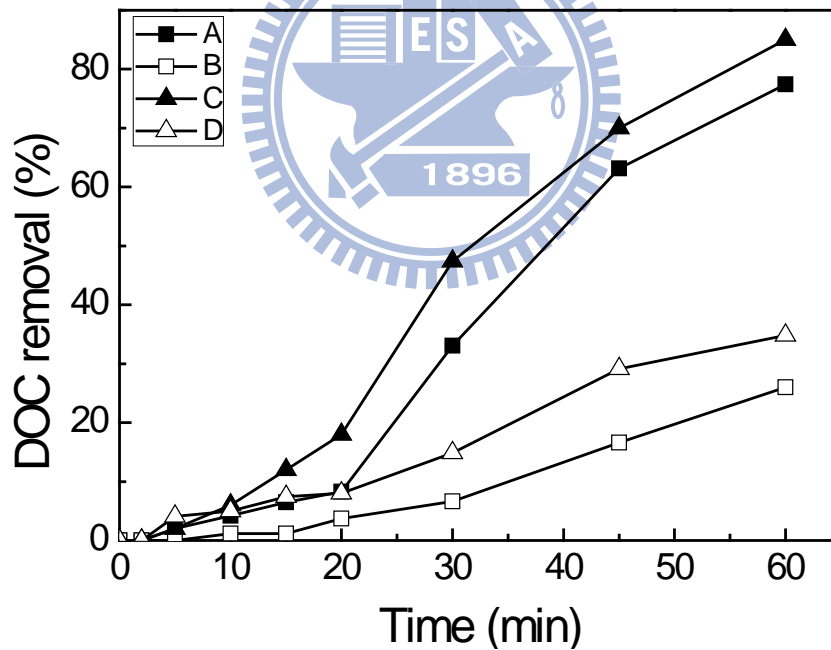
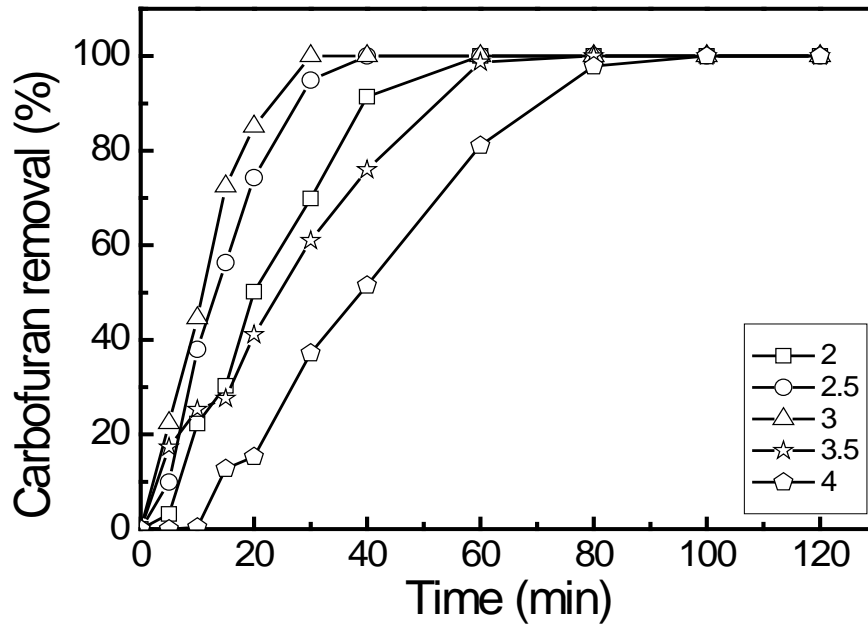


Fig. 4-2. The profiles of (a) carbofuran (b) DOC removals with time at pH 3, using H_2O_2 : $1.3 \text{ mg L}^{-1} \text{ min}^{-1}$, Fe^{3+} : 10 mg L^{-1} (A and B) and H_2O_2 : $1.3 \text{ mg L}^{-1} \text{ min}^{-1}$, Fe^{3+} : 40 mg L^{-1} (C and D) (Solid points represent carbofuran 21 mg L^{-1} and hollow points represent carbofuran 81 mg L^{-1}).

(a)



(b)

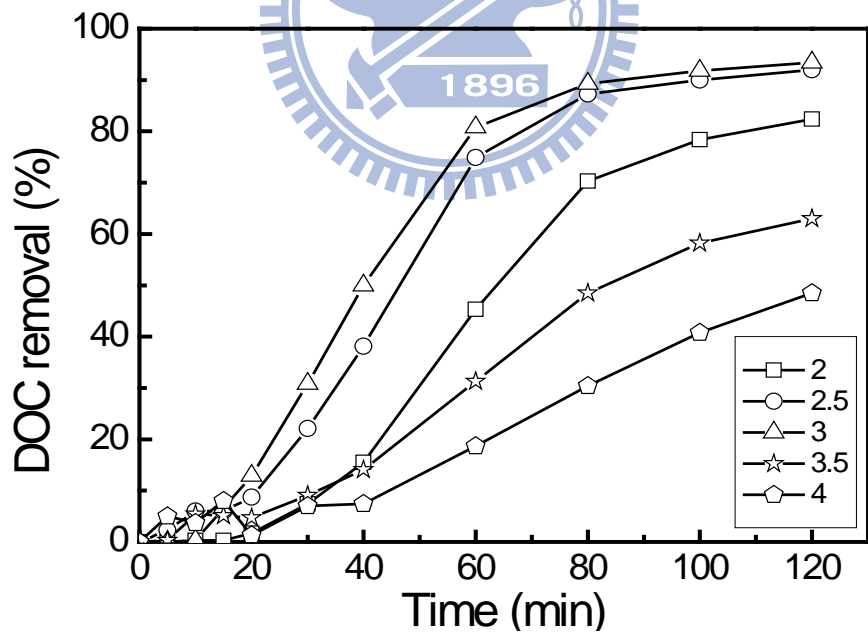


Fig. 4-3. The profiles of (a) carbofuran (b) DOC removals with time at various pH (Fe^{3+} dosage at 35 mg L^{-1} , H_2O_2 dosage rate at $4 \text{ mg L}^{-1} \text{ min}^{-1}$ and carbofuran 50 mg L^{-1}).

Table 4-1. Effect of various pH on carbofuran and DOC removals (Fe^{3+} dosage at 35 mg L^{-1} , H_2O_2 dosage rate at 4 $\text{mg L}^{-1} \text{min}^{-1}$ and carbofuran 50 mg L^{-1}).

pH	Carbofuran		DOC		Pseudo-first order carbofuran removal kinetics	
	removal (%)		removal (%)		$k_{app} (\times 10^{-2} \text{min}^{-1})$	R^2
	30 min	120 min	30 min	120 min		
2	70	100	7	82	3.5	0.92
2.5	95	100	22	92	8.1	0.88
3	100	100	31	93	8.6	0.94
3.5	61	100	9	63	3.2	0.96
4	37	100	7	49	2.1	0.85

achieved in between 100-120 minutes of the photo-Fenton process under all initial pH values (Fig. 4-3a). At the end of 30 minutes, 37% degradation of carbofuran was observed at pH 4, whereas it was 61% at pH 3.5 and almost 100% at pH 3. This indicates that the lower pH values are better for the photo-Fenton decomposition of carbofuran. However, the decomposition of carbofuran was reduced to 95% and 70% under pH 2.5 and 2, respectively at the end of 30 minutes of photo-Fenton reaction. Similar trends can be seen in Fig. 4-3b, where the DOC removal at the end of 120 minutes increased from 49% at pH 4 to 93% at pH 3, and then decreased to 82% at pH 2.

It can also be seen in Table 4-1 that increasing solution pH from 2 to 3 enhances the removal of carbofuran at 30 min reaction from 70% to 100%; however, further

increase in pH (above 3) decreases the removal efficiency, and at pH 4 the removal efficiency decreased to 37%. The reduced efficiency at higher pH values ($\text{pH} > 3$) is due to the precipitation of Fe^{3+} as inactive $\text{Fe}(\text{OH})_3$ thus hindering the reaction between Fe^{2+} and H_2O_2 . Furthermore, H_2O_2 can also be hydrolyzed to water and oxygen (Eq. 4-1) at higher pH values [14]. The decomposition performance under low pH condition ($\text{pH} < 3$) decreases since excess H^+ will react with $\cdot\text{OH}$ via Eq. 2-17 and produce water [33]. The consumption of H_2O_2 and $\cdot\text{OH}$ can decrease the oxidation performance of target compounds. Moreover, the dominant $\text{Fe}(\text{OH})^{2+}$ reaches a maximum at pH around 3 [14]. The lower quantity of $\text{Fe}(\text{OH})^{2+}$ at pH below 3 causes lower amount of Fe^{2+} reduction and $\cdot\text{OH}$ production in Eq. 2-12 resulted in poor performance of carbofuran removal.



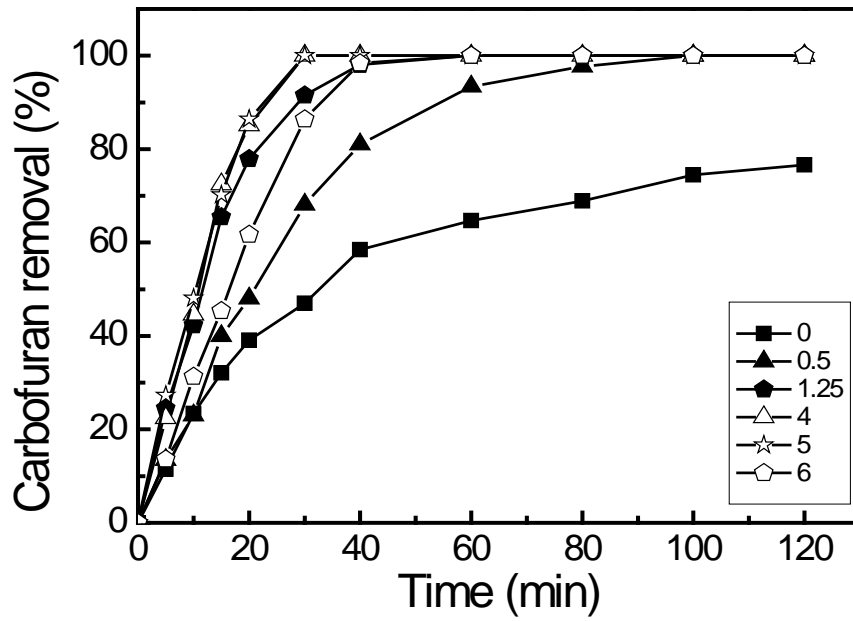
The variations of DOC removal at 30 min and 120 min are similar with the results of carbofuran removal. At pH value of 3, the DOC removals at 30 min and 120 min were found to be 31% and 93%, respectively. Furthermore, the carbofuran removals were fitted well with the pseudo-first order reaction model and the R^2 values ranged between 0.85 to 0.96. The apparent rate constants of carbofuran removal were increased with the decrease in pH value from 4 to 3. Further decrease in pH (below 3) decreased the apparent rate constant of carbofuran removal. The highest apparent rate constant ($8.6 \times 10^{-2} \text{ min}^{-1}$) was obtained at pH 3. Base on the results obtained, the optimal pH for the oxidation of carbofuran using photo-Fenton process is 3, which is in good agreement with the previous photo-Fenton studies conducted for the destruction of various organic compounds [27,74].

4.4 Effect of H₂O₂ dosage rate on carbofuran degradation

In order to identify a better dosage rate of H₂O₂ required for the photo-Fenton reaction, the experiments were repeated at 50 mg L⁻¹ carbofuran concentration and pH 3, with a Fe³⁺ dosage of 35 mg L⁻¹ and varying H₂O₂ dosage rates (0-6 mg L⁻¹ min⁻¹). Carbofuran and DOC removals under various dosage rates of H₂O₂ are shown in Fig. 4-4 and Table 4-2. It can be noticed in Fig. 4-4a that the carbofuran degradation increases under the higher dosage rates of H₂O₂, which is mainly due to the generation of $\cdot\text{OH}$ with extra H₂O₂ addition. In the absence of H₂O₂, i.e. UV/Fe³⁺ process, the degradation and mineralization of carbofuran were reached around 77% and 13%, respectively, within 120 minutes of reaction. The result proves that dosage of H₂O₂ is necessary to enhance the mineralization of carbofuran. At a H₂O₂ dosage of 0.25 mg L⁻¹ min⁻¹, more than 90% carbofuran removal was observed corresponding to a DOC removal of 33% at the end of 100 minutes of photo-Fenton reaction. Both carbofuran and DOC removals distinctly amplified with the increased additions of H₂O₂. When the H₂O₂ dosage was increased to 4 mg L⁻¹ min⁻¹, almost 100% of carbofuran was decomposed within 30 minutes reaction and a maximum carbofuran mineralization of 94% was observed after 120 minutes of reaction (Fig. 4-4b). At higher H₂O₂ dosage conditions, the DOC removal reveals a sharp increase within 20-60 minutes (10-60%), and then followed a gradual increase after 60 minutes (60-94%).

On the other hand, carbofuran removals have improved greatly, i.e. 32 to 73%, 39 to 90% and 47 to 100% within 15, 20 and 30 min reaction, respectively, when the H₂O₂ dosage rate was increased from 0 to 4 mg L⁻¹ min⁻¹ (Table 4-2). At the same condition, the DOC removal efficiency has increased from 13% to 93% after 120 min reaction. However, no improvement in the carbofuran and DOC removals were observed when

(a)



(b)

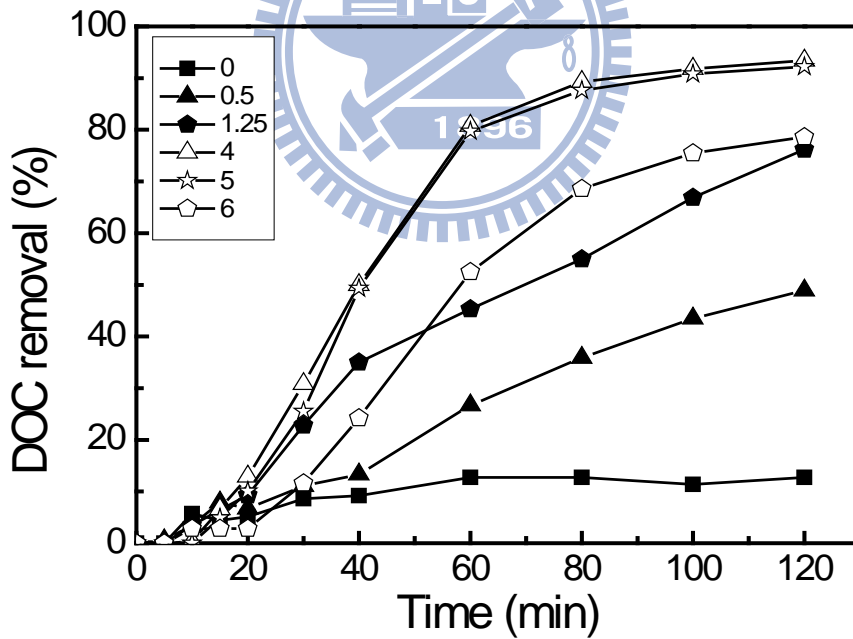


Fig. 4-4. The profiles of (a) carbofuran (b) DOC removals with time at various H_2O_2 dosage rates (Fe^{3+} dosage at 35 mg L^{-1} , pH 3 and carbofuran 50 mg L^{-1}).

the H_2O_2 was overdosed, i.e. beyond $4 \text{ mg L}^{-1} \text{ min}^{-1}$. Several researchers have also reported the negative effect of H_2O_2 dosage under H_2O_2 overdosed photo-Fenton systems for the degradation of target compound [27,66]. Under this overdosed rate, H_2O_2 could react with $\cdot\text{OH}$, and as a result, less powerful $\text{HO}_2\cdot$ is formed as shown in Eq. 2-14. Moreover, $\text{HO}_2\cdot$ could further react with $\cdot\text{OH}$ and form water and oxygen as per Eq. 2-15 [27,42]. Therefore, the H_2O_2 dosage rate beyond $4 \text{ mg L}^{-1} \text{ min}^{-1}$ can reduce the oxidative capacity of the photo-Fenton reaction by decreasing the amount of $\cdot\text{OH}$ and oxidant in the system [74].

The variation of residual H_2O_2 concentration as shown in Fig. 4-5 is in good agreement with the DOC profile. The residual H_2O_2 concentration under H_2O_2 dosage rates of 4 and $5 \text{ mg L}^{-1} \text{ min}^{-1}$ decrease at reaction time 15-40 min, and then, increases gradually after 40 min (Fig. 4-5). The carbofuran removals were fitted using the pseudo-first order reaction model; the highest apparent rate constant of $8.8 \times 10^{-2} \text{ min}^{-1}$ was observed at the H_2O_2 dosage rate of $4 \text{ mg L}^{-1} \text{ min}^{-1}$ (Table 4-2). This reveals that H_2O_2 dosage rate at $4 \text{ mg L}^{-1} \text{ min}^{-1}$ has accelerated the oxidation rate of carbofuran. The experimental outcomes, i.e. carbofuran degradation, mineralization and ratio of DOC removal/carbofuran degradation, at the end of 120 minutes of the photo-Fenton process are shown in Table 4-3. The ratio of DOC removal/carbofuran degradation increases with increasing H_2O_2 dosage rate, which demonstrates that the addition of H_2O_2 is useful for enhancing the mineralization of carbofuran in the photo-Fenton process. Throughout the experiments, the solution pH remains relatively unchanged (2.8-3.4) as shown in Fig. 4-6. The increase of pH in the initial stage of reaction is due to OH^- generated through Eq. 2-1. Also, it can be noted that at the end of experiment the pH value decreased (Fig. 4-6). The carbamic acid formed during the reaction might be the reason for this decrease in pH.

Table 4-2. Effect of various H₂O₂ dosage rates on carbofuran and DOC removals

(Fe³⁺ dosage at 35 mg L⁻¹, pH 3 and carbofuran 50 mg L⁻¹).

H ₂ O ₂ dosage rate (mg L ⁻¹ min ⁻¹)	Carbofuran removal (%)			DOC removal (%)		Pseudo-first order carbofuran removal kinetics	
	15 min	20 min	30 min	30 min	120 min	k_{app} ($\times 10^{-2}$ min ⁻¹)	R ²
0	32	39	47	9	13	1.4	0.87
0.5	40	48	68	11	49	4.5	0.98
1.25	66	78	92	23	76	7.7	0.98
4	73	90	100	31	93	8.8	0.94
5	73	87	100	26	92	8.6	0.95
6	45	62	86	12	79	5.6	0.91

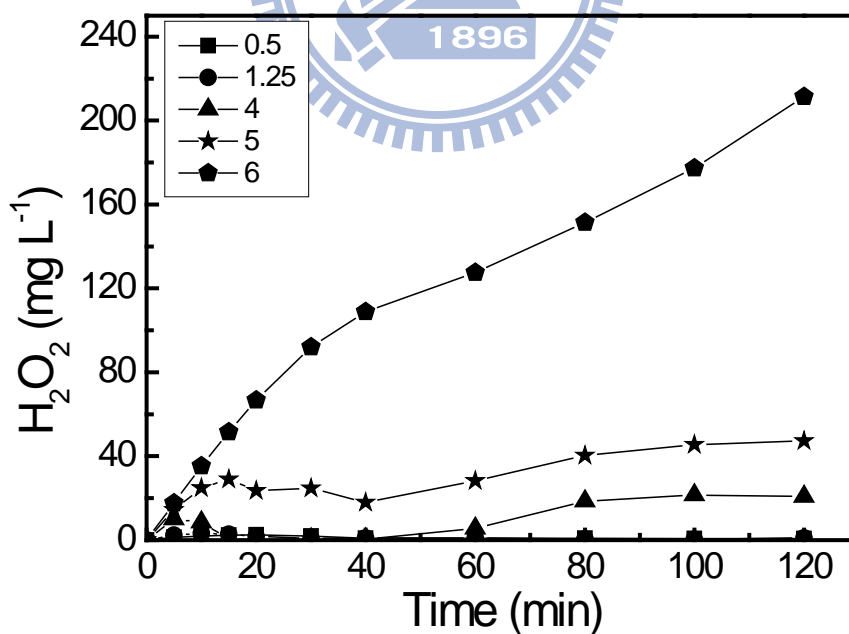


Fig. 4-5. Profiles of residual H₂O₂ with time at various H₂O₂ dosage rates (Fe³⁺ 35 mg L⁻¹, pH 3 and carbofuran 50 mg L⁻¹).

Table 4-3. Summarization of carbofuran degradation, DOC removal and the ratio of DOC removal/carbofuran degradation by the photo-Fenton reaction at various H₂O₂ dosage rates (Fe³⁺ 35 mg L⁻¹, pH 3 and carbofuran 50 mg L⁻¹).

H ₂ O ₂ dosage rate (mg L ⁻¹ min ⁻¹)	Carbofuran degradation (%) [A]	DOC removal (%) [B]	B/A
0	77	13	0.17
0.5	100	49	0.49
1.25	100	76	0.76
4	100	93	0.93
5	100	92	0.92
6	100	79	0.79

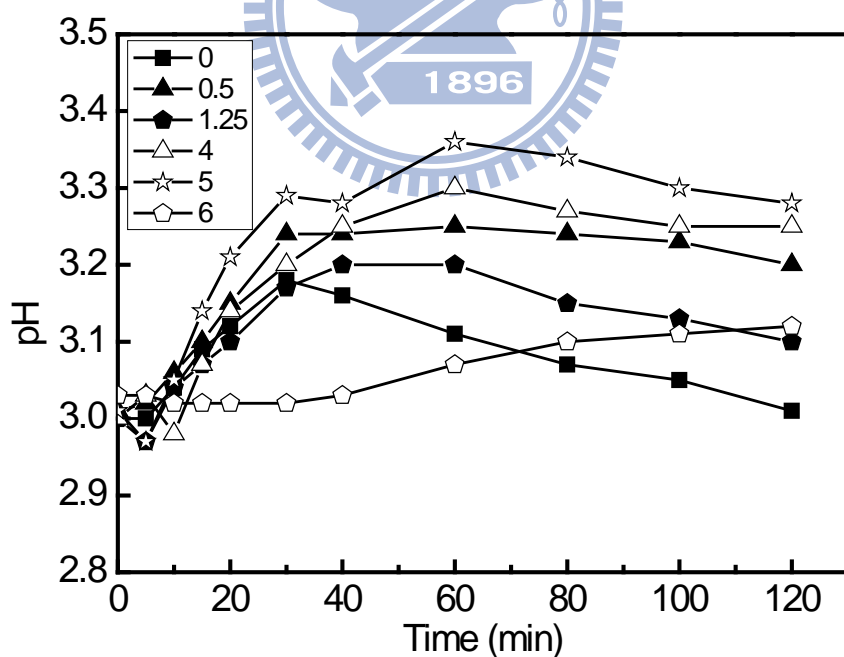


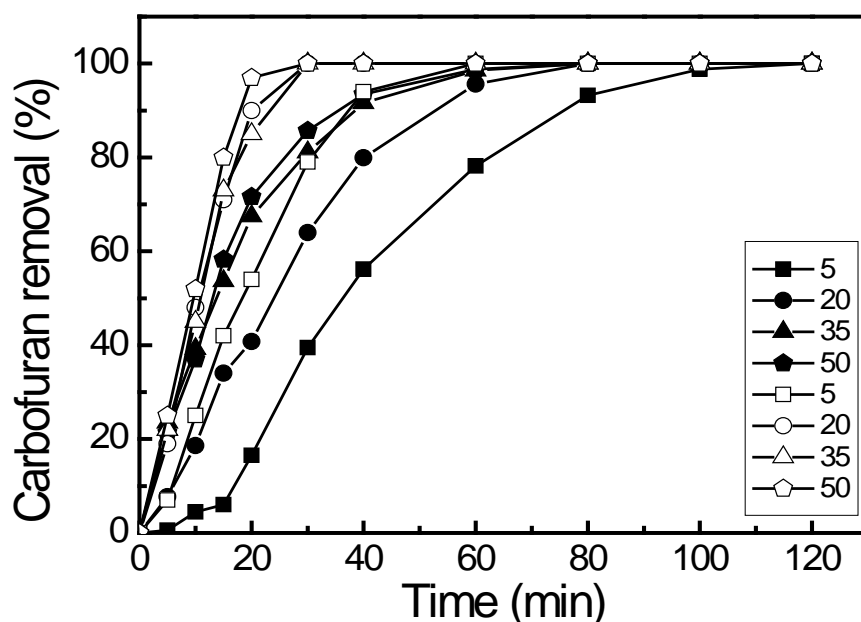
Fig. 4-6. Profiles of pH at various H₂O₂ dosage rates (Fe³⁺ dosage at 35 mg L⁻¹, pH 3 and carbofuran 50 mg L⁻¹).

4.5 Effect of Fe³⁺ dosage on carbofuran degradation

The photo-Fenton experiments were repeated under 50 mg L⁻¹ carbofuran concentration at different Fe³⁺ dosages (5-50 mg L⁻¹) and H₂O₂ dosage rates (0.8 and 4 mg L⁻¹ min⁻¹), and at fixed pH, i.e. pH 3. The experimental outcomes are shown in Fig. 4-7 and Table 4-4. The profiles of H₂O₂ consumption are shown in Fig. 4-8. Throughout the study not much variation in pH (2.9-3.3) was observed as shown in Fig. 4-9. The carbofuran removal increases with increasing Fe³⁺ dosages due to the production of more •OH through Fenton reaction. It can be seen from Fig. 4-7a that even at the Fe³⁺ dosage of 5 mg L⁻¹ carbofuran was completely oxidized after 100 and 60 min of reaction time under H₂O₂ dosage rates of 0.8 and 4 mg L⁻¹ min⁻¹, respectively. At higher Fe³⁺ dosages (> 35 mg L⁻¹), the reaction times to reach 100% carbofuran removal were reduced to 60 and 30 min with around 30 and 80% of DOC mineralized. But there were no obvious further improvements on carbofuran degradation and mineralization for Fe³⁺ dosage higher than 35 mg L⁻¹ (Figs. 4-7a and b). This observation is in good agreement with the results reported in the previous studies [27,33,78]. The main reason for the limited degradation of carbofuran at H₂O₂ dosage rate of 0.8 mg L⁻¹ min⁻¹ is due to the insufficient residual H₂O₂ concentration in the system (Fig. 4-8). The higher removal at a H₂O₂ dosage rate of 4 mg L⁻¹ min⁻¹ could be attributed to the increased residual H₂O₂ concentration in the system; however, the increase in Fe³⁺ dosage beyond 35 mg L⁻¹ at this condition has produced similar carbofuran removal owing to the photostationary equilibrium between Fe²⁺ and Fe³⁺ [5].

Table 4-4 also demonstrates that carbofuran and DOC removal efficiencies could be improved by increasing the Fe³⁺ dosage. The increasing in Fe³⁺ dosage facilitates the

(a)



(b)

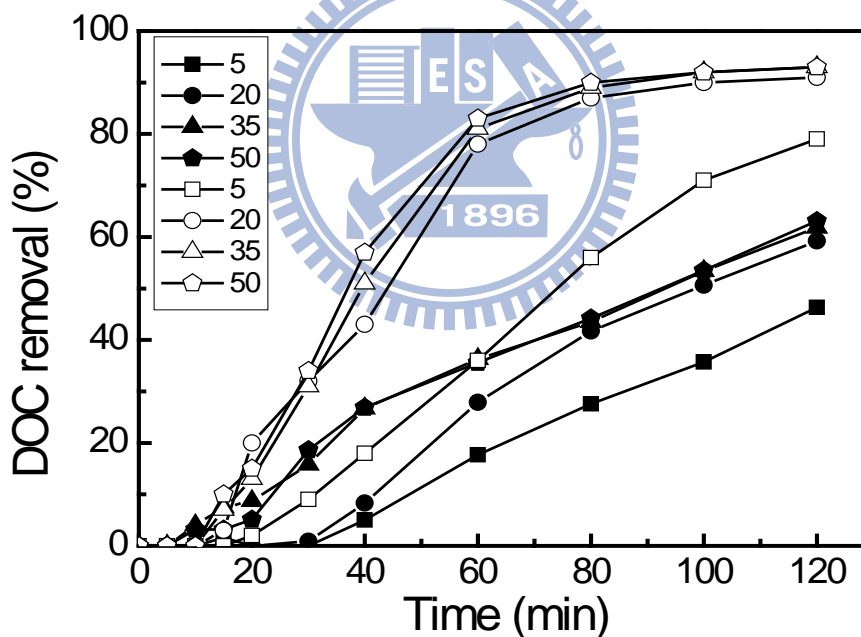


Fig. 4-7. The profiles of (a) carbofuran (b) DOC removals with time under various Fe^{3+} dosages at pH 3 and carbofuran 50 mg L^{-1} (Solid points represent H_2O_2 dosage rate 0.8 $\text{mg L}^{-1} \text{min}^{-1}$ and hollow points represent H_2O_2 dosage rate 4 $\text{mg L}^{-1} \text{min}^{-1}$).

Table 4-4. Effect of various Fe³⁺ dosages on carbofuran and DOC removals under H₂O₂ dosage rates 0.8 and 4 mg L⁻¹ min⁻¹ at pH 3 and carbofuran 50 mg L⁻¹.

H ₂ O ₂ dosage rate (mg L ⁻¹ min ⁻¹)	Fe ³⁺ dosage (mg L ⁻¹)	Carbofuran removal (%)			DOC removal (%)		Pseudo-first order carbofuran removal kinetics	
		15 min	20 min	30 min	30 min	120 min	<i>k_{app}</i> (×10 ⁻² min ⁻¹)	R ²
0.8	5	6	17	40	0	46	2.6	0.95
	20	34	41	64	12	59	4.4	0.92
	35	54	68	81	16	62	6.5	0.98
	50	58	72	85	19	63	6.9	0.99
4	5	42	54	79	9	79	5.2	0.96
	20	71	85	100	32	91	8.3	0.96
	35	73	90	100	31	93	8.6	0.94
	50	80	97	100	34	93	10.5	0.94

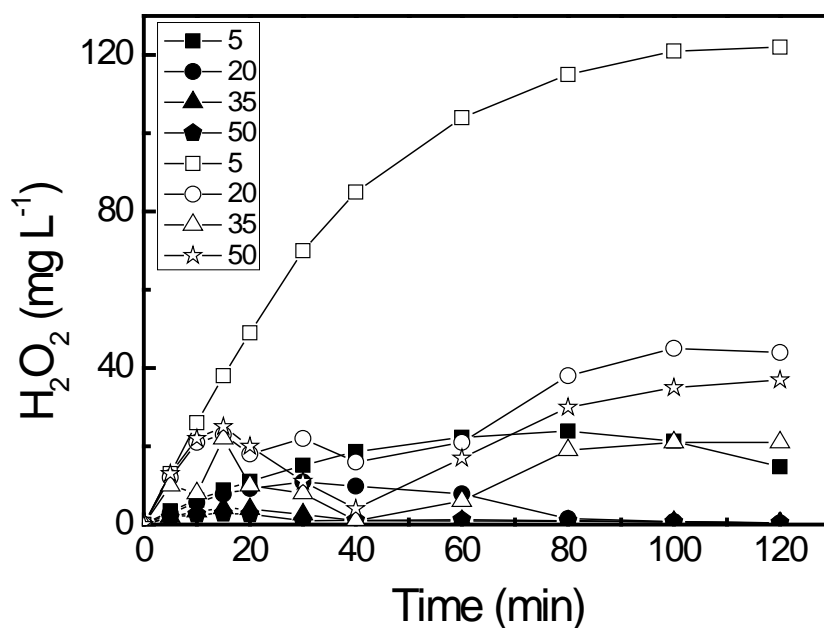


Fig. 4-8. Profiles of residual H₂O₂ with time under various Fe³⁺ dosages at pH 3 and carbofuran 50 mg L⁻¹ (Solid points represent H₂O₂ dosage rate 0.8 mg L⁻¹ min⁻¹ and hollow points represent H₂O₂ dosage rate 4 mg L⁻¹ min⁻¹).

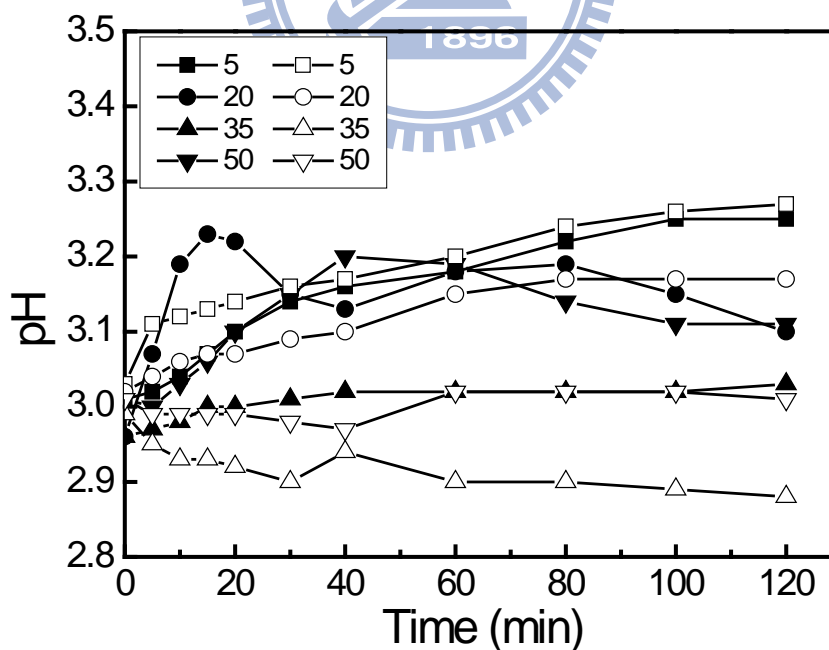


Fig. 4-9. Profiles of pH with time under different Fe³⁺ dosages at pH 3 and carbofuran 50 mg L⁻¹ (Solid points represent H₂O₂ dosage rate 0.8 mg L⁻¹ min⁻¹ and hollow points represent H₂O₂ dosage rate 4 mg L⁻¹ min⁻¹).

higher carbofuran and DOC removal efficiencies. The carbofuran removals shown in Table 4-4 were fitted using the pseudo-first order reaction model. The apparent rate constants are shown in Table 4-4, which indicate that increase in Fe^{3+} dosages and the dosage rates of H_2O_2 have the capability of increasing the carbofuran removal rate to a certain extent. The highest carbofuran removal rate constant of $10.5 \times 10^{-2} \text{ min}^{-1}$ was observed at $50 \text{ mg L}^{-1} \text{ Fe}^{3+}$ dosage with $4 \text{ mg L}^{-1} \text{ min}^{-1}$ of H_2O_2 dosage rate.

4.6 Chemical degradability of carbofuran

A summary of different experiments and their main outcomes are presented in Table 4-5. This could be useful to evaluate the efficiency of each process in carbofuran degradation/mineralization. It can be seen in Table 4-5 that no carbofuran volatilization was observed in 120 min reaction; therefore, the carbofuran removal in the present study was solely by the treatment technique adopted. The simple oxidation techniques, i.e. H_2O_2 , Fe^{3+} , UV irradiation and the combination of H_2O_2 and Fe^{3+} , have produced low carbofuran removal and insignificant DOC removal efficiencies. While H_2O_2 and Fe^{3+} were combined with UV irradiation, i.e. $\text{UV} + \text{H}_2\text{O}_2$ and $\text{UV} + \text{Fe}^{3+}$, the carbofuran removal was increased to 84% and 77%, respectively, after 120 min reaction. However, the DOC removal was reached only less than 17% in these combinations. In these two cases, H_2O_2 had an oxidation potential of 1.78 V/SHE and high valence iron was responsible for the direct attack to organic matter justifying the results obtained [26,68,93]. These results reveal that even in the absence of Fe^{3+} and H_2O_2 , the degradation and mineralization of carbofuran occur.

On the other hand, the photo-Fenton reaction has produced complete carbofuran removal (100%) in 30 min and up to 93% DOC removal in 120 min. These results

Table 4-5. Carbofuran and DOC removals under various experimental conditions.

Experiment	H ₂ O ₂ (mg L ⁻¹ min ⁻¹)	Fe ³⁺ (mg L ⁻¹)	Carbofuran (mg L ⁻¹)	pH	Removals after 120	
					min	
					Carbofuran (%)	DOC (%)
Control	0	0	50	3	0	0
UV	0	0	50	3	7	0
H ₂ O ₂	4	0	50	3	10	0
Fe ³⁺	0	35	50	3	0	0
Fe ³⁺ + H ₂ O ₂	4	35	50	3	18	5
UV + H ₂ O ₂	4	0	50	3	84	17
UV + Fe ³⁺	0	35	50	3	77	13
Photo-Fenton ¹	4	35	50	3	100	93

¹UV + Fe³⁺ + H₂O₂

indicate that the photo-Fenton treatment is highly effective for the rapid degradation and mineralization of carbofuran. Also, in literature, the photo-Fenton system was reported as efficient process for the degradation of several pollutants [24,26,27]. In this study, H₂O₂ was supplied at a constant flow rate during the treatment, which could minimize the reagent cost. As a whole, the application of the photo-Fenton reaction with constant supply of H₂O₂ can generate rapid removal of carbofuran from aqueous systems.

4.7 CCD of experiments for the photo-Fenton process

As mentioned in the introduction, several parameters i.e. pH, dosages of H_2O_2 and Fe^{3+} and carbofuran concentration affect the photo-Fenton degradation and mineralization efficiency of carbofuran. From Eqs. 2-1 to 2-3, it is expected the complex sequential reactions are pH dependent. Furthermore, the generation and consumption of $\cdot\text{OH}$ and iron species (Fe^{2+} , Fe^{3+}) all strongly influenced by pH [37]. The optimum pH value varies with different target compounds treated by photo-Fenton reaction. In addition, carbofuran concentration shows great negative effect on the oxidation of carbofuran. Therefore, plenty of experiments need to be conducted with the application of a four factor CCD. For this reason, pH and carbofuran concentration were selected to fix at 3 and 100 mg L^{-1} according to the previous investigation, respectively.

The CCD is the most popular response surface design methodologies for fitting second-order polynomial equations in the design of experiment [36]. With the aim to find out favorable reagent dosages in the carbofuran degradation by estimating the coefficients of the second-order polynomial equation and constructing the response surface and contour plots, a two factor CCD was carried out using H_2O_2 dosage rate ranging from 1 to $10 \text{ mg L}^{-1} \text{ min}^{-1}$ and Fe^{3+} dosage from 1 to 100 mg L^{-1} . The responses (carbofuran and DOC removals and BOD_5/DOC ratio) at different reaction times are shown in Table 4-6. The influence of H_2O_2 dosage rate and Fe^{3+} dosage on carbofuran and DOC removals were determined at 45 and 60 min, while their influence on BOD_5/DOC ratio were determined at 60 min. The central point was repeated three times (Runs 4, 5, 6) in Table 4-6 and the similar results were obtained indicating the reproducibility of experiment was quite well. The carbofuran removals were fitted well with the pseudo-first order reaction model (R^2 value greater than 0.96) and the highest

apparent rate constant of $6.3 \times 10^{-2} \text{ min}^{-1}$ was observed. However, this table can only provide the results of carbofuran and DOC removals and BOD₅/DOC ratio at certain experimental conditions. Therefore, CCD along with RSM is necessary to estimate the maximum responses at different H₂O₂ dosage rate and Fe³⁺ dosage.

4.7.1 The regression model coefficients

The coefficients of the second-order polynomial equation corresponding to each dependent variable were developed by multiple regression analysis using the MINITAB[®] 14 statistical software. Carbofuran removals (Y_{1, 45 min}, Y_{2, 60 min}), DOC removals (Y_{3, 45 min}, Y_{4, 60 min}) and BOD₅/DOC ratio (Y_{5, 60 min}) were expressed as a function of H₂O₂ dosage rate (X₁) and Fe³⁺ dosage (X₂) as per Eqs. 4-2 to 4-6. The responses can be estimated from these empirical equations; moreover, the surface and contour plots constructed based on these equations can be used to find out the optimal reaction condition.

The regression coefficients and the probability P-values for all linear, quadratic and interaction effects of the variable on responses are shown in Table 4-7. The coefficient of variable in the equation represents the weight of itself to individual response, i.e. the contribution of first-order, quadratic and cross effects, the trend of response and interaction among variable. A positive sign for the coefficients of H₂O₂ dosage rate and Fe³⁺ dosage in the fitted model for all responses indicated that the responses increased with increased levels of reagent dosages.

The P-value was used to estimate the statistical significance and its value less than 0.05 in analysis of variance (ANOVA) indicates that the component is considered as statistically significant [96]. Table 4-7 shows that the P-values for both H₂O₂ dosage

Table 4-6. Experimental results of CCD for the photo-Fenton degradation of carbofuran (pH 3 and carbofuran 100 mg L⁻¹).

Experimental runs	Actual value (coded value)		Carbofuran removal (%)		DOC removal (%)		BOD ₅ /DOC ratio	Pseudo-first order carbofuran removal kinetics	
	H ₂ O ₂ dosage rate (mg L ⁻¹ min ⁻¹)	Fe ³⁺ dosage (mg L ⁻¹)	45 min	60 min	45 min	60 min	60 min	k_{app} ($\times 10^{-2}$ min ⁻¹)	R ²
1	2.3 (-1)	15 (-1)	68	81	17	26	0.37	2.8	0.99
2	2.3 (-1)	86 (1)	72	86	15	25	0.41	2.9	0.99
3	5.5 (0)	100 (1.414)	90	100	24	30	0.82	3.8	0.99
4	5.5 (0)	51 (0)	97	100	30	42	0.93	5.2	0.99
5	5.5 (0)	51 (0)	93	100	29	39	0.81	4.6	0.99
6	5.5 (0)	51 (0)	95	100	27	41	0.86	4.9	0.99
7	5.5 (0)	1 (-1.414)	55	67	7	15	0.36	2.0	0.96
8	8.7 (1)	86 (1)	92	100	24	43	0.53	5.1	0.99
9	10.0 (1.414)	51 (0)	100	100	42	70	0.38	6.3	0.99
10	1.0 (-1.414)	51 (0)	68	81	17	27	0.33	2.8	0.99
11	8.7 (1)	15 (-1)	80	95	17	25	0.24	3.2	0.96

Table 4-7. Estimated regression coefficient and corresponding P-value for response.

Component	Carbofuran removal				DOC removal				BOD ₅ /DOC	
	45 min		60 min		45 min		60 min		60 min	
	Coefficient	P	Coefficient	P	Coefficient	P	Coefficient	P	Coefficient	P
Constant	95.0	0.000	100.0	0.000	28.7	0.000	40.7	0.000	0.867	0.000
X ₁	9.7	0.005	6.9	0.026	5.5	0.045	9.7	0.018	0.008	0.809
X ₂	8.2	0.011	7.1	0.023	3.6	0.141	4.8	0.148	0.123	0.009
X ₁ ²	-5.6	0.073	-3.9	0.198	-0.6	0.805	2.5	0.490	-0.277	0.001
X ₂ ²	-11.3	0.006	-7.4	0.037	-7.6	0.027	-10.5	0.025	-0.160	0.006
X ₁ X ₂	2.0	0.524	0.0	1.000	2.3	0.479	4.8	0.284	0.063	0.197

rate and Fe^{3+} dosage are always smaller than 0.05, except Fe^{3+} dosage for DOC removal and H_2O_2 dosage rate for BOD_5/DOC ratio, indicating these variables affect the responses significantly. In addition, H_2O_2 dosage rate presents greater impact than Fe^{3+} dosage on carbofuran and DOC removals. On the other hand, Fe^{3+} dosage has greater effect than H_2O_2 dosage rate on BOD_5/DOC ratio. The cross effects are negligible for all responses.

$$Y_{1, 45 \text{ min}} = 95.0 + 9.7X_1 + 8.2X_2 - 5.6X_1^2 - 11.3X_2^2 + 2.0X_1X_2 \quad \text{Eq. (4-2)}$$

$$Y_{2, 60 \text{ min}} = 100.0 + 6.9X_1 + 7.1X_2 - 3.9X_1^2 - 7.4X_2^2 \quad \text{Eq. (4-3)}$$

$$Y_{3, 45 \text{ min}} = 28.7 + 5.5X_1 + 3.6X_2 - 0.6X_1^2 - 7.6X_2^2 + 2.3X_1X_2 \quad \text{Eq. (4-4)}$$

$$Y_{4, 60 \text{ min}} = 40.7 + 9.7X_1 + 4.8X_2 + 2.5X_1^2 - 10.5X_2^2 + 4.8X_1X_2 \quad \text{Eq. (4-5)}$$

$$Y_{5, 60 \text{ min}} = 0.867 + 0.008X_1 + 0.123X_2 - 0.277X_1^2 - 0.160X_2^2 + 0.063X_1X_2 \quad \text{Eq. (4-6)}$$

Since the coefficients (R^2) always increases with increasing regressor variables in a regression model. The adjusted R^2 coefficients considering the number of regressor variables is usually selected in statistical modeling [37]. Therefore, the adjusted R^2 coefficients were determined for all responses in this study and their values were found to be greater than 0.71 in all the cases. This indicates that at least 71% of quadratic model is in good agreement with experimental data. As can be seen in the Fig. 4-10 the experimental results are in good agreement with the values calculated by the second-order polynomial equations. Fig. 4-10 also shows that the values of DOC removal are smaller than those of carbofuran removal which indicate that several intermediates produced in the photo-Fenton oxidation of carbofuran. This graph of carbofuran removal reveals that there were some problems with fitting the second-order polynomial equation in wide ranges which resulting in several calculated values above 100%. This observation agrees with other researches which point out that the failure of

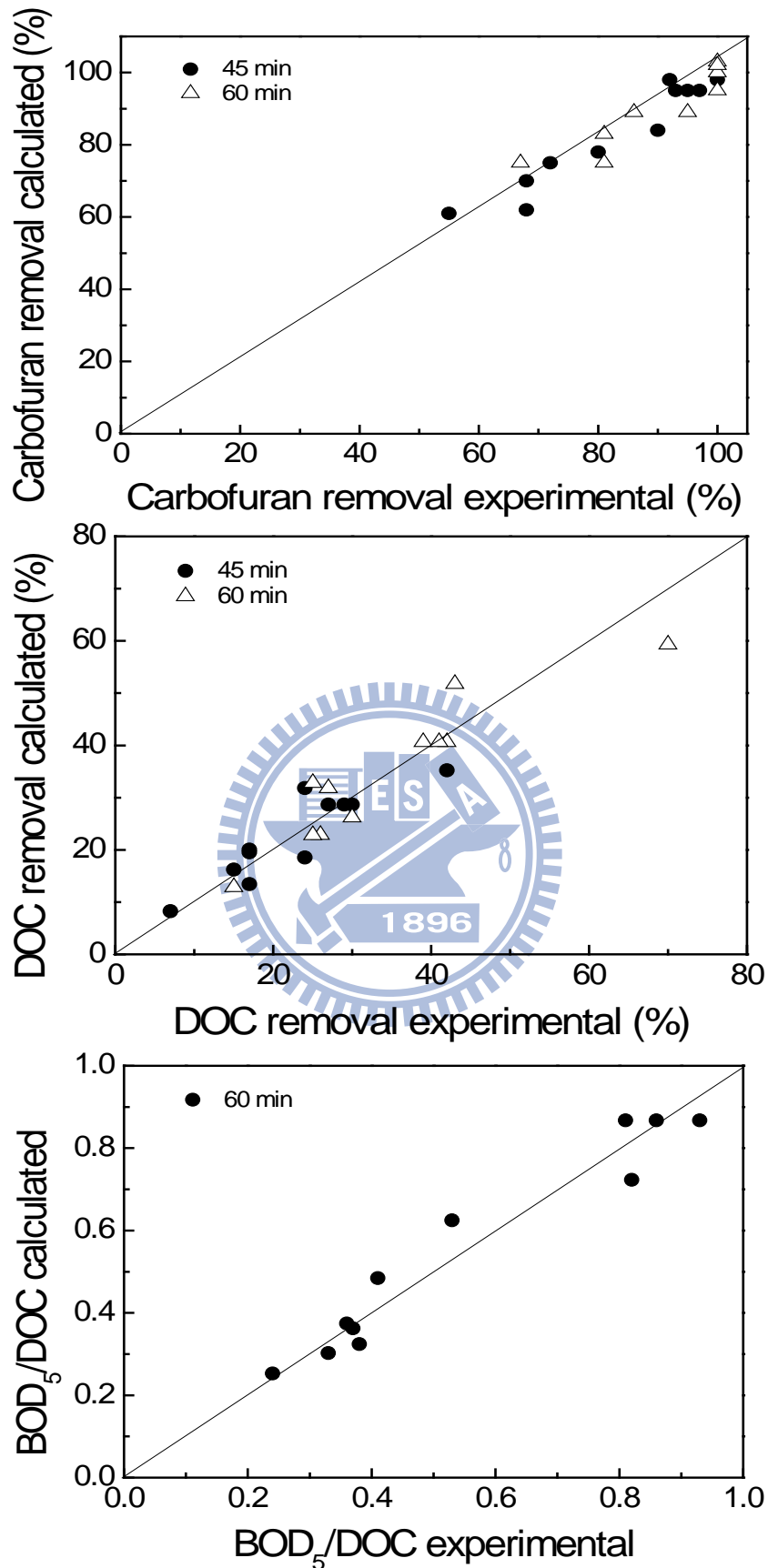


Fig. 4-10. Experimental and calculated values for carbofuran and DOC removals and BOD₅/DOC ratio in the photo-Fenton degradation of carbofuran.

this approach is often obtained due to the complexity of the system while the model covers wide range of results [36,68]. Figs. 4-11a to e demonstrate that the normal probability plots of residuals of the fitted models for all responses are in the straight line. Moreover, the plots of residuals versus predicted values for the responses (Figs. 4-12a to e) are structureless. These evidences reveal that the fitted models of all responses are quite adequate.

4.7.2 Influence of H₂O₂ dosage rate and Fe³⁺ dosage on response

In order to better understand the influence of independent variables, the 3-D response surface plots and contour plots were constructed according to the second-order polynomial equations and are shown in Fig. 4-13. It can be noticed in Fig. 4-13a that H₂O₂ dosage rate has little effect on carbofuran removal at low Fe³⁺ dosage. This may be due to the low Fe³⁺ dosage which restrict the generation of •OH. The carbofuran degradation increases with the increasing H₂O₂ dosage rate under higher Fe³⁺ dosage. Moreover, HO₂• could further react with •OH and form water and oxygen as per Eq. 2-15 [16,27,42]. Therefore, this scavenging effect can reduce the oxidative capacity of the photo-Fenton reaction by decreasing the amount of •OH and oxidant in the system [74].

A similar behavior was observed in the effect of Fe³⁺ dosage on carbofuran removal. The increase in Fe³⁺ dosage enhances the production of more •OH through the Fenton reaction and facilitates the higher carbofuran removal efficiencies. Moreover, no significant improvement in carbofuran removal was observed when the Fe³⁺ dosage increased beyond 60 mg L⁻¹. The detrimental effect on carbofuran removal caused by

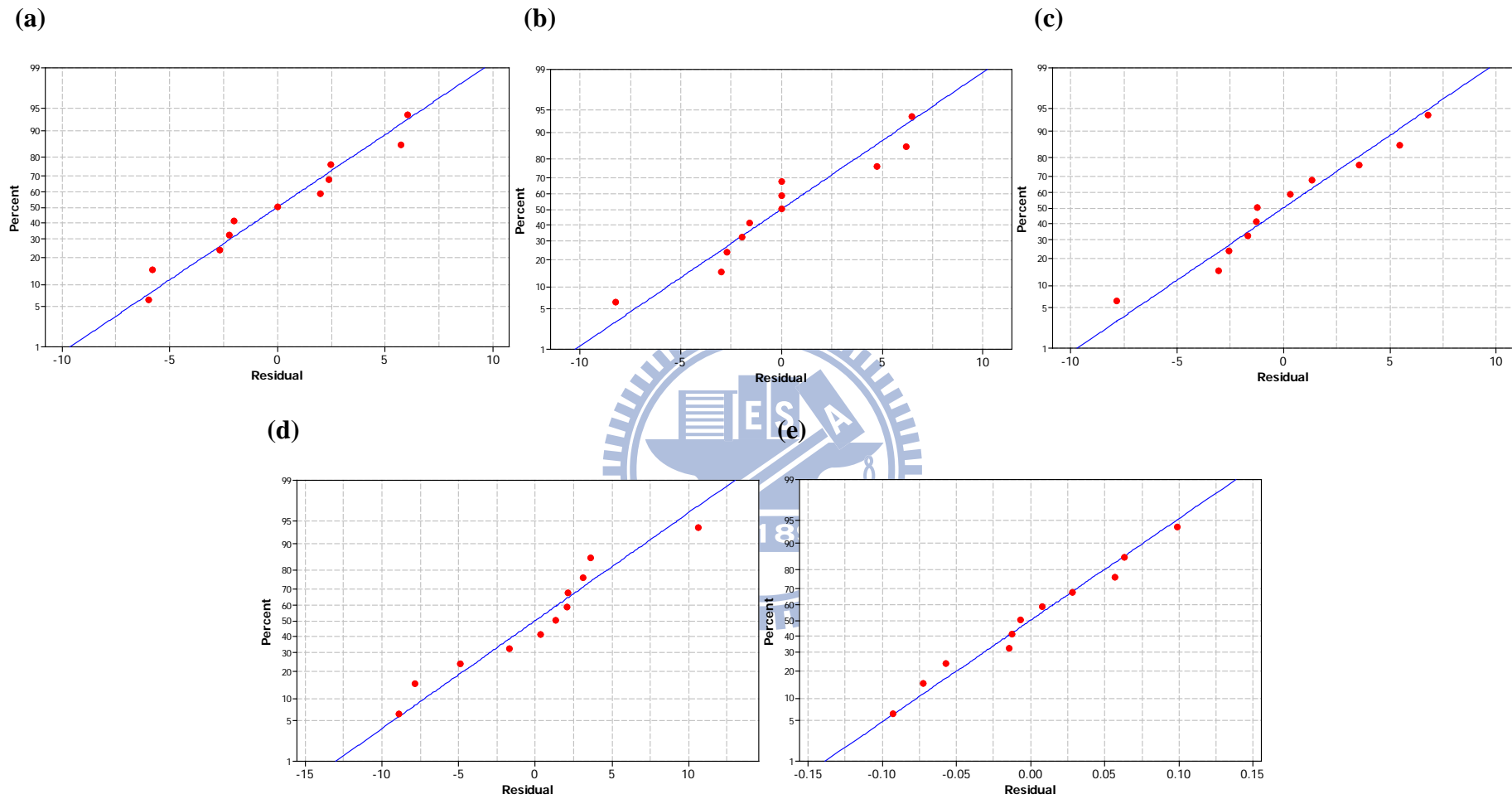


Fig. 4-11. Normal probability plots of responses (a) carbofuran removal at 45 min (b) carbofuran removal at 60 min (c) DOC removal at 45 min (d) DOC removal at 60 min (e) BOD₅/DOC ratio at 60 min.

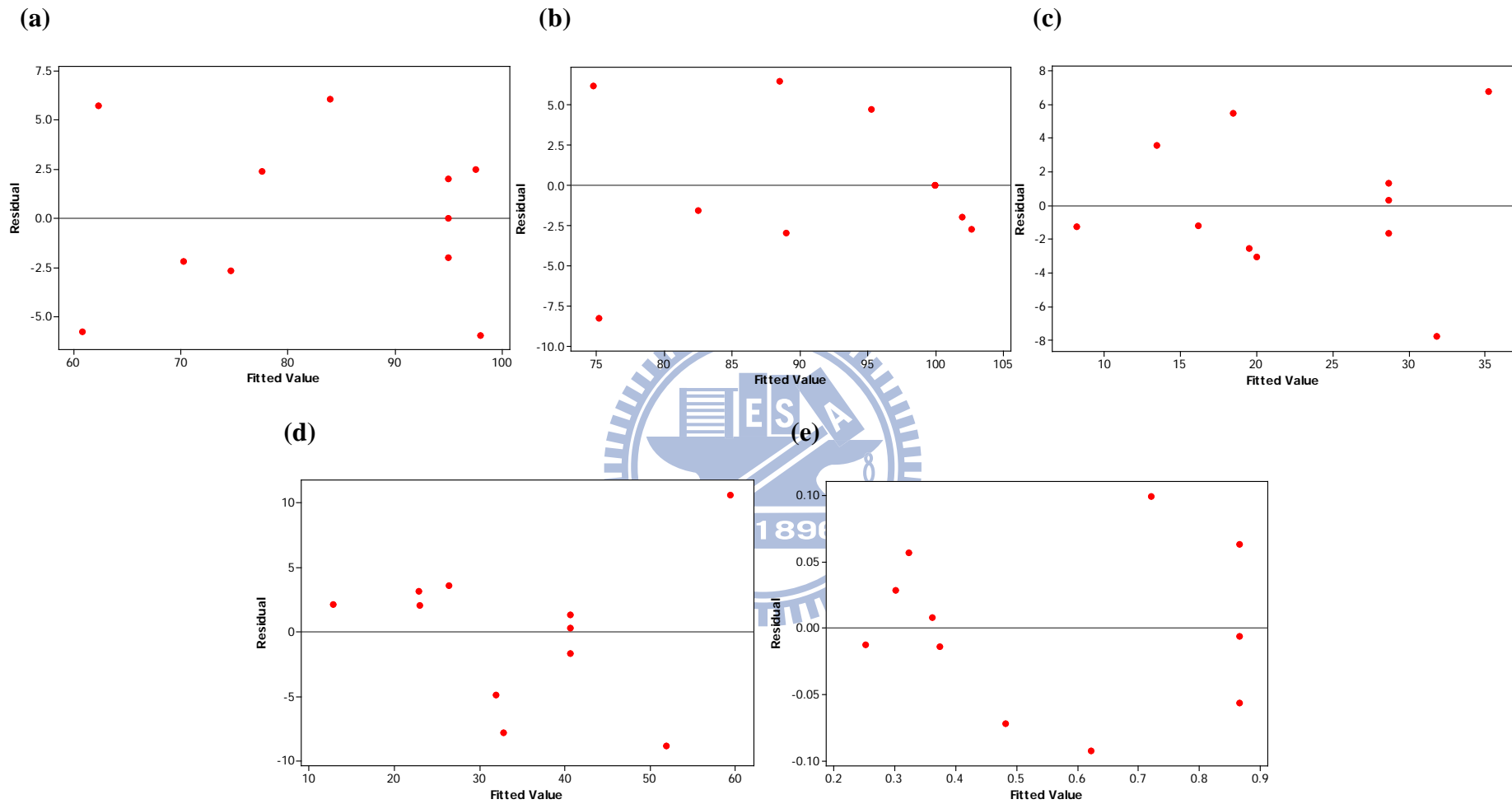
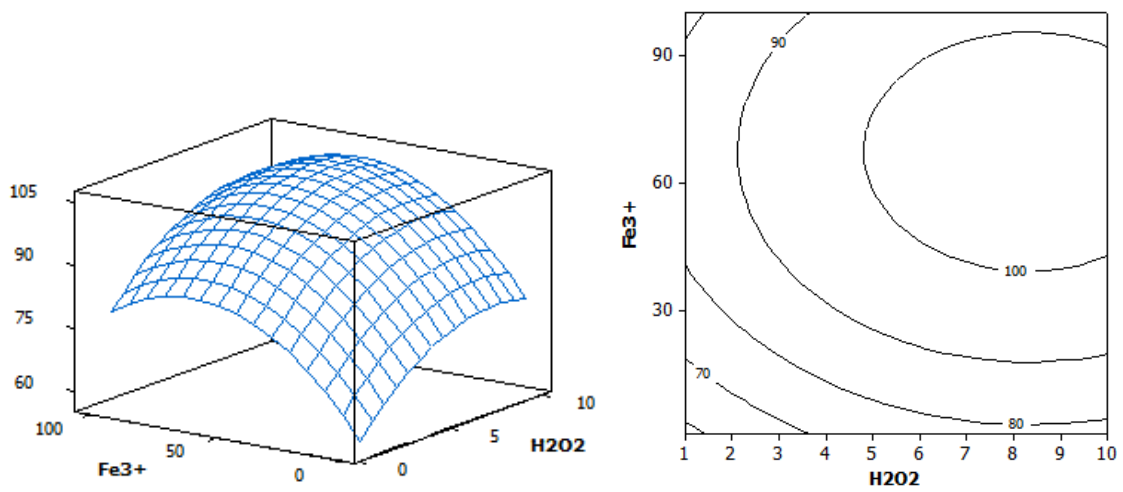
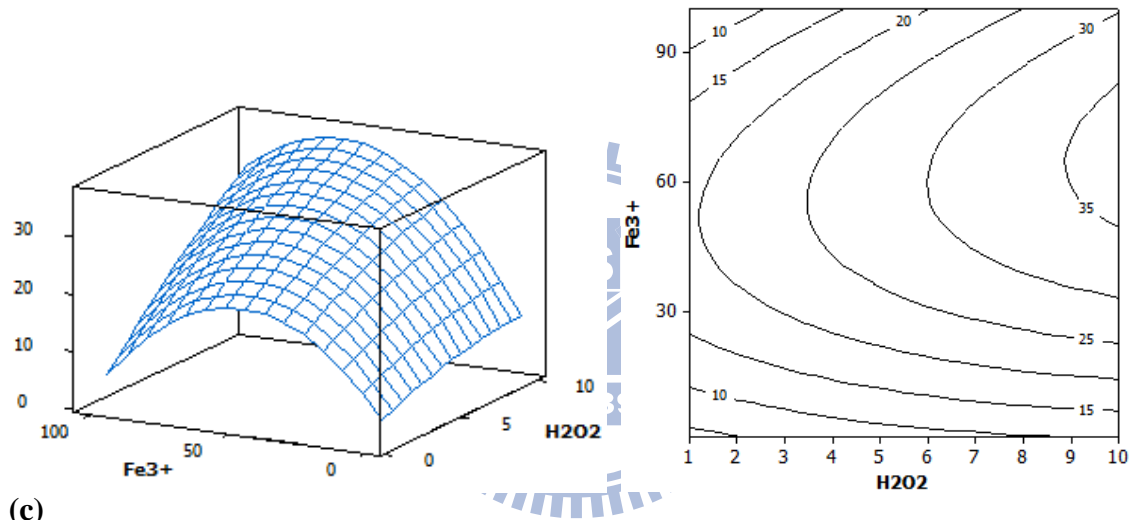


Fig. 4-12. Plots of residuals versus predicted values for responses (a) carbofuran removal at 45 min (b) carbofuran removal at 60 min (c) DOC removal at 45 min (d) DOC removal at 60 min (e) BOD₅/DOC ratio at 60 min.

(a)



(b)



(c)

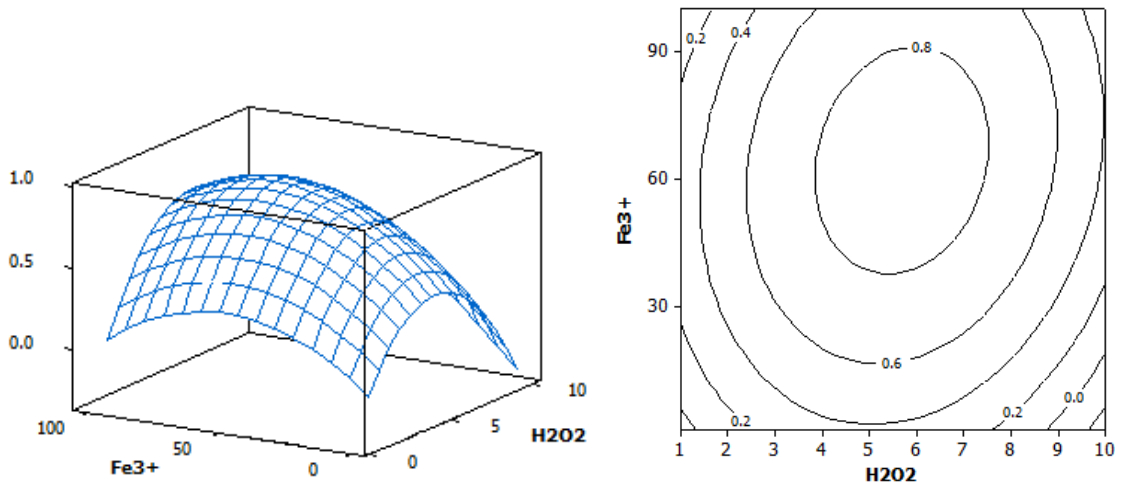


Fig. 4-13. The response surface and contour plot as a function of H_2O_2 dosage rate and Fe^{3+} dosage of (a) carbofuran removal at 60 min (b) DOC removal at 45 min (c)

BOD_5/DOC ratio at 60 min.

excessive Fe^{3+} dosage was due to the scavenging effect of Fe^{3+} dosage as per Eq. 2-16 and resulted in a poor performance of the photo-Fenton reaction. Several researchers have also reported the negative effect of Fe^{3+} dosage under Fe^{3+} overdosed system for the degradation of various target compounds [31,82].

Fig. 4-13b shows that the carbofuran mineralization is significantly influenced by H_2O_2 dosage rate. DOC removal reflects the extent of mineralization of target compound and highly depends on the amount of H_2O_2 dosage rate. The increase in H_2O_2 dosage rate enhances the mineralization of carbofuran. However, H_2O_2 dosage rate reveals little effect on DOC removal with Fe^{3+} dosage below 30 mg L^{-1} due to the limitation of $\cdot\text{OH}$ production. The curvature type relationship exists between the DOC removal and Fe^{3+} dosage. In contrast, the detrimental effects of high loading of H_2O_2 dosage rate, based on the fact that consuming the $\cdot\text{OH}$ in the system, were not observed at high levels of reagent dosage in the set of DOC removal. The DOC removal increased almost linear while higher level of H_2O_2 dosage rate employed without reaching any limiting value that changes the tendency. Moreover, the DOC removal could be maximized at Fe^{3+} dosage range of 55 to 65 mg L^{-1} while H_2O_2 dosage rate controlled at $10 \text{ mg L}^{-1} \text{ min}^{-1}$.

It can be seen in Fig. 4-13c that both H_2O_2 dosage rate and Fe^{3+} dosage had positive effect on BOD_5/DOC ratio to a certain dosage level and then negative effect on BOD_5/DOC ratio was observed. The BOD_5/DOC ratio increases with H_2O_2 dosage rate and Fe^{3+} dosage to $5 \text{ mg L}^{-1} \text{ min}^{-1}$ and 60 mg L^{-1} , respectively. Thereafter, BOD_5/DOC ratio decreases at high levels of H_2O_2 dosage rate and Fe^{3+} dosage. A maximum BOD_5/DOC ratio (> 0.8) was observed when the H_2O_2 dosage rate and Fe^{3+} dosage were controlled at the range of 5 to $6 \text{ mg L}^{-1} \text{ min}^{-1}$ and 55 to 65 mg L^{-1} , respectively.

4.7.3 Favorable reagent dosages for carbofuran degradation under the photo-Fenton as a pretreatment process

Table 4-8 shows the optimum levels of H₂O₂ dosage rate and Fe³⁺ dosage for maximizing carbofuran removal, DOC removal and BOD₅/DOC ratio with different reaction times. Comparing the results shown in Table 4-8, it is understood that CCD coupled with contour plot can help the researchers to find out the optimal reaction condition for each response. For carbofuran removal, it could be observed from Table 4-8 that as the reaction time increases, the optimum H₂O₂ dosage rate shifts toward low level of dosage rate. For example, an initial carbofuran concentration of 100 mg L⁻¹ could be degraded completely by using 6.5 mg L⁻¹ min⁻¹ of H₂O₂ dosage rate at 45 min reaction time or by using 4.9 mg L⁻¹ min⁻¹ of H₂O₂ dosage rate at 60 min reaction time.

Table 4-8. Optimum levels of H₂O₂ dosage rate and Fe³⁺ dosage for maximum carbofuran and DOC removals and BOD₅/DOC ratio.

Dependent variable	Reaction time (min)	H ₂ O ₂ (mg L ⁻¹ min ⁻¹)	Fe ³⁺ (mg L ⁻¹)	Calculated value ^a
Carbofuran removal (%)	45	6.5	62	100
	60	4.9	61	100
DOC removal (%)	45	10	61	37
	60	10	61	61
BOD ₅ /DOC	60	5.4	59	0.89

^a The value simulated by the quadratic models obtained from experimental design.

In addition, a maximum DOC removal of 61% could be achieved after 60 min reaction at H₂O₂ dosage rate of 10 mg L⁻¹ min⁻¹ and Fe³⁺ dosage of 61 mg L⁻¹. Several researchers reported that DOC removal is highly related with H₂O₂ concentration in the system [68,82,93]. Therefore, high loading of H₂O₂ dosage rate must be employed to achieve high carbofuran mineralization within a short reaction time. Residual DOC after the photo-Fenton reaction indicates that the carbofuran intermediates generated in the treatment are not completely degraded. In the aspect of BOD₅/DOC ratio, a maximum BOD₅/DOC ratio of around 0.89 was obtained at H₂O₂ dosage rate of 5.4 mg L⁻¹ min⁻¹ and Fe³⁺ dosage of 59 mg L⁻¹. Higher BOD₅/DOC ratio represents that more organic carbon compounds are oxidized to easily biodegradable intermediates. In this study, the photo-Fenton reaction was selected as a pretreatment coupling with biological treatment for carbofuran degradation; thus, mineralization efficiency is not a concerning parameter. Based on the results of carbofuran removal and BOD₅/DOC ratio, H₂O₂ dosage rate of 5.4 mg L⁻¹ min⁻¹ and Fe³⁺ dosage of 59 mg L⁻¹ are found to be the favorable reagent dosages for pretreatment of carbofuran by the photo-Fenton process. Comparing the results obtained in Fig. 4-2, maximum carbofuran and DOC removals were 97% and 34% with 81 mg L⁻¹ carbofuran concentration, respectively. Under the favorable reagent dosage estimated by experimental design, carbofuran (100 mg L⁻¹) was completely removed within 30 min reaction and 41% DOC removal was reached. Moreover, the H₂O₂/Fe³⁺ ratio was found to be varied from 0.75 to 9.04 within 60 min reaction.

From Fig. 4-10, it can be seen that a high correlation was observed between the experimentally observed and predicted values. However, to confirm the applicability of the second-order quadratic model; two sets of experiments in which H₂O₂ dosage rate fixed at 5.4 mg L⁻¹ min⁻¹ and Fe³⁺ dosage controlled at 59 mg L⁻¹, respectively, were

conducted. The experimental results were compared with the simulated results of quadratic model (Table 4-9) to check the validity of the developed models. From the results, it can be seen from Table 4-9 that the predicted values of the quadratic model are in good agreement with the experimental data.

4.8 Degradation pathway

The experimental samples collected under favorable reagent dosages obtained by experimental design, i.e. Fe^{3+} dosage at 59 mg L^{-1} , H_2O_2 dosage rate at $5.4 \text{ mg L}^{-1} \text{ min}^{-1}$, were used for identifying the intermediates of carbofuran degradation and its degradation pathway. The carbofuran concentration and pH were 100 mg L^{-1} and 3, respectively. Five major intermediates, i.e. 3-Hydroxy-2,2-dimethyl-2,3-dihydro-1-benzofuran-7-yl methylcarbamate, 2,2-Dimethyl-3-oxo-2,3-dihydro-1-benzofuran-7-yl

Table 4-9. Comparison of the simulated data of carbofuran removal and DOC removal with experimental data.

Item	Carbofuran removal (%)		DOC removal (%)	
	45 min	60 min	45 min	60 min
Quadratic models ^a	96	100	29	41
Set 1 ^b	96	100	30	48
Set 2 ^b	97	100	24	48

^a The value simulated by the quadratic models obtained from experimental design.

^b The experimental value obtained while H_2O_2 dosage rate and Fe^{3+} dosage controlled at $5.4 \text{ mg L}^{-1} \text{ min}^{-1}$ and 59 mg L^{-1} , respectively.

methylcarbamate, 2,2-Dimethyl-2,3-dihydro-1-benzofuran-7-ol, 2,2-Dimethyl-2,3-dihydro-1-benzofuran-3,7-diol and 7-Hydroxy-2,2-dimethyl-1-benzofuran-3(2H)-one, were identified and their full scan mass spectra are shown in Figs. 4-14b to f, respectively, along with mass spectra of carbofuran in Fig. 4-14a. Based on the spectral analysis of the intermediates, the possible carbofuran degradation pathway(s) are proposed in Fig. 4-15, and numbers 1-5 are assigned to five intermediates. The first step in the degradation of carbofuran is found to be the cleavage of C-O bond in carbamate group and the formation of intermediate 1 (m/z 164) [97]. This intermediate has also been detected in the photolysis, TiO₂ catalyzed photolysis and anodic Fenton treatment of carbofuran [19,63,97]. The carbamate group appeared to be the primary attack site by \cdot OH in the photo-Fenton reaction. Alternatively, it is envisaged that hydroxylation of carbofuran and intermediate 1 also play an important role in the initial degradation owing to \cdot OH attack at the 3-C position of furan ring. This leads to the formation of intermediates 2 (m/z 237) and 3 (m/z 180) [48]. The successive oxidation of these two compounds, i.e. m/z 237 and 180, at their 3-C position of the furan ring might have induced the formation of intermediates 4 (m/z 235) and 5 (m/z 178) [68].

In addition to the hydroxylation and further oxidation of 3-C position in the furan ring, the cleavage of carbamate group from intermediates 2 and 4 can also result in the formation of intermediates 3 and 5. Moreover, the decrease of DOC up to 48% indicates that the furan ring and benzene ring are decomposed to ring open intermediates, and subsequently, mineralized to inorganic carbon dioxide and water. Carbamic acid and methyl amine are also formed simultaneously through the degradation of carbamate group as reported in previous investigations [5,19]. In addition to these five compounds, there may be other intermediates of carbofuran, which are not detected at this moment owing to their lower concentrations.

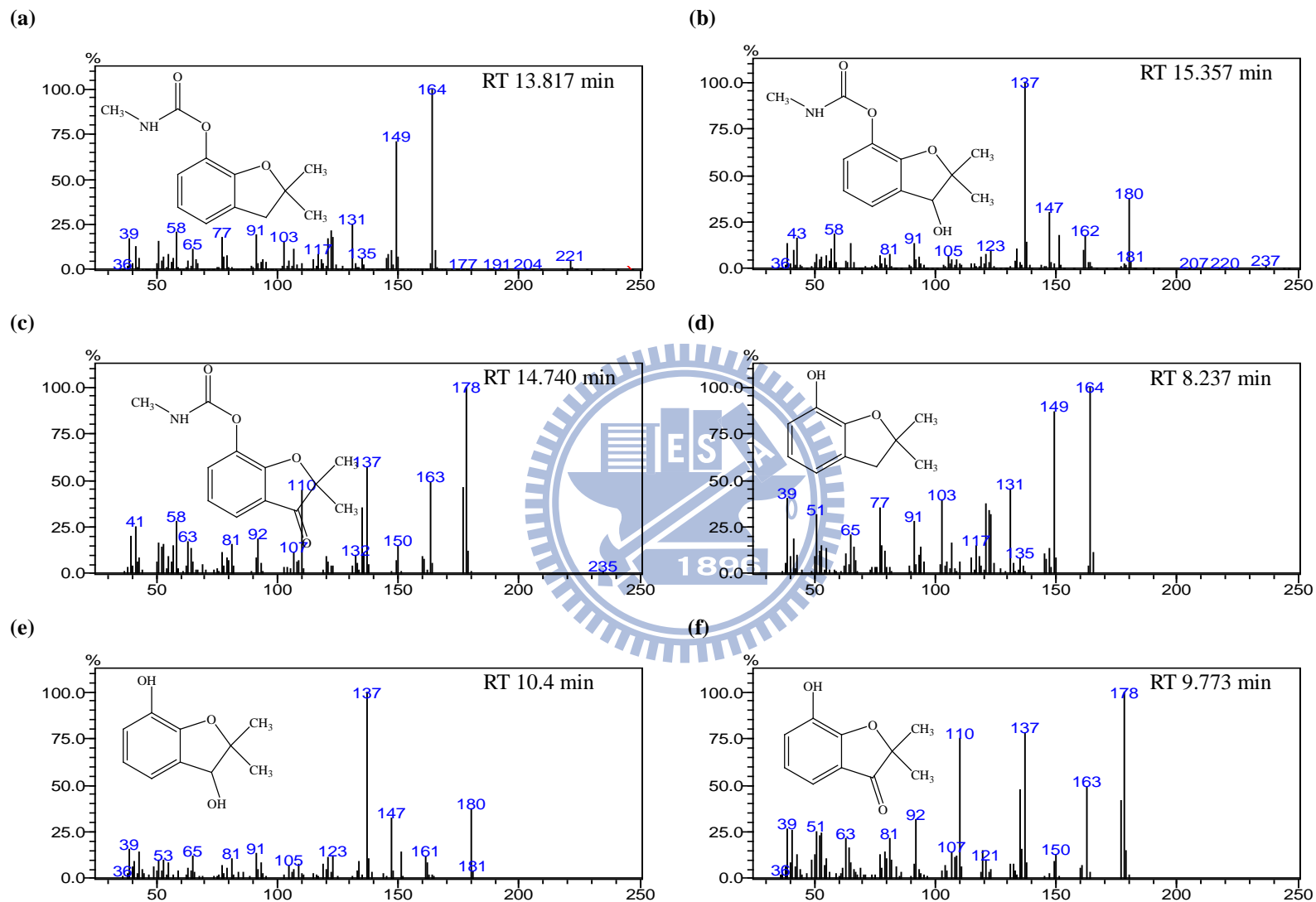


Fig. 4-14. GC-MS spectra of carbofuran and its degradation intermediates (RT means retention time).

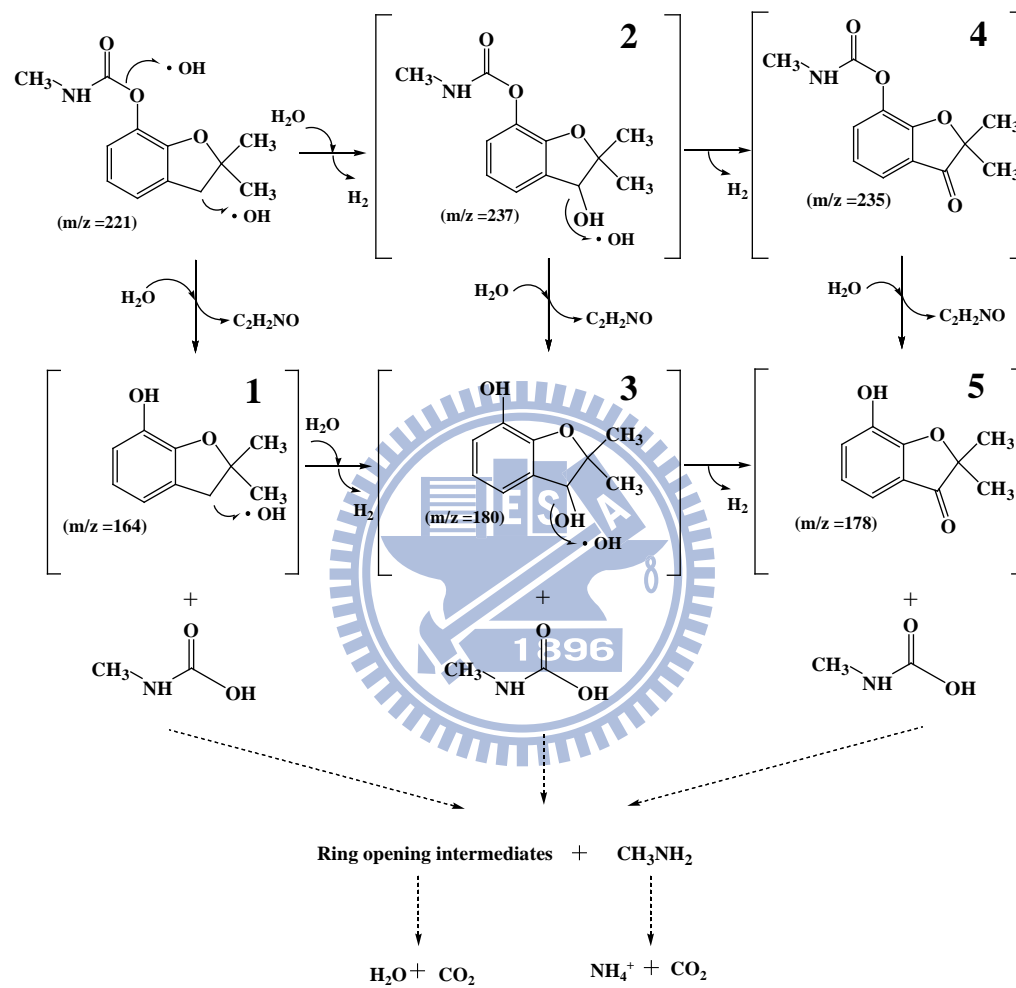


Fig. 4-15. Proposed degradation pathways of carbofuran by photo-Fenton process (dotted lines reflect the hypothesized carbofuran degradation pathway).

4.9 Toxicity and oxidation state assessment

Microtox[®] test has been proved to be a suitable global indicator to evaluate the biodegradability of effluent pretreated by photochemical process [35]. Therefore, acute toxicity of the photo-Fenton effluent was evaluated by Microtox[®] test to find out the extent of carbofuran detoxification in the photo-Fenton process under the predetermined H₂O₂ dosage rate of 5.4 mg L⁻¹ min⁻¹, Fe³⁺ dosage of 59 mg L⁻¹ and carbofuran concentration of 100 mg L⁻¹ at pH 3. TU₅ and TU₁₅ variations of the photo-Fenton effluent with reaction times are shown in Fig. 4-16. Both the profiles have shown similar trends throughout the treatment process. A sharp decrease in toxicity was observed in the first 10 min of the photo-Fenton reaction. Subsequently, a sudden increase in TU₅ as well as TU₁₅ profiles were observed between 10 and 20 min with carbofuran and DOC removals increased from 31% to 65% and 1% to 9%, respectively, which demonstrate that the intermediates produced during the photo-Fenton degradation of carbofuran are more toxic than the parent compound. However, the toxicity decreased gradually after 20 min reaction time and reached a lowest TU value of 4 at the end of reaction. The decrease implies that the toxic intermediate are further oxidized to less harmful compounds with increase of DOC removal from 9% to 48%. The variation of TU agrees with the toxicity result of single pesticide solution reported in previous studies [35,43,44].

On the other hand, AOS and COS are the useful parameters that can be employed for evaluating the extent of carbofuran oxidation and also the oxidation of intermediates. Therefore, AOS and COS were calculated according to Eq. 4-7 and Eq. 4-8 [11,15], respectively, where DOC₀ represents the initial DOC of carbofuran.

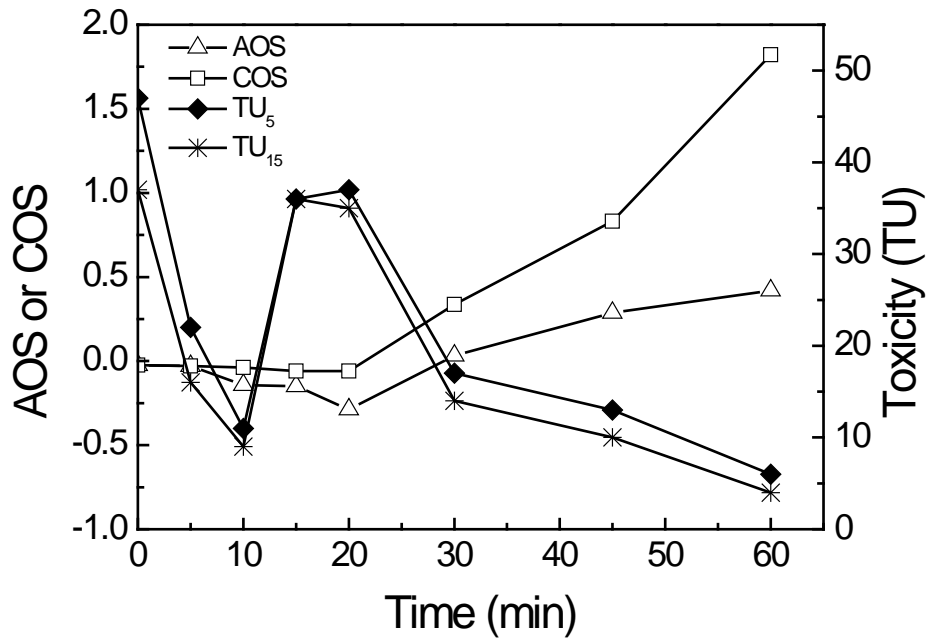
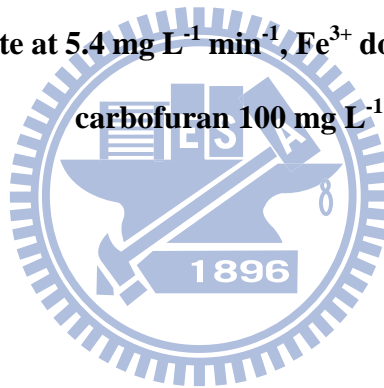


Fig. 4-16. Variations in the Microtox[®] test, AOS and COS as a function of reaction time (H_2O_2 dosage rate at $5.4 \text{ mg L}^{-1} \text{ min}^{-1}$, Fe^{3+} dosage at 59 mg L^{-1} , pH 3 and carbofuran 100 mg L^{-1}).



$$\text{AOS} = 4 - 1.5 \frac{\text{COD}}{\text{DOC}} \quad \text{Eq. (4-7)}$$

$$\text{COS} = 4 - 1.5 \frac{\text{COD}}{\text{DOC}_0} \quad \text{Eq. (4-8)}$$

As shown in Fig. 4-16, the initial AOS and COS of 100 mg L^{-1} carbofuran were -0.03 which indicate the presence of reduced organic matter. After 60 min of reaction, AOS and COS values increased from -0.03 to 0.42 and 1.82, respectively. These increases clearly demonstrate the strong mineralization and generation of oxidized organic intermediates during the photo-Fenton treatment of carbofuran. The high AOS and COS values at the end of experiment may be characteristic of well oxidized compounds such as carbamic acid resulting in the reduction of pH value from 3 to 2.89.

4.10 Biodegradability assessment

The BOD₅/COD ratio has been reported as an important indicator for biodegradability of toxic compounds [15]. Results of BOD₅ and BOD₅/COD ratio at different treatment times under predetermined H₂O₂ dosage rate of 5.4 mg L⁻¹ min⁻¹, Fe³⁺ dosage of 59 mg L⁻¹ and carbofuran concentration of 100 mg L⁻¹ are shown in Fig. 4-17. The BOD₅ of initial 100 mg L⁻¹ carbofuran solution was found to be around zero, which confirmed the biorefractory characteristic of carbofuran. There are slight decreases in BOD₅ at 10 and 20 min due to the increase of TU₅ from 11 to 37 during this period. Thereafter, the BOD₅ of the photo-Fenton effluent gradually increases with the treatment time indicating the improvement of biodegradability due to the generation

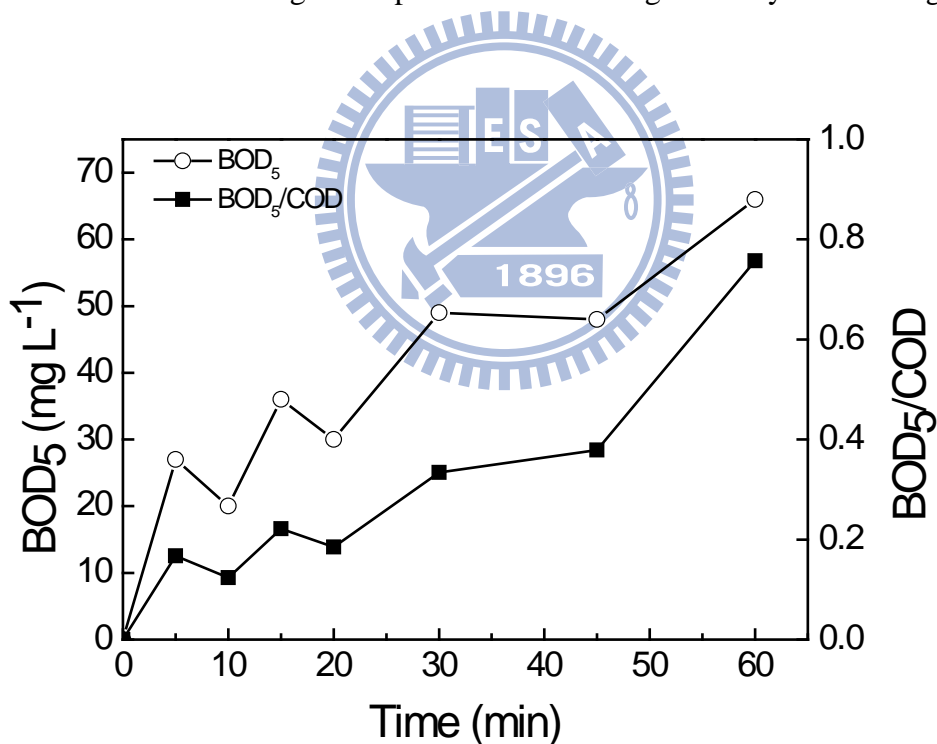


Fig. 4-17. Variations in the BOD₅ and BOD₅/COD ratio as a function of reaction time (H₂O₂ dosage rate at 5.4 mg L⁻¹ min⁻¹, Fe³⁺ dosage at 59 mg L⁻¹, pH 3 and carbofuran 100 mg L⁻¹).

of more biodegradable intermediates during the photo-Fenton reaction. Throughout the study, the profile of BOD₅/COD ratio followed similar trend as BOD₅ profile. It has been widely reported in the literature that BOD₅/COD ratio greater than 0.5 is an indication of readily biodegradable effluent [11,41]. At initial stage of photo-Fenton process, the biodegradable intermediates may also present in the system, but the activity of microorganism is inhibited by carbofuran. After 45 min reaction time, BOD₅/COD ratio was increased more than 0.38 due to the enhancement in BOD₅ together with the reduction in COD; representing an easily biodegradable effluent (BOD₅/COD for municipal wastewater is around 0.4). The highest BOD₅/COD ratio of 0.76 was achieved at the end of experiment in this study.

Based on the results of Microtox[®] test and BOD₅/COD ratio, a reaction time of 45 min can be chosen as the appropriate time for coupling the photo-Fenton process with biological treatment. Under these circumstances, around 96% carbofuran removal can be achieved, the TU₁₅ can be reduced to 10 and the BOD₅/COD ratio can be increased to 0.38. The reduction of TU and increase of biodegradability represented an easily biodegradable effluent.

Chapter 5

Conclusions and recommendations

5.1 Summary of findings

Carbofuran degradation was accelerated in the photo-Fenton system and the apparent degradation rate was influenced by many factors such as irradiation time, carbofuran concentration, pH, dosage rate of H_2O_2 and dosage of Fe^{3+} applied. Furthermore, this study has demonstrated that CCD along with RSM can provide statistically reliable results in the photo-Fenton degradation of carbofuran. The second-order polynomial equations for carbofuran with DOC removals and BOD_5/DOC ratio at different reaction times have been successfully developed. The adjusted R^2 coefficients determined were all greater than 71%, indicating the experimental results obtained are in good agreement with the values calculated by the second-order polynomial equations. The major findings from photo-Fenton degradation of carbofuran are summarized as follows:

- (1) The degradation and mineralization were maximized at pH 3 and minimized at pH 2 and 4. Carbofuran (50 mg L^{-1}) was completely removed within 30 min and 93% DOC removal was achieved by the photo-Fenton process under H_2O_2 dosage rate of $4 \text{ mg L}^{-1} \text{ min}^{-1}$ and Fe^{3+} dosage of 35 mg L^{-1} at pH 3.
- (2) The scavenging effects of H_2O_2 dosage rate and Fe^{3+} dosage were observed in overdosed system, i.e. H_2O_2 dosage rate $4 \text{ mg L}^{-1} \text{ min}^{-1}$ and Fe^{3+} dosage 35 mg L^{-1} ,

with carbofuran 50 mg L⁻¹.

- (3) According to the results of carbofuran removal and BOD₅/DOC ratio in experimental design, H₂O₂ dosage rate of 5.4 mg L⁻¹ min⁻¹ and Fe³⁺ dosage of 59 mg L⁻¹ are the favorable reagent dosages for degradation of 100 mg L⁻¹ carbofuran. Under these conditions, carbofuran (100 mg L⁻¹) was completely removed within 30 min reaction and 41% DOC removal was reached.
- (4) Five intermediate products of carbofuran were identified under the the favorable reagent dosages, which indicate that C-O bond of the carbamate group and 3-C position of the furan ring were oxidized. Moreover, the increase of DOC removal up to 48% indicates that the furan ring or benzene ring was decomposed to ring open intermediates during the process. Carbamic acid and methyl amine were also formed simultaneously through the degradation of carbamate group.
- (5) Under the favorable reagent dosages, the toxicity unit measured by Microtox[®] test with 5 min exposure was decreased from 47 to 6 and the biodegradability evaluated by BOD₅/COD ratio was increased from 0 to 0.76 after 60 min reaction. The reduction of TU and increase of biodegradability represented an easily biodegradable effluent.
- (6) Based on the results of Microtox[®] test and BOD₅/COD ratio at the favorable reagent dosages, a reaction time of 45 min was chosen as the appropriate time for coupling the photo-Fenton process with biological treatment. Under this circumstance, around 96% carbofuran removal and 29% DOC removal were achieved for degradation of cabofuran (100 mg L⁻¹). Moreover, the TU₁₅ was reduced to 10 and the BOD₅/COD ratio increased to 0.38.

As a whole, the experimental results demonstrate that the photo-Fenton process has great potential for degradation and mineralization of carbofuran contaminated water.

Furthermore, the photo-Fenton treatment can be considered as a promising pretreatment for coupling with biological treatment.

5.2 Recommendations for future work

Based on the findings of the present study, the following points are suggested for future work:

- (1) Further research is necessary to evaluate the effects of factors other than pH, dosage rate of H_2O_2 and dosage of Fe^{3+} , i.e. light intensity, temperature and $\text{H}_2\text{O}_2/\text{Fe}^{3+}$ ratio, on the carbofuran degradation. This knowledge can provide a complete understanding in degradation and mineralization of carbofuran in a complex system conditions.
- (2) Since the Fe^{3+} solution in this study was added once in batch experiments, it can be expected to reduce the usage of iron source by continuous addition at fixed flow rate under similar operating conditions.
- (3) There are only five intermediates detected in the present study. The residual DOC value means that other intermediates could be exist in the system. Further research is necessary to quantify the intermediates and establish the degradation pathways of carbofuran using photo-Fenton reaction.
- (4) The present study has already demonstrated that carbofuran can be effectively treated via photo-Fenton process. And, the photo-Fenton process was successfully initiated as a pretreatment to enhance the biodegradability and reduce the toxicity of carbofuran. The feasibility of coupling photo-Fenton process and biological treatment in acclimated batch reactors needs to be further investigated.

Chapter 6

References

- [1] 行政院農委會, 台灣農業年報 (2010).
- [2] C.W. Worthing, The pesticide manual, ninth ed., British crop protection council, London (1991).
- [3] I. Hua, U. Pfalzer-Thompson, Ultrasonic irradiation of carbofuran: Decomposition kinetics and reactor characterization, *Water Res.* 35(6) (2001) 1445-1452.
- [4] R. Jaramillo, W. Bowen, J. Stoorvogel, Carbofuran presence in soil leachate, groundwater, and surface water in the potato growing area in Carchi, Ecuador, CIP Program Report for 1999-2000 (2001) 355-360.
- [5] H. Katsumata, K. Matsuba, S. Kaneco, T. Suzuki, K. Ohta, Y. Yobiko, Degradation of carbofuran in aqueous solution by Fe(III) aquacomplexes as effective photocatalysts, *J. Photochem. Photobiol. A* 170(3) (2005) 239-245.
- [6] D.V. Brkic, S.L. Vitorovic, S.M. Gasic, N.K. Neskovic, Carbofuran in water: Subchronic toxicity to rats, *Environ. Toxicol. Pharmacol.* 25(3) (2008) 334-341.
- [7] EPA, National primary drinking water regulations, carbofuran, Office of Water U.S. Environmental Protection Agency (1995) EPA 811-F-95-003f-T.
- [8] WHO, Carbofuran in drinking-water, World Health Organization, international programme on chemical safety (2004).
- [9] P.L. Huston, J.J. Pignatello, Degradation of selected pesticide active ingredients and commercial formulations in water by the photo-assisted Fenton reaction, *Water*

- Res. 33(5) (1999) 1238-1246.
- [10] S. Malato, J. Blanco, A. Vidal, D. Alarcon, M.I. Maldonado, J. Caceres, W. Gernjak, Applied studies in solar photocatalytic detoxification: an overview, *Sol. Energy* 75(4) (2003) 329-336.
- [11] A.M. Amat, A. Arques, A. Garcia-Ripoll, L. Santos-Juanes, R. Vicente, I. Oller, M.I. Maldonado, S. Malato, A reliable monitoring of the biocompatibility of an effluent along an oxidative pre-treatment by sequential bioassays and chemical analyses, *Water Res.* 43(3) (2009) 784-792.
- [12] C. Sirtori, A. Zapata, I. Oller, W. Gernjak, A. Aguera, S. Malato, Decontamination industrial pharmaceutical wastewater by combining solar photo-Fenton and biological treatment, *Water Res.* 43(3) (2009) 661-668.
- [13] W.C. Paterlini, R.F.P. Nogueira, Multivariate analysis of photo-Fenton degradation of the herbicides tebuthiuron, diuron and 2,4-D, *Chemosphere* 58(8) (2005) 1107-1116.
- [14] J.J. Pignatello, E. Oliveros, A. MacKay, Advanced oxidation processes for organic contaminant destruction based on the Fenton reaction and related chemistry, *Crit. Rev. Env. Sci. Technol.* 36(1) (2006) 1-84.
- [15] A. Arques, A.M. Amat, A. Garcia-Ripoll, R. Vicente, Detoxification and/or increase of the biodegradability of aqueous solutions of dimethoate by means of solar photocatalysis, *J. Hazard. Mater.* 146(3) (2007) 447-452.
- [16] E.C. Catalkaya, F. Kargi, Effects of operating parameters on advanced oxidation of diuron by the Fenton's reagent: A statistical design approach, *Chemosphere* 69(3) (2007) 485-492.
- [17] E. Brillas, I. Sires, M.A. Oturan, Electro-Fenton process and related electrochemical technologies based on Fenton's reaction chemistry, *Chem. Rev.*

- 109(12) (2009) 6570-6631.
- [18] F.J. Benitez, J.L. Acero, F.J. Real, Degradation of carbofuran by using ozone, UV radiation and advanced oxidation processes, *J. Hazard. Mater.* 89(1) (2002) 51-65.
- [19] M. Mahalakshmi, B. Arabindoo, M. Palanichamy, V. Murugesan, Photocatalytic degradation of carbofuran using semiconductor oxides, *J. Hazard. Mater.* 143(1-2) (2007) 240-245.
- [20] Y.S. Ma, M. Kumar, J.G. Lin, Degradation of carbofuran-contaminated water by the Fenton process, *J. Environ. Sci. Health. Part A Toxic/Hazard. Subst. Environ. Eng.* 44(9) (2009) 914-920.
- [21] Y.S. Ma, C.F. Sung, Investigation of carbofuran decomposition by a combination of ultrasonic and Fenton process, *Sustain. Environ. Res.* 20 (2010) 213-219.
- [22] A.K. Abdessalem, N. Bellakhal, N. Oturan, M. Dachraoui, M.A. Oturan, Treatment of a mixture of three pesticides by photo and electro-Fenton processes, *Desalination* 250(1) (2010) 450-455.
- [23] Y.S. Ma, C.F. Sung, J.G. Lin, Degradation of carbofuran in aqueous solution by ultrasound and Fenton processes: Effect of system parameters and kinetic study, *J. Hazard. Mater.* 178(1-3) (2010) 320-325.
- [24] F.A. Al Momani, A.T. Shawaqfeh, M.S. Shawaqfeh, Solar wastewater treatment plant for aqueous solution Of pesticide, *Sol. Energy* 81(10) (2007) 1213-1218.
- [25] M.R.A. Silva, A.G. Trovo, R.F.P. Nogueira, Degradation of the herbicide tebuthiuron using solar photo-Fenton process and ferric citrate complex at circumneutral pH, *J. Photochem. Photobiol. A* 191(2-3) (2007) 187-192.
- [26] M.J. Xu, Q.S. Wang, Y.L. Hao, Removal of organic carbon from wastepaper pulp effluent by lab-scale solar photo-Fenton process, *J. Hazard. Mater.* 148(1-2)

- (2007) 103-109.
- [27] M. Tamimi, S. Qourzal, N. Barka, A. Assabbane, Y. Ait-Ichou, Methomyl degradation in aqueous solutions by Fenton's reagent and the photo-Fenton system, *Sep. Purif. Technol.* 61(1) (2008) 103-108.
- [28] F. Torrades, S. Saiz, A. Garcia-Hortal, J. Garcia-Montano, Degradation of wheat straw black liquor by Fenton and photo-Fenton processes, *Environ. Eng. Sci.* 25(1) (2008) 92-98.
- [29] J. De Laat, H. Gallard, S. Ancelin, B. Legube, Comparative study of the oxidation of atrazine and acetone by $\text{H}_2\text{O}_2/\text{UV}$, $\text{Fe(III)}/\text{UV}$, $\text{Fe(III)}/\text{H}_2\text{O}_2/\text{UV}$ and Fe(II) or $\text{Fe(III)}/\text{H}_2\text{O}_2$, *Chemosphere* 39(15) (1999) 2693-2706.
- [30] M. Panizza, I. Sires, G. Cerisola, Anodic oxidation of mecoprop herbicide at lead dioxide, *J. Appl. Electrochem.* 38(7) (2008) 923-929.
- [31] F. Torrades, M. Perez, H.D. Mansilla, J. Peral, Experimental design of Fenton and photo-Fenton reactions for the treatment of cellulose bleaching effluents, *Chemosphere* 53(10) (2003) 1211-1220.
- [32] F. Wu, N.S. Deng, Photochemistry of hydrolytic iron (III) species and photoinduced degradation of organic compounds. A minireview, *Chemosphere* 41(8) (2000) 1137-1147.
- [33] C.S. Chiou, Y.H. Chen, C. Chang-Tang, C.Y. Chang, J.L. Shie, Y.S. Li, Photochemical mineralization of di-n-butyl phthalate with $\text{H}_2\text{O}_2/\text{Fe}^{3+}$, *J. Hazard. Mater.* 135(1-3) (2006) 344-349.
- [34] I. Oller, S. Malato, J.A. Sanchez-Perez, M.I. Maldonado, R. Gasso, Detoxification of wastewater containing five common pesticides by solar AOPs-biological coupled system, *Catal. Today* 129(1-2) (2007) 69-78.
- [35] M. Lapertot, S. Ebrahimi, I. Oller, M.I. Maldonado, W. Gernjak, S. Malato, C.

- Pulgarin, Evaluating Microtox (c) as a tool for biodegradability assessment of partially treated solutions of pesticides using Fe³⁺ and TiO₂ solar photo-assisted processes, *Ecotoxicol. Environ. Saf.* 69(3) (2008) 546-555.
- [36] J. Herney-Ramirez, M. Lampinen, M.A. Vicente, C.A. Costa, L.M. Madeira, Experimental design to optimize the oxidation of Orange II dye solution using a clay-based Fenton-like catalyst, *Ind. Eng. Chem. Res.* 47(2) (2008) 284-294.
- [37] M. Ahmadi, F. Vahabzadeh, B. Bonakdarpour, E. Mofarrah, M. Mehranian, Application of the central composite design and response surface methodology to the advanced treatment of olive oil processing wastewater using Fenton's peroxidation, *J. Hazard. Mater.* 123(1-3) (2005) 187-195.
- [38] A.R. Khataee, Application of central composite design for the optimization of photodestruction of a textile dye using UV/S₂O₈²⁻ process, *Polish J. Chem. Technol.* 11(4) (2009) 38-45.
- [39] L.A. Lu, M. Kumar, J.C. Tsai, J.G. Lin, High-rate composting of barley dregs with sewage sludge in a pilot scale bioreactor, *Bioresource Technology* 99(7) (2008) 2210-2217.
- [40] I. Arslan-Alaton, A.E. Caglayan, Toxicity and biodegradability assessment of raw and ozonated procaine penicillin G formulation effluent, *Ecotoxicol. Environ. Saf.* 63(1) (2006) 131-140.
- [41] P. Kajitvichyanukul, N. Suntronvipart, Evaluation of biodegradability and oxidation degree of hospital wastewater using photo-Fenton process as the pretreatment method, *J. Hazard. Mater.* 138(2) (2006) 384-391.
- [42] M.I. Pariente, F. Martinez, J.A. Melero, J.A. Botas, T. Velegraki, N.P. Xekoukoulotakis, D. Mantzavinos, Heterogeneous photo-Fenton oxidation of benzoic acid in water: Effect of operating conditions, reaction by-products and

- coupling with biological treatment, *Appl. Catal., B* 85(1-2) (2008) 24-32.
- [43] M. Lapertot, C. Pulgarin, P. Fernandez-Ibanez, M.I. Maldonado, L. Perez-Estrada, I. Oller, W. Gernjak, S. Malato, Enhancing biodegradability of priority substances (pesticides) by solar photo-Fenton, *Water Res.* 40(5) (2006) 1086-1094.
- [44] M. Lapertot, S. Ebrahimi, S. Dazio, A. Rubinelli, C. Pulgarin, Photo-Fenton and biological integrated process for degradation of a mixture of pesticides, *J. Photochem. Photobiol. A* 186(1) (2007) 34-40.
- [45] D.W. Kolpin, E.M. Thurman, D.A. Goolsby, Occurrence of selected pesticides and their metabolites in near-surface aquifers of the midwestern United States, *Environ. Sci. Technol.* 30(1) (1996) 335-340.
- [46] K.G. Varshney, A. Gupta, K.C. Singhal, The adsorption of carbofuran on the surface of antimony(V) arsenosilicate: a thermodynamic study, *Colloids Surf. A* 104(1) (1995) 7-10.
- [47] T.L. Hsieh, M.M. Kao, Adsorption of carbofuran on lateritic soils, *J. Hazard. Mater.* 58(1-3) (1998) 275-284.
- [48] W.S. Kuo, Y.H. Chiang, L.S. Lai, Degradation of carbofuran in water by solar photocatalysis in presence of photosensitizers, *J. Environ. Sci. Health., Part B* 41(6) (2006) 937-948.
- [49] V.K. Gupta, I. Ali, Suhas, V.K. Saini, Adsorption of 2,4-D and carbofuran pesticides using fertilizer and steel industry wastes, *J. Colloid Interface Sci.* 299(2) (2006) 556-563.
- [50] G.H.N. Farahani, I. Bin Sahid, Z. Zakaria, A. Kuntom, D. Omar, Study on the downward movement of carbofuran in two Malaysian soils, *Bull. Environ. Contam. Toxicol.* 81(3) (2008) 294-298.

- [51] A. Detomaso, G. Mascolo, A. Lopez, Characterization of carbofuran photodegradation by-products by liquid chromatography/hybrid quadrupole time-of-flight mass spectrometry, *Rapid Commun. Mass Spectrom.* 19(15) (2005) 2193-2202.
- [52] C. Yuan, Annual report of Taiwan's agriculture, Council of Agriculture (2010).
- [53] W.J. Hayes, E.R. Laws, Handbook of pesticide toxicology, academic press, New York, (1991) 1042.
- [54] M. Arias-Estevez, E. Lopez-Periago, E. Martinez-Carballo, J. Simal-Gandara, Carbofuran sorption kinetics by corn crop soils, *Bull. Environ. Contam. Toxicol.* 77(2) (2006) 267-273.
- [55] D. Finlayson, J. Graham, R. Greenhalgh, J. Roberts, E. Smith, P. Whitehead, R. Willes, I. Williams, Carbofuran: criteria for interpreting the effects of its use on environmental quality, *Nat. Res. Coun. Canada, Publ. NRCC 16740* (1979) 191.
- [56] PHG, Carbofuran in drinking water. California Public Health Goal, (2000).
- [57] D. Lee, C. Chen, K. Houn, Behavior assessment of eight major pesticides used in Taiwan in soils by mechanistic models, *Soils Fert. in Taiwan* (1990).
- [58] S. Nicosia, N. Carr, D. Gonzales, M. Orr, Off-field movement and dissipation of soil-incorporated carbofuran from three commercial rice fields, *J. Environ. Qual.* 20(3) (1991) 532.
- [59] R.A. Chapman, C.M. Cole, Observations on the influence of water and soil-pH on the persistence of insecticides, *J. Environ. Sci. Health., Part B* 17(5) (1982) 487-504.
- [60] S. Campbell, M.D. David, L.A. Woodward, Q.X. Li, Persistence of carbofuran in marine sand and water, *Chemosphere* 54(8) (2004) 1155-1161.
- [61] W.G. Johnson, T.L. Lavy, Persistence of carbofuran and molinate in flooded rice

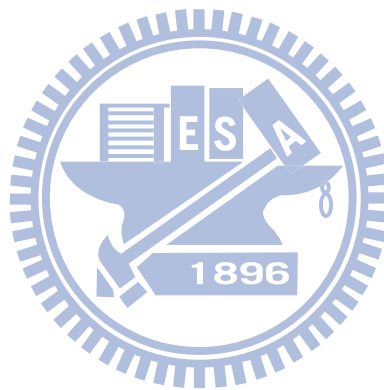
- culture, *J. Environ. Qual.* 24(3) (1995) 487-493.
- [62] W. Chu, T.K. Lau, S.C. Fung, Effects of combined and sequential addition of dual oxidants ($\text{H}_2\text{O}_2/\text{S}_2\text{O}_8^{2-}$) on the aqueous carbofuran photodegradation, *J. Agric. Food. Chem.* 54(26) (2006) 10047-10052.
- [63] Q.Q. Wang, A.T. Lemley, Oxidative degradation and detoxification of aqueous carbofuran by membrane anodic Fenton treatment, *J. Hazard. Mater.* 98(1-3) (2003) 241-255.
- [64] Y.H. Huang, S.T. Tsai, Y.F. Huang, C.Y. Chen, Degradation of commercial azo dye reactive Black B in photo/ferrioxalate system, *J. Hazard. Mater.* 140(1-2) (2007) 382-388.
- [65] S. Chen, D.Z. Sun, J.S. Chung, Treatment of pesticide wastewater by moving-bed biofilm reactor combined with Fenton-coagulation pretreatment, *J. Hazard. Mater.* 144(1-2) (2007) 577-584.
- [66] M. Perez, F. Torrades, X. Domenech, J. Peral, Fenton and photo-Fenton oxidation of textile effluents, *Water Res.* 36(11) (2002) 2703-2710.
- [67] F. Martinez, G. Calleja, J.A. Melero, R. Molina, Heterogeneous photo-Fenton degradation of phenolic aqueous solutions over iron-containing SBA-15 catalyst, *Appl. Catal., B* 60(3-4) (2005) 181-190.
- [68] M. Perez-Moya, M. Graells, L.J. del Valle, E. Centelles, H.D. Mansilla, Fenton and photo-Fenton degradation of 2-chlorophenol: Multivariate analysis and toxicity monitoring, *Catal. Today* 124(3-4) (2007) 163-171.
- [69] A. Santos, P. Yustos, S. Rodriguez, E. Simon, F. Garcia-Ochoa, Abatement of phenolic mixtures by catalytic wet oxidation enhanced by Fenton's pretreatment: Effect of H_2O_2 dosage and temperature, *J. Hazard. Mater.* 146(3) (2007) 595-601.

- [70] J.A. Melero, G. Calleja, F. Martinez, R. Molina, M.I. Pariente, Nanocomposite Fe₂O₃/SBA-15: An efficient and stable catalyst for the catalytic wet peroxidation of phenolic aqueous solutions, *Chem. Eng. J.* 131(1-3) (2007) 245-256.
- [71] L. Mater, E.V.C. Rosa, J. Berto, A.X.R. Correa, P.R. Schwingel, C.M. Radetski, A simple methodology to evaluate influence of H₂O₂ and Fe²⁺ concentrations on the mineralization and biodegradability of organic compounds in water and soil contaminated with crude petroleum, *J. Hazard. Mater.* 149(2) (2007) 379-386.
- [72] I. Sires, C. Arias, P.L. Cabot, F. Centellas, J.A. Garrido, R.M. Rodriguez, E. Brillas, Degradation of clofibric acid in acidic aqueous medium by electro-Fenton and photoelectro-Fenton, *Chemosphere* 66(9) (2007) 1660-1669.
- [73] D. Mantzavinos, Removal of cinnamic acid derivatives from aqueous effluents by Fenton and Fenton-like processes as an alternative to direct biological treatment, *Water Air Soil Pollut. Focus* 3(3) (2003) 211-221.
- [74] P. Bautista, A.F. Mohedano, M.A. Gilarranz, J.A. Casas, J.J. Rodriguez, Application of Fenton oxidation to cosmetic wastewaters treatment, *J. Hazard. Mater.* 143(1-2) (2007) 128-134.
- [75] F. Torrades, S. Saiz, J.A. Garcia-Hortal, Using central composite experimental design to optimize the degradation of black liquor by Fenton reagent, *Desalination* 268(1-3) (2011) 97-102.
- [76] M. Rios-Enriquez, N. Shahin, C. Duran-de-Bazua, J. Lang, E. Oliveros, S.H. Bossmann, A.M. Braun, Optimization of the heterogeneous Fenton-oxidation of the model pollutant 2, 4-xylydine using the optimal experimental design methodology, *Sol. Energy* 77(5) (2004) 491-501.
- [77] H. Kusic, N. Koprivanac, I. Selanec, Fe-exchanged zeolite as the effective heterogeneous Fenton-type catalyst for the organic pollutant minimization: UV

- irradiation assistance, *Chemosphere* 65(1) (2006) 65-73.
- [78] P. Kajitvichyanukul, M.C. Lu, A. Jamroensan, Formaldehyde degradation in the presence of methanol by photo-Fenton process, *J. Environ. Manage.* 86(3) (2008) 545-553.
- [79] I. Arslan-Alatori, A.B. Yalabik, T. Olmez-Hanci, Development of experimental design models to predict Photo-Fenton oxidation of a commercially important naphthalene sulfonate and its organic carbon content, *Chem. Eng. J.* 165(2) (2010) 597-606.
- [80] C.M. Sanchez-Sanchez, E. Exposito, J. Casado, V. Montiel, Goethite as a more effective iron dosage source for mineralization of organic pollutants by electro-Fenton process, *Electrochem. Commun.* 9(1) (2007) 19-24.
- [81] J.J. Wu, M. Muruganandham, J.S. Yang, S.S. Lin, Oxidation of DMSO on goethite catalyst in the presence of H₂O₂ at neutral pH, *Catal. Commun.* 7(11) (2006) 901-906.
- [82] C. Segura, C. Zaror, H.D. Mansilla, M.A. Mondaca, Imidacloprid oxidation by photo-Fenton reaction, *J. Hazard. Mater.* 150(3) (2008) 679-686.
- [83] M.N. Chong, B. Jin, C.W.K. Chow, C. Saint, Recent developments in photocatalytic water treatment technology: A review, *Water Res.* 44(10) (2010) 2997-3027.
- [84] R. Munter, Advanced oxidation processes-current status and prospects, *Proc. Estonian Acad. Sci. Chem* 50(2) (2001) 59-80.
- [85] G.C. Glatzmaier, R.G. Nix, M.S. Mehos, Solar destruction of hazardous chemicals, *Journal of environmental science and health. Part A, Environmental science and engineering* 25(5) (1990) 571-581.
- [86] G.C. Glatzmaier, T.A. Milne, C. Tyner, J. Sprung, Innovative solar technologies for

- treatment of concentrated organic wastes, *Solar energy materials* 24(1-4) (1991) 672-673.
- [87] R. Oliveira, M.F. Almeida, L. Santos, L.M. Madeira, Experimental design of 2,4-dichlorophenol oxidation by Fenton's reaction, *Ind. Eng. Chem. Res.* 45(4) (2006) 1266-1276.
- [88] E. Neyens, J. Baeyens, A review of classic Fenton's peroxidation as an advanced oxidation technique, *J. Hazard. Mater.* 98(1-3) (2003) 33-50.
- [89] H. Gallard, J. De Laat, B. Legube, Spectrophotometric study of the formation of iron (III)-hydroperoxy complexes in homogeneous aqueous solutions, *Water Res.* 33(13) (1999) 2929-2936.
- [90] C. Techapun, T. Charoenrat, M. Watanabe, K. Sasaki, N. Poosaran, Optimization of thermostable and alkaline-tolerant cellulase-free xylanase production from agricultural waste by thermotolerant *Streptomyces* sp Ab106, using the central composite experimental design, *Biochemical Engineering Journal* 12(2) (2002) 99-105.
- [91] M.J. Diaz, M.E. Eugenio, L. Jimenez, E. Madejon, F. Cabrera, Modelling vinasse/cotton waste ratio incubation for optimum composting, *Chem. Eng. J.* 93(3) (2003) 233-240.
- [92] D.C. Montgomery, *Design and Analysis of Experiments*. fifth ed., John Wiley & Sons (2001).
- [93] J.H. Ramirez, C.A. Costa, L.M. Madeira, Experimental design to optimize the degradation of the synthetic dye Orange II using Fenton's reagent, *Catal. Today* 107(8) (2005) 68-76.
- [94] C. Satterfield, A. Bonnell, Interferences in Titanium Sulfate Method for Hydrogen Peroxide, *Anal. Chem.* 27(7) (1955) 1174-1175.

- [95] APHA-AWWA-WPCF, Standard methods for the examination of water and wastewater, Twentieth ed, American public health association, Washington DC (1998).
- [96] M. Diaz, M. Eugenio, L. Jimenez, E. Madejon, F. Cabrera, Modelling vinasse/cotton waste ratio incubation for optimum composting, Chem. Eng. J. 93(3) (2003) 233-240.
- [97] J. Bachman, H.H. Patterson, Photodecomposition of the carbamate pesticide carbofuran: Kinetics and the influence of dissolved organic matter, Environ. Sci. Technol. 33(6) (1999) 874-881.



Curriculum vitae

Name: Li-An Lu

Address: Institute of Environmental Engineering,

National Chiao Tung University,

1001 University Road, Hsinchu 300, Taiwan, ROC.

Tel : +886-3-5712121 Ext. 55531

E-mail: sigma.ev92g@nctu.edu.tw

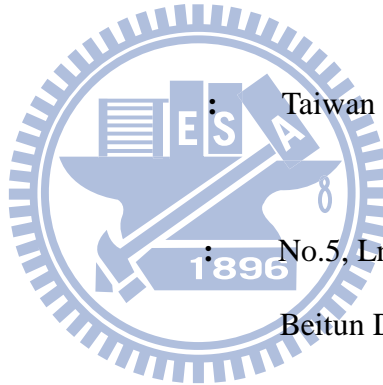


PERSONAL INFORMATION

Date of Birth : 21st March, 1981

Nationality : Taiwan

Present Address : No.5, Ln. 71, Sec. 1, Rehe Rd.,
Beitun Dist., Taichung City 406,
Taiwan (R.O.C.)



EDUCATION

Ph.D. (2005-2011) : Institute of Environmental
Engineering, National Chiao Tung
University

M.S. (2003-2005) : Institute of Environmental
Engineering, National Chiao Tung
University

B.S. (1999-2003) : Department of civil Engineering
National Chi Nan University

THESIS TITLE

Title of Ph.D. Thesis : Application of photo-Fenton process
in the degradation and detoxification
of carbofuran contaminated water

Advisor : Dr. Jih-Gaw Lin

Title of M.S. Thesis : High-rate composting of barley
dregs with sewage sludge and its
application



Advisor : Dr. Jih-Gaw Lin

COMPUTER SKILLS

M.S. Office, Origin, Minitab

AWARDS AND HONORS

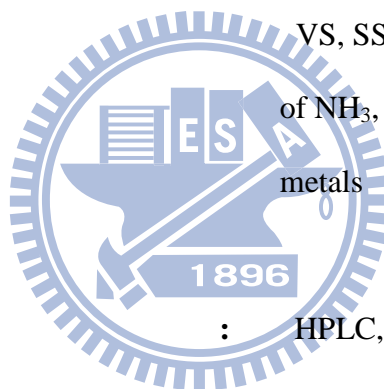
- Scholarship of Ministry of Education, sustainable campus (2008)
- Scholarship of Taiwan Water Environmental Regeneration Agency (2008)

RESEARCH INTERESTS

- Composting of solid waste
- Oxidation of hazardous and biorefractory compounds using AOPs
- Municipal and industrial waste water treatment

TECHNICAL SKILLS

Environmental chemistry : Physico-chemical measurements
such as pH, BOD₅, DO, COD, TS,
VS, SS, turbidity, and concentrations
of NH₃, NO₂⁻, NO₃⁻, PO₄³⁻, and heavy



Analytical chemistry : HPLC, TOC analyzer, TKN
analyzer, UV/Visible
spectrophotometer, microwave
digestion and AA

PAPERS PUBLISHED IN INTERNATIONAL JOURNALS

- **L.A. Lu**, M. Kumar, J.C. Tsai, J.G. Lin, High-rate composting of barley dregs with sewage sludge in a pilot scale bioreactor, *Bioresource Technology* 99(7) (2008) 2210-2217.

- **L.A. Lu**, Y.S. Ma, M. Kumar, J.G. Lin, Photochemical degradation of carbofuran and elucidation of removal mechanism, Chem. Eng. J. 166(1) (2010) 150-156.
- **L.A. Lu**, Y.S. Ma, M. Kumar, J.G. Lin, Influence of pH and H₂O₂ dosage on the decomposition of carbofuran during the photo-Fenton process, Sustain. Environ. Res. 20(5) (2010) 293-297.
- **L.A. Lu**, Y.S. Ma, M. Kumar, J.G. Lin., Photo-Fenton pretreatment of carbofuran – Analyses via experimental design, detoxification and biodegradability enhancement, Separ. Purif. Technol. (**In press**).
- **L.A. Lu**, Y.S. Ma, A. Daverey, J.G. Lin, Optimization of Photo-Fenton Process Parameters on Carbofuran Degradation Using Central Composite Design, J. Environ. Sci. Health part B (**In press**).

➤

PAPERS PUBLISHED IN INTERNATIONAL CONFERENCES

-
- **L.A. Lu**, M. Kumar, J.G. Lin, Influence of H₂O₂ dosage in the decomposition of aqueous carbofuran by photo-Fenton process, The 3rd IWA-ASPIRE Conference and Exhibition, Oct 18-22 (2009) Taipei, Taiwan.
 - **L.A. Lu**, J.C. Tsai, V. Pugalenti and J.G. Lin, High-rate composting of sludge with barley dregs and use of compost as a novel biosorbent. IWA Specialized Conference – Sustainable Sludge Management: State of the Art, Challenges and Perspectives, May 29-31 (2006) Moscow, Russia.
 - **L.A. Lu**, J.C. Tsai, V. Pugalenti, S.W. Sung, J.G. Lin, Optimization of a high-rate composting of barley dregs with sewage sludge, WEF 2006 Residuals and

Biosolids Management Conference, March 12-15 (2006) Greater Cincinnati, Ohio, USA.

- V. Pugalenti, J.C. Tsai, **L.A. Lu**, J.G. Lin, Fast Composting of Beer Manufactory Wastes Using Thermophilic Bioreactor, International Conference on Advances in Industrial Wastewater Treatment, February 9-11 (2005) Chennai, India.

PAPERS PUBLISHED IN DOMESTIC CONFERENCES

- **呂理安**、蘇義雄、庫瑪、馬英石、林志高，利用Fenton法降解受加保扶污染之水體。第十八屆下水道與水環境再生研討會，中華民國 97 年，台北科技大學，台北市。
- **呂理安**、庫瑪、蔡人傑、林志高，麥粕與下水污泥快速堆肥之研究。第九屆海峽兩岸環境保護學術研討會，中華民國 96 年，交通大學，西安，中國。
- **呂理安**、蔡人傑、葛蘭斯、林志高，麥粕與下水污泥快速堆肥之最適化研究。第十七屆環工年會暨第二十屆廢棄物處理技術研討會，中華民國 94 年 11 月 18 至 19 日，國立中央大學，桃園縣中壢市。
- 林志高、何公亮、蔡人傑、**呂理安**，啤酒廠廢麥粕堆肥化之研究。2004 產業環保工程實務技術研討會，中華民國 93 年 11 月 11 日，國立台灣大學，台北市。